NASA CR-72858
WANL-PR(VVV)- 001
March, 1971

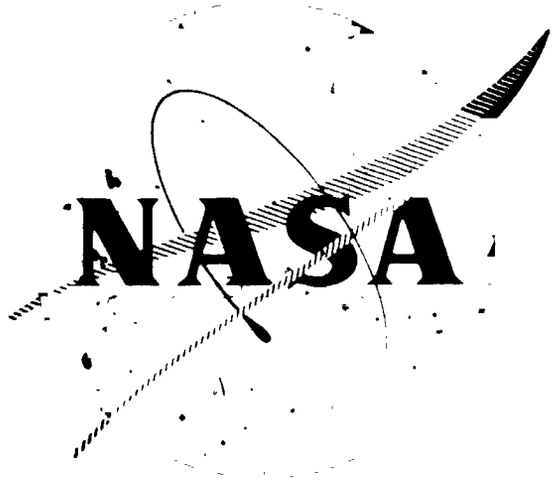

INFLUENCE OF RESTRAINT AND THERMAL EXPOSURE ON WELDS IN T-111 AND ASTAR-811C

By

R.E. Gold and G.G. Lessmann

Westinghouse Astronuclear Laboratory

Prepared for
National Aeronautics And Space Administration
NASA Lewis Research Center
Task I of Contract NAS 3-11827
Paul Moorhead, Project Manager

NOTICE

This report was prepared as an account of Government-sponsored work. Neither the United States, nor the National Aeronautics and Space Administration (NASA), nor any person acting on behalf of NASA:

A.) Makes any warranty or representation, expressed or implied, with respect to the accuracy, completeness, or usefulness of the information contained in this report, or that the use of any information, apparatus, method, or process disclosed in this report may not infringe privately-owned rights; or

B.) Assumes any liabilities with respect to the use of, or for damages resulting from the use of, any information, apparatus, method or process disclosed in this report.

As used above, "person acting on behalf of NASA" includes any employee or contractor of NASA, or employee of such contractor, to the extent that such employee or contractor of NASA or employee of such contractor prepares, disseminates, or provides access to any information pursuant to his employment or contract with NASA, or his employment with such contractor.

Requests for copies of this report should be referred to:

National Aeronautics and Space Administration
Scientific and Technical Information Facility
P. O. Box 33
College Park, Maryland 20740

Astronuclear Laboratory

NASA CR-72858
WANL-PR(VVV)-001

FINAL REPORT

INFLUENCE OF RESTRAINT AND THERMAL EXPOSURE ON WELDS IN T-111 AND ASTAR-811C

by

R. E. Gold and G. G. Lessmann

WESTINGHOUSE ASTRONUCLEAR LABORATORY
Pittsburgh, Pennsylvania 15236

prepared for

NATIONAL AERONAUTICS AND SPACE ADMINISTRATION

March, 1971

Task I of Contract NAS 3-11827

Fracture and Hot Crack Resistance of Welds in T-111 and ASTAR-811C

NASA Lewis Research Center
Cleveland, Ohio
Paul E. Moorhead, Project Manager
Materials and Structures Division

Astronuclear Laboratory

FOREWORD

This program was conducted by the Westinghouse Astronuclear Laboratory under NASA Contract NAS 3-11827. Mr. P. E. Moorhead of the NASA Lewis Research Center, Materials and Structures Division, was the NASA Project Manager for the program.

The objectives delineated and the results reported herein represent the requirements of Task I of Contract NAS 3-11827. Additional investigations which were performed as a part of this program are the subjects of additional reports. The final reports for this contract are the following :

Task	Title	Report Number
I	Influence of Restraint and Thermal Exposure on Welds in T-111 and ASTAR-811C	NASA CR-72858
II	The Varestraint Test for Refractory Metals	NASA CR-72828
III	Investigation of High Temperature Fracture of T-111 and ASTAR-811C	NASA CR-72859

TABLE OF CONTENTS

LIST OF ILLUSTRATIONS

LIST OF ILLUSTRATIONS (Continued)

LIST OF TABLES

LIST OF TABLES (Continued)

ABSTRACT

The notched-tensile, tensile, and bend properties of GTA welds in T-111 and ASTAR-811C sheet were determined following a wide range of thermal exposures in order to define changes in ductility and mechanical property behavior due to weld aging response. No notch sensitivity or unusual tensile response was noted for any of the conditions evaluated. As had been previously reported* , however, an aging response was noted for the bend ductile-brittle transition temperature determinations on both T-111 and ASTAR-811C welds. A tentative explanation for the observed response of each alloy is presented.

In addition, the interrelationship of mechanical and chemical factors leading to underbead cracking in T-111 was investigated. The problem was shown to be amenable primarily to chemical solutions, such as alloy compositional changes. This was demonstrated by the improved performance of ASTAR-811C over T-111 in plate weld studies. Only modest success was achieved with procedural techniques as a means of eliminating underbead cracking.

---

* Lessmann, G. G. and Gold, R. E., "Long-Time Elevated Temperature Stability of Refractory Metal Alloys", NASA-CR-1608, September, 1970.

1.0 SUMMARY

The mechanical behavior of GTA welds in T-111 and ASTAR-811C sheet was characterized as a function of a wide range of post-weld therm· ·xposures. This investigation was prompted by recent observations showing that T-111 welds respond to long-time high temperature exposure with potential ductility impairment. This study was consequently undertaken to determine the reproducibility of this response and its engineering significance. The advanced tantalum-base alloy ASTAR-811C was included in this investigation both because of its metallurgical similarities to T-111 and to provide a timely evaluation of its thermal stability. To provide sufficient material for this program the first commercial scale ASTAR-811C ingot (> 300 lb.) was produced and processed to the required sheet, wire and plate with a net 42% yield. Thermal exposures included post-weld annealing from 1205°C (2200°) through 1982°C (3600°F) followed by 1000 hour aging at 1149°C (2100°F). Post exposure evaluation included notched-unnotched tensile testing, high temperature tensile testing, bend testing, and structural evaluations.

Notched tensile tests were conducted at temperatures as low as -196°C (-320°F). Not a single incidence of notch sensitivity was noted in as-welded, post-weld annealed, or aged GTA welds in either T-111 or ASTAR-811C. It appeared both the fracture appearance transition temperature (FATT) and the ductility transition temperature (DTT) of GTA welds in T-111 are well below -196°C (-320°F). ASTAR-811C welds at -196°C (-320°F) are above the DTT but seem to be below the FATT.

A series of tensile tests were performed on as-welded post-weld annealed, and aged GTA welds in T-111 and ASTAR-811C at RT, 538°, 982°, 1149°, 1316° and 1427°C (1000°, 1800°, 2100°, 2400° and 2600°F). No unusual features in either the mechanical properties or the fracture behavior were observed which were attributable to the thermal exposures. In additional tests to 2316°C (4200°F) a region of decreased tensile ductility was observed in the vicinity of 1649°C (3000°F) for both alloys. This is in no way unique to welds or to these alloys. The temperature range over which the ductility decrease persisted was signif-

icantly greater for T-111 than for ASTAR-811C. This appears related to the presence of a stable carbide precipitate in ASTAR-811C.

Bend transition temperatures were determined for post-weld annealed-plus-aged T-111 and ASTAR-811C welds using 1t, 2t, and 4.5t bend radii. Results were in general agreement with those of a previous study (Reference Contract NAS 3-2540) which had indicated a potential ductility impairment resulted from long-time aging at temperatures between 982° and 1149°C (1800° and 2100°F). The ductility impairment was qualitatively followed by noting the change in the bend DBTT on aging. 1149°C (2100°F) aging of GTA sheet welds of T-111 resulted in a slight increase in the bend transition temperature. However, the magnitude of the increase was much less than had been observed and reported previously. The unaged bend transition temperature of ASTAR-811C GTA welds -- i.e. in the as-welded and as-welded plus post-weld annealed conditions -- was found to be in the range of 52° to 65°C (125° to 150°F). This represented an increase of nearly 222°C (400°F) relative to the as-received condition. Subsequent aging at 1149°C (2100°F) had essentially no further effects. Differences in the 1t, 2t, and 4.5t bend transition temperatures of welds in either alloy were negligible.

The microstructural responses of the weld specimens to the thermal exposures were characterized in detail by the use of light microscopy. In T-111 only two effects were noted. First, post-weld anneals up to about 1649°C (3000°F) or aging at 1149°C (2100°F) resulted in the development of an interdendritic precipitate in the fusion zone. Second, post-weld anneals at 1871° and 1982°C (3400° and 3600°F) resulted in extensive grain growth and complete homogenization of the weld structures, after which aging had no effect. In ASTAR-811C the reactions were somewhat more complicated. In addition to the effects noted for T-111, post-weld anneals above 1649°C (3000°F) or aging 1000 hours at 1149°C (2100°F) resulted in the precipitation of intragranular and grain boundary carbides. The grain boundary carbide was present in two distinct morphologies -- as a blocky, cellular precipitate and as a semi-continuous grain boundary phase. The development of the carbide precipitates was not confined to the fusion zone but was a general feature of the heat-affected zone and base metal regions as well.

An additional phase of this program was addressed to the recently observed grain boundary underpass cracking problem which exists in multipass GTA plate welds in T-111 and ASTAR-811C. This problem is particularly important since it is typical of advanced alloys designed for high creep strength coupled with liquid alkali metal corrosion resistance. Efforts were directed toward developing an understanding of the factors which control cracking, both mechanical and chemical, and their interactions. Considerable success was achieved in this regard. The cracking can be identified with the high creep strength of T-111 coupled with segregation of hafnium to grain boundaries. At high temperatures, encountered in welding but not in normal applications, the grain boundaries are weakened relative to the high strength matrix. Consequently, weld thermal strains are disproportionately accommodated by the grain boundaries. In practice this results in grain boundary cracking in the first passes of a multipass plate weld as successive passes are applied. Results of this study showed that ASTAR-811C is virtually insensitive to this problem, and that underbead cracking should lend itself to solution using modified filler wire compositions for T-111.

2.0 INTRODUCTION

This report presents the results of a weldability and weld property study of plate and sheet welds in the tantalum-base alloys, T-111 and ASTAR-811C. This investigation was sponsored by the National Aeronautics and Space Administration, and provided the first comprehensive weldability evaluation of ASTAR-811C as well as advancing the general state-of-the-art in the area of weld aging response. ASTAR-811C is a later generation alloy than T-111 and was developed to combine many of the attributes of T-111 with improved high temperature creep strength[1]. The possibility of the utilization of ASTAR-811C to replace or supplement T-111 in critical applications provided justification for its inclusion in this program.

Two important aspects of weld performance were investigated in this program. These are first, the influence of restraint resulting from heavy section welding, and secondly, weld stability during exposures at typical application temperatures. Previous NASA-sponsored research on the elevated temperature stability of refractory metal alloys[2] had implied a possible ductility impairment in the mechanical properties of T-111 welds due to long time ultra-high vacuum exposures between 982° and 1149°C (1800° and 2100°F). The aging response was detected only in measurements of the bend ductile-brittle transition temperature using a 1t bend radius. No evidence of a response was noted for tensile tests at room or elevated temperatures. Hence, in the present program the engineering significance of the aging response in T-111 and ASTAR-811C welds was investigated using notched tensile tests, bend tests using several bend radii, and room and elevated temperature tensile tests. The pre-test thermal exposures were expanded to encompass 1 hour post-weld annealing at temperatures from 1205° through 1982°C (2200° through 3600°F). In addition tests were performed after 1000 hour aging at 1149°C (2100°F) in ultra-high vacuum.

Observations of grain boundary cracking in multipass GTA plate welds in T-111[3] provided the impetus for the plate weld investigation portion of this program. The approach employed was to screen a number of procedural variations in making multipass plate welds and to evaluate their relative effectiveness in alleviating the grain boundary underpass cracking problem. This

provided a comparison between T-111 and two heats of ASTAR-811C. An excellent assessment of the Varestraint test (see reference 5) was thereby afforded by direct comparison with plate welding results. In this respect the plate weld study provided a definite correlation between Varestraint results and field welding performance.

Primary units in this report are the International System of Units (or Systeme International d' Unites ; Reference NASA SP-7012) . For clarity the customary engineering units have also been provided as secondary units. The exception to this is for engineering drawings where the customary units are primary. Where required due to quantity of data involved duplicate figures or tables are provided, the SI figure or table being suffixed with an "a".

3.0 TECHNICAL PROGRAM

3.1 Background

Typical of all but the most highly alloyed tantalum-base refractory metal alloys, T-111 and ASTAR-811C possess excellent weldability characteristics. Particular evidence in support of this statement is provided by the fact that in the more than 300 GTA sheet welds prepared for the various tasks of this program, not a single incidence of poor weld quality was observed either by visual, dye penetrant or radiographic inspection of the as-welded specimens or by subsequent metallographic examination.

The above facts notwithstanding, numerous instances of grain boundary cracking have been observed in multipass GTA plate welds in both T-111 and ASTAR-811C. The cracks are located in weld metal deposited during previous filler passes; i.e. metallographic examination of the weld at various stages of completion has established the fact cracks are not found in the filler pass deposited immediately preceding the examination. The first documented observations of this problem were made during efforts on Contract NAS 3 - 10602 ("Development of Large Diameter T-111 Tubing"). Some of the conclusions and observations from that program regarding this problem follow [3]:

- Joint thickness and geometry strongly influence the occurrence and severity of the cracking. The use of a double U-groove joint design greatly reduced the extent of cracking.
- Trial plate welds in T-222 and FS-85 refractory metal alloys, which are similar in general chemistry to T-111 having a refractory metal base and a reactive metal addition, displayed similar grain boundary cracking while a trial weld in Ta-10W plate was crack free. These results suggest the presence of the reactive metal (i.e. hafnium or zirconium) in a high strength matrix aggravates the cracking problem.
- Single pass weld procedures, such as full penetration EB welding, completely avoided the problem. Obviously this offers no solution for GTA welding since it is impractical to deposit a single filler pass weld on 0.952 cm. (0.375 in.) plate.
- A 14.60 cm. (5.75 inch) OD T-111 tube which had been GTA welded and found to contain underpass grain boundary cracks in the weld metal was reduced a total of 92% by tube rocking. Subsequent examinations revealed no residual evidence of the previously existing cracks. The fact the tube was able to accommodate over 65%

reduction in area at a single stage, that is, between in-process anneals, despite the presence of cracks attests to the superior fracture toughness of the alloy. This fact was further established during the notched-unnotched tensile evaluation in this program.

A review of the above indicates the underpass grain boundary cracking problem can be avoided by exercising proper joint design or by post-weld deformation. Unfortunately, many hardware components must be welded in place or are of such geometry to preclude either of these solutions. Hence, further efforts to understand and circumvent this behavior were warranted.

In addition to the plate weld problem, recent studies of the elevated temperature stability of T-111 and other refractory metal alloys[2] revealed a modest loss of ductility following long time aging at temperatures from 982° through 1149°C (1800° through 2100°F). The ductility decrease was observed by measurements of the 1t bend ductile-brittle transition temperature as a function of aging time and temperature. Aging times to 10,000 hours were used. The nature of the ductility response observed can be characterized as follows:

- The magnitude of the response, as measured by the increase in the 1t bend DBTT, was greater for GTA welds than for EB welds. Base metal did not exhibit a similar effect.
- The use of 1 hour post-weld anneals at temperatures to 1649°C (3000°F) were ineffective in stabilizing the weld structure with respect to the aging phenomenon.
- Tensile properties and hardness traverses did not reveal any aging response. Weld tensile ductility remained excellent irrespective of thermal history. Hence, the aging response is peculiar to bend testing.
- In all conditions the bend specimens failed by intergranular "tearing" rather than by a brittle cleavage mode and hence did not demonstrate a true shift in ductile-brittle behavior.

Several of the preceding statements suggest the likely possibility the ductility decrease may be rather insignificant. The fact tensile ductility did not suffer a decrease implies the aging may merely result in a metallurgical structure unable to accommodate the rather severe 33% strain of the 1t bend test. Hence, one of the chief aims of this program was to obtain a more comprehensive understanding of this problem and its implications. To do this required a more complete definition of the observed ductility impairment noted in the aged weld structures.

3.2 Test Program

The outline of the testing program is shown in Figure 1. In the plate weld study welds were prepared from T-111 and ASTAR-811C using a variety of welding procedures selected to evaluate their effectiveness in alleviating the grain boundary underpass cracking problem. Within the rather limited scope of the present program it was not realistic to assume a solution would be obtained, but, rather, to identify some of the more critical aspects of the problem. In this respect, the goal of this task was to identify if possible the most promising avenues of study by which an ultimate solution might be achieved. The welding variables considered included ;

- type of filler metal used
- effect of interpass time
- number of filler passes employed
- effect of reversing direction each successive pass
- the use of a "buttered" weld joint technique

Joint design and mechanical fixturing were not varied.

The purpose of the remaining tasks was to evaluate the fracture toughness of welds in T-111 and ASTAR-811C. In addition to evaluation in the as-welded condition, the influence of one hour post-weld anneals at pressures below 1.33×10^{-3} N/m^2 (10^{-5} torr) at temperatures from 1205° through 1982°C (2200° through 3600°F) and aging for 1000 hours at 1149°C (2100°F) in ultra-high vacuum was also evaluated. Notched-unnotched tensile tests were used in the first phase of the evaluation to assess the effects of a multiaxial stress system on the fracture behavior of the weld specimens. The combined influence of relatively low test temperatures and multiaxial stresses tend to create conditions under which brittle failure is promoted. Hence, the performance of a given material in this type of test provides a quantitative evaluation of its resistance to brittle fracture.

The next phase of the evaluation (Task IC on Figure 1) consisted of the evaluation of conventional tensile properties of post-weld annealed and post-weld annealed-plus-aged longitudinal weld specimens. Testing was performed at room temperature, 538°, 982°, 1149°,

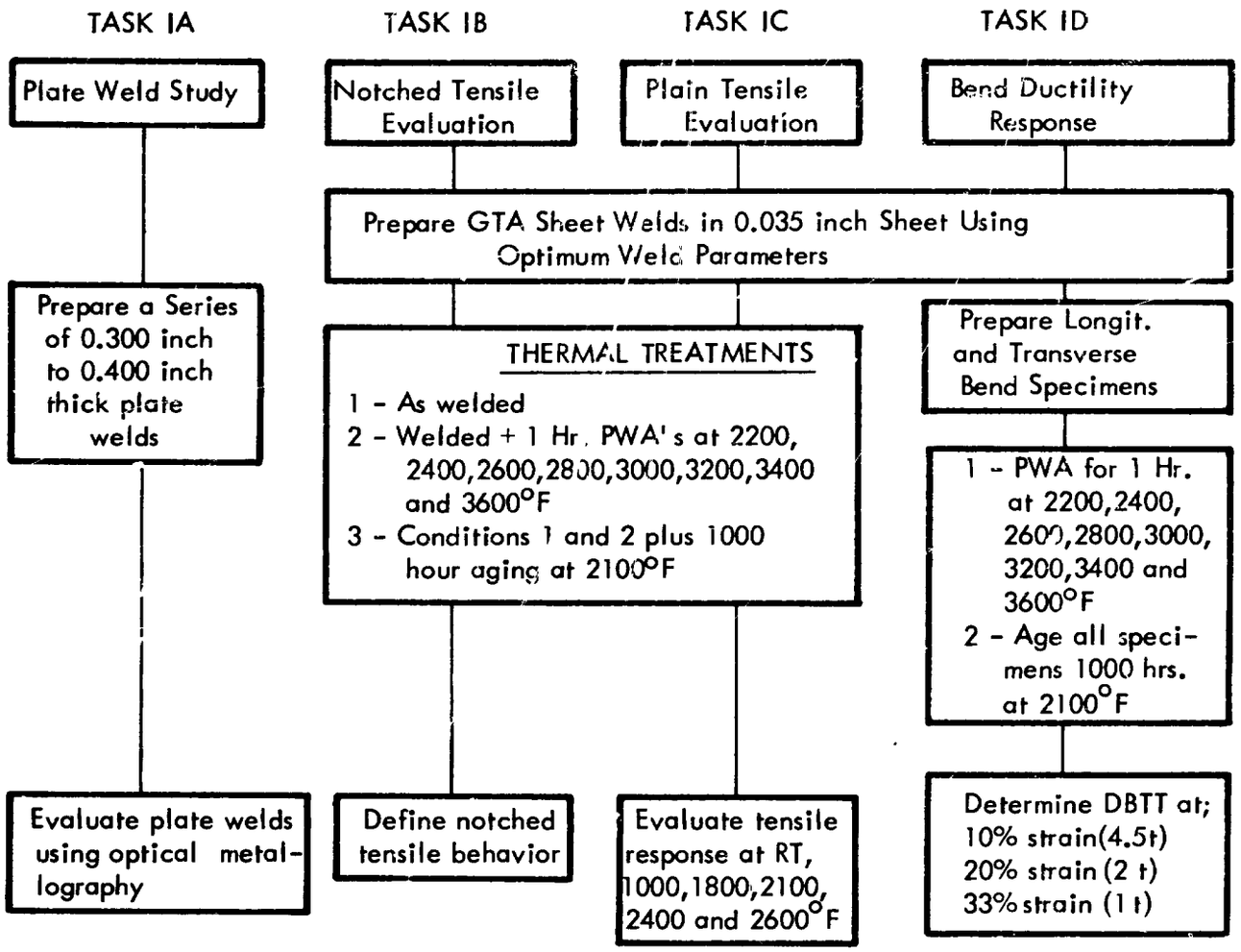

FIGURE 1 - Outline of Test Program for T-111 and ASTAR-811C.

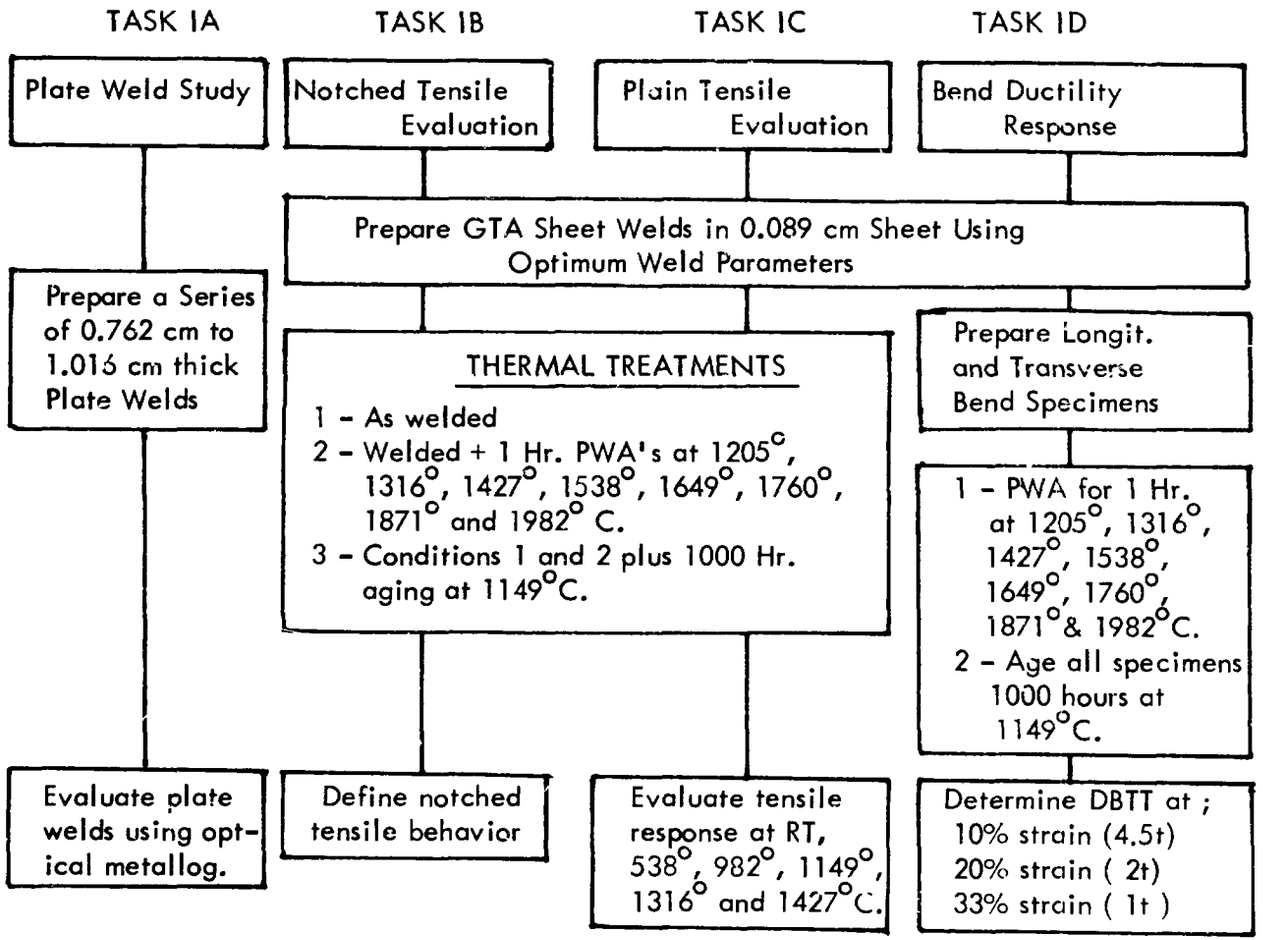

FIGURE 1a - Outline of Test Program for T-111 and ASTAR-811C.

1316° and 1427°C (1000°, 1800°, 2100°, 2400° and 2600°F). This phase of the program was designed to provide information regarding the effect of thermal exposures on both the conventional tensile properties as well as the ensuing fracture behavior. In this way the test results could be assigned perspective with regard to their engineering significance.

The remaining task of this program (Task ID) was addressed to the correlation of 1t bend tests , which correspond to an outer fiber strain of 33%, with bend tests accomplished at 2t and 4.5t bend radii , corresponding to outer fiber strains of 20% and 10%, respectively. The question which inevitably arises when evaluating bend test results is that of how to interpret the data. Generally treated as a simple "go no go" test, it is nevertheless hoped the results will lend themselves to a more quantitative interpretation. The direct relationship between bend radius and outer fiber strain necessitate close inspection of as-tested specimens to ensure uniformity in the test results. In addition, particularly when a ductility impairment is suggested by the results, the details of the fractures themselves are extremely important. It must be pointed out that in all but the most highly alloyed tantalum-base alloys, and in T-111 and ASTAR-811C in particular, the failure mode observed in bend tested specimens can invariably be described as ductile grain boundary tearing in the weld metal rather than the more classic brittle cleavage fractures associated with transition temperature behavior. Logically then one must attempt to determine if the failures observed reflect a significant loss of ductility or merely indicate an inability of the coarse-grained weld specimens to accommodate the bending strain of the bend tests.

3.3 Procedures

3.3.1 Welding Procedures

The gas-tungsten-arc (GTA) welding process was used exclusively for all plate and sheet welding. All welding was performed in a vacuum purged weld chamber using an ultra-high purity helium atmosphere. The weld atmosphere was continuously monitored for oxygen and water vapor contents during all welding operations. For the bead-on-plate sheet welding the oxygen and water vapor were maintained at less than 5 ppm by volume whereas for the greater heat input plate welding the maximum level was set as 10 ppm by volume. All weld

ing was done using straight polarity direct current (SPDC).

All bead-on-plate sheet welds in both T-111 and ASTAR-811C sheet were made using the following welding parameters;

Weld Current		115 amps
Weld Speed	38.1 cpm	(15 ipm)
Arc Gap	0.157 cm.	(0.062 inches)

Electrodes were made of 0.24 cm. (0.094 in.) diameter centerless ground 2% thoriated tungsten which had been ground to a blunted 0.079 cm. (0.031 in.) diameter tip. Welding was done semi-automatically using a traversing table which permitted a uniform, reproducible travel speed of the workpiece relative to the electrode. All sheet welds were inspected for basic quality using visual, dye penetrant and radiographic techniques.

Due to the importance of the various parameters in the plate welding study and the fact numerous variations were employed, specification of the plate weld parameters will be deferred to the discussion of the plate weld studies. The weld joint designs used are shown in Figure 2.

3.3.2 Tensile Testing

Specimen configurations used for tensile testing are shown in Figure 3 for the room and elevated temperature tensile tests and in Figure 4 for the notched-unnotched tests. Room temperature tests were performed using a strain rate of 0.005 min^{-1} to 0.6% strain, then 0.05 min^{-1} to specimen fracture. Elevated temperature tensile testing was conducted using 0.05 min^{-1} strain rate throughout the test. The bulk of the notched-unnotched tensile tests were conducted at -196°C (-320°F) and -46°C (-50°F) using a constant crosshead speed of 0.0127 cm/minute (0.005 inch/minute). A few tests on aged T-111 specimens were run at -196°C (-320°F) using a crosshead speed of 1.27 cm/minute (0.5 inch/minute) to assess the effect of a higher strain rate on the notched tensile behavior. All elevated temperature tests were performed at pressures below 1.33×10^{-3} N/m^2 (10^{-5} torr). Specimen gage sections were wrapped in tantalum foil for additional contamination protection during testing. Weld surfaces were ground flat during specimen machining operations.

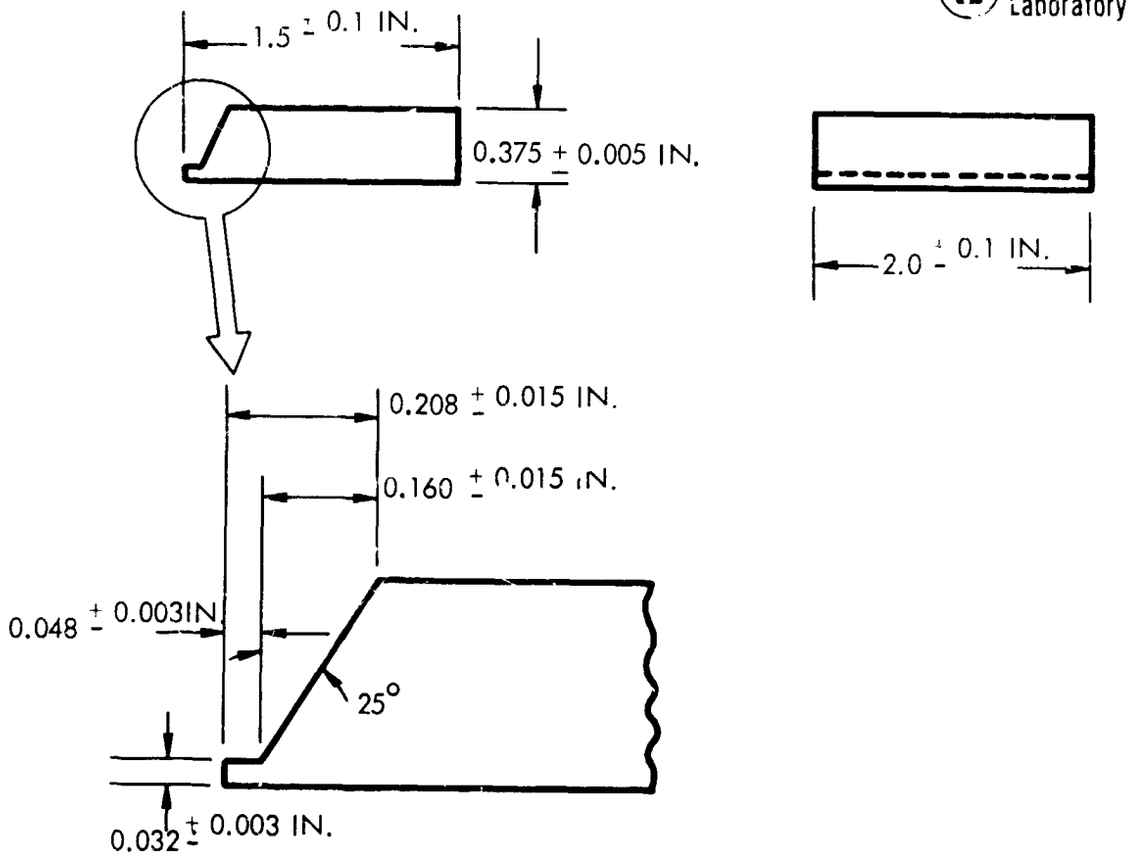

Configuration (a), Basic preparation for fusion root pass.

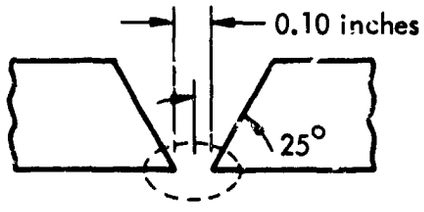

Configuration (b), Utilizing a filler root pass.

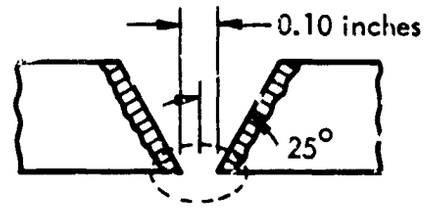

Configuration (c), T-111 plate "buttered" with ASTAR-811C filler wire, remachined and welded with ASTAR-811C filler wire.

FIGURE 2 - Butt Joint Weld Preparations Used This Program.

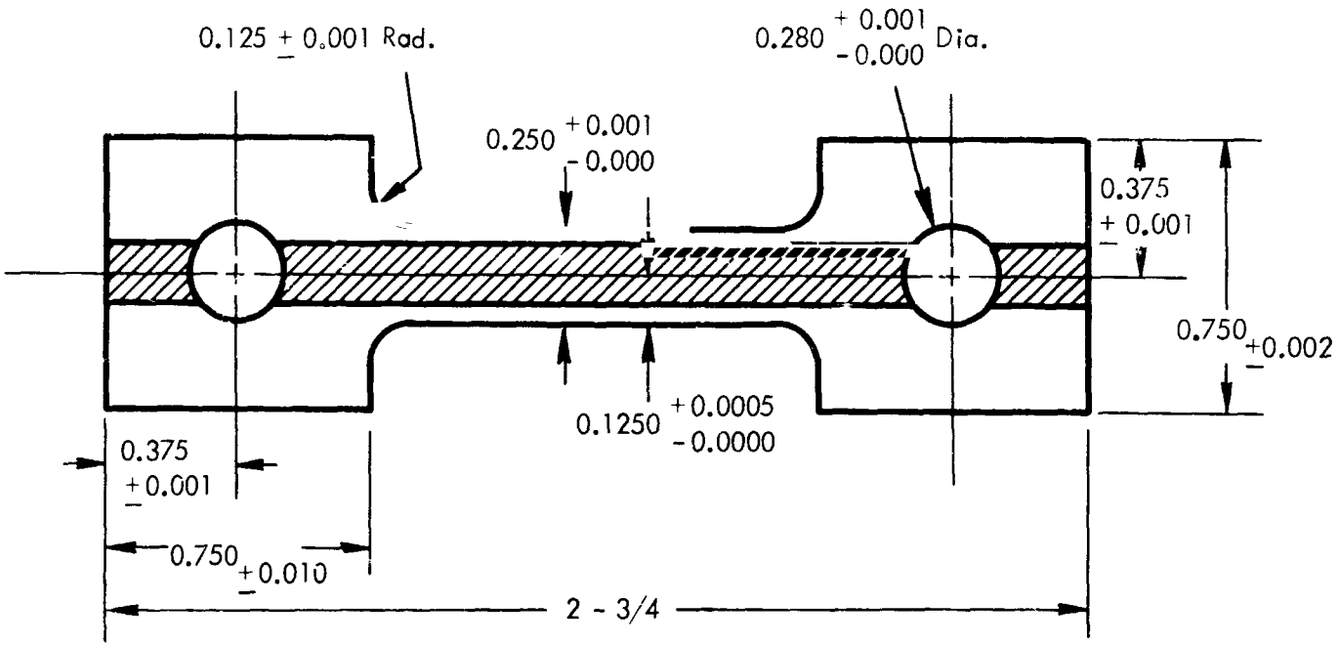

FIGURE 3 - Specimen Configuration Used for Room Temperature and High Temperature Tests on T-111 and ASTAR-811C GTA Sheet Welds.

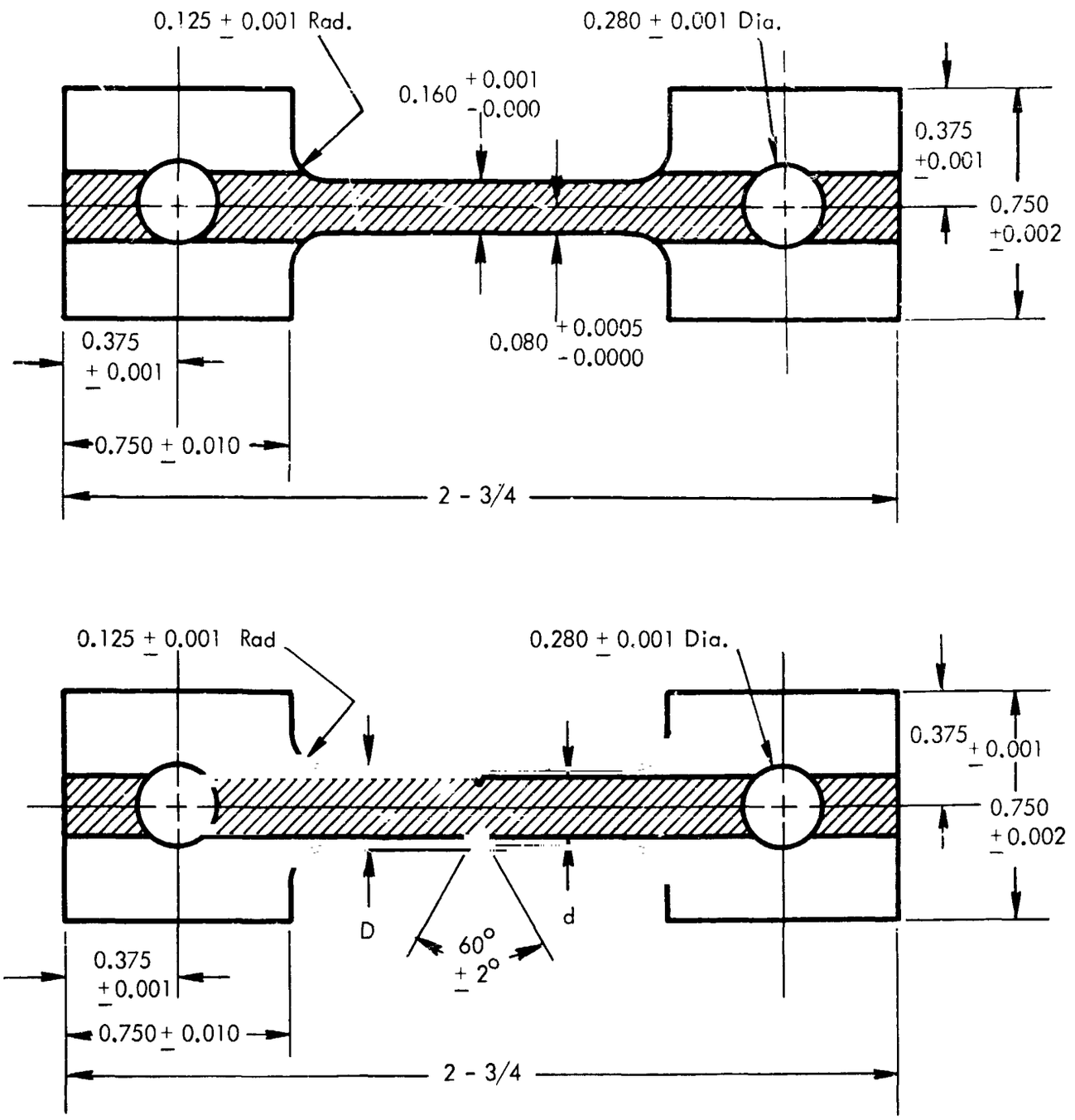

Special Notes: $D = 0.210^{+0.001}_{-0.000}$ $d = 0.150^{+0.001}_{-0.000}$

Notch Root Radius = 0.004 inches

FIGURE 4 - Specimen Configuration Used for Notched-Unnotched Tensile Tests on T-111 and ASTAR-811C GTA Welds in 0.089 cm (0.035 inch) Sheet.

3.3.3 Bend Testing

The bend test parameters are shown in Figure 5. To satisfy the requirements of the bend ductility response evaluation tests were conducted using 1t , 2t , and 4.5 t punch radii. These correspond to outer fiber strains of 33% , 20% , and 10% , respectively.

Bend specimens were prepared directly from the inspected welds by shearing to the 12t x 24t specimen size. Surface grinding was unnecessary due to the uniformly high quality of the welds. Specimens were bent with the top surface of the weld in tension to an angle of 90° to 105° after springback. Four specimens are normally required to define the transition temperature. The bend test data are recorded graphically as shown by reference to the data plots in the Appendix. This method of presentation identifies all pertinent data including crack location and the extent of crack propagation for each specimen as well as the transition curve defined by the bend angle achieved as a function of test temperature. Longitudinal and transverse curves are coded for presentation on the same graph.

3.4 Program Materials

3.4.1 T-111

The T-111 material evaluated in this program was procured in the form of plate, sheet and wire. The material was purchased from Wah Chang Corporation of Albany, Oregon and represented three different heats of T-111. Metallurgical data and certified chemical analyses relevant to the as-received condition are presented in Tables 1 and 2. All forms of T-111 were obtained in the fully recrystallized condition.

3.4.2 ASTAR-811C

To provide sufficient material for this program ASTAR-811C was produced in a commercial size ingot for the first time. A 138 kg (304 lb.) ingot was prepared by Wah Chang Corporation of Albany, Oregon using double vacuum-arc melting practice. The 18.4 cm (7.25 inch) diameter ingot was canned in molybdenum and extruded at 1649°C (3000°F) using an extrusion ratio of 3:1. The machined ingot and molybdenum extrusion can are shown prior to assembly

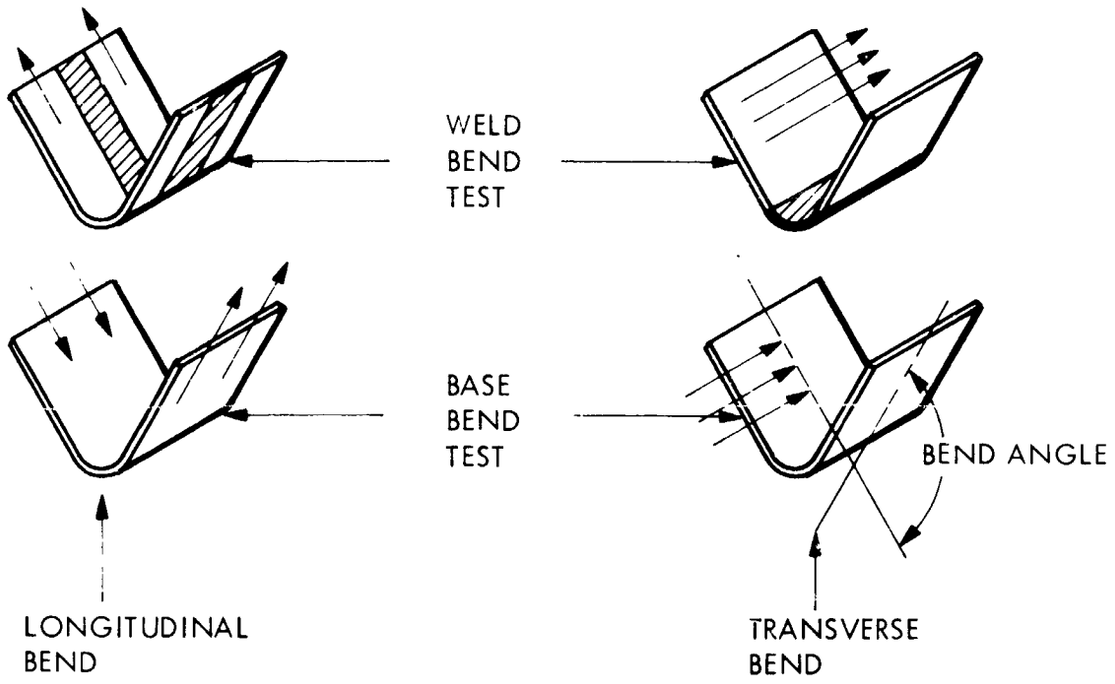

NOTE: ARROWS SHOW ROLLING DIRECTION

THICKNESS, t = 0.035 INCH
WIDTH = 12t
LENGTH = 24t
TEST SPAN = 15t
PUNCH SPEED = 1 IPM
TEMPERATURE - VARIABLE
PUNCH RADIUS - VARIABLE, GENERALLY 1t, 2t, 4t, or 6t

BEND DUCTILE TO BRITTLE TRANSITION TEMPERATURE =
LOWEST TEMPERATURE FOR 90° + BEND WITHOUT CRACKING

596924A

FIGURE 5 - Bend Test Parameters

TABLE 1 - Metallurgical Data for As-Received T-111

Form	Heat No.	Hardness[a] DPH	Grain Size		Used For
			ASTM No.	Avg. Dia., μm	
0.508/0.762 cm(0.200/0.300 in.) Plate	650043	240	7 - 7.5	32	Plate weld studies
0.203 cm (0.080 inch) diam. Wire	65059	230	9	18	Filler wire-plate welds
0.089 cm (0.035 inch) Sheet	650043	219	8.5	22	Tensile evaluations
0.089 cm (0.035 inch) Sheet	650050	214	7.5	30	Bend ductility eval.

(a) 98.06 N (10 kg) load used for hardness determinations.

TABLE 2 - Chemical Analysis of As-Received T-111[a]

Form	Heat No.	Certified Analysis						Check Analysis		
		Ta	W	Hf	C	O	N	C	O	N
Plate	650043	Bal	8.30	2.00	<40	100	25	-	-	-
Wire	65059	Bal	8.85	2.07	70	40	10	80	27	<5
Sheet	650043	Bal	8.30	2.00	<40	90	12	33	40	12
Sheet	650050	Bal	8.00	1.95	<40	50	12	38	65	<5

(a) Metal analyses in w/o ; interstitial analyses in wt. ppm.

in Figure 6. Following extrusion and cleanup the usable yield, weighing 111 kg (244 lbs.), was annealed 1 hour at 1649°C (3000°F), then forged to sheet bar at 1260°C (2300°F). After cleanup the as-forged sheet bar was processed to plate, sheet and wire as required to satisfy the testing requirements of the experimental program. An excellent product yield from ingot exceeding 42% was realized.

Metallurgical data and chemical analyses of the as-received material are presented in Tables 3 and 4, respectively. Also shown in Table 4 are the analyzed chemistry values for the original development heat of ASTAR-811C produced at the Astronuclear Laboratory under Contract NAS 3-2542 [1]. The slightly higher W and Re contents of the program heat (Heat 650078) suggested the desirability of characterizing the base metal mechanical properties of this material. Base metal tensile properties were determined at -196°, RT, 1205°, 1649° and 1982°C (-320°, RT, 2200°, 3000° and 3600°F) using sheet specimens. These results are presented in Table 5 along with the data for comparable tests conducted under NAS 3-2542. The program heat is seen to be somewhat stronger than the development heat, particularly at the lower test temperatures, although the ductility, measured in terms of the tensile elongation, is quite similar. 1t bend tests (33% outer fiber strain) indicated a bend DBTT of -157°C (-250°F) for Heat 650078 as compared to < -196°C (< -320°F) for the development heat. The high yield and ultimate tensile strength is likely due to the slightly higher tungsten and rhenium contents. Rhenium, in particular, has been observed to be a potent solid solution strengthener at low temperatures when present in the tantalum matrix[4]. The relevance of the difference in materials is discussed later in the appropriate Results section of this report.

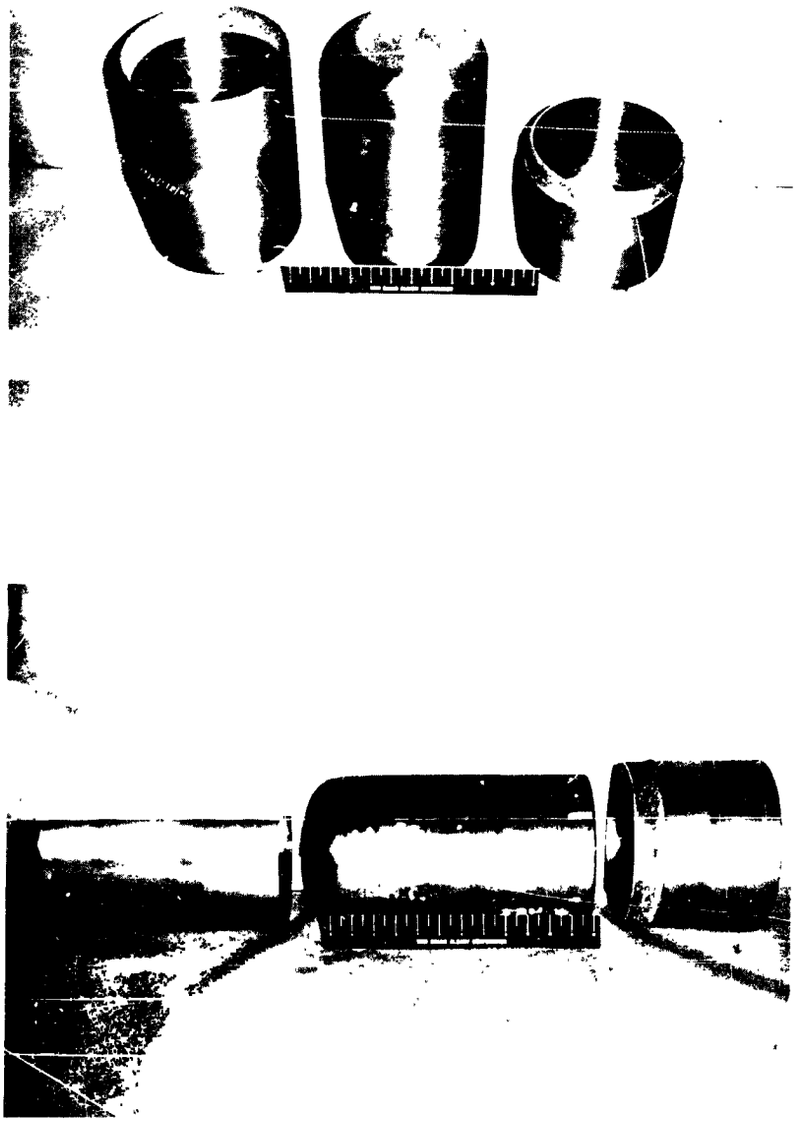

FIGURE 6 - ASTAR - 811C Ingot and Molybdenum Container Prior to Assembly for Extrusion.

TABLE 3 - Metallurgical Data for As-Received ASTAR-811C
(Heat 650078)

Form	Hardness[a] DPH	Grain Size		Used For
		ASTM No.	Avg. Dia., μm	
0.089 cm. (0.035 inch) Sheet	276	8.5	19	Bend ductility evaluation
0.559/0.952 cm. (0.220/0.375 in.) Plate	- -	8.5	22	Plate weld studies
0.318 cm. (0.125 inch) Plate	283	9.5	13	Varestraint testing [b]
0.089 cm. (0.035 inch) Sheet	281	9.5	13	Fracture studies [c]

(a) 9.806 N (10 kg) load used for hardness determinations.
(b) Subject of Task II ; see Reference (5)
(c) Subject of Task III ; see Reference (6)

TABLE 4 - Chemical Analyses of As-Received ASTAR-811C[a]

Heat	Form	Certified Analysis							Check Analysis		
		Re	Ta	W	Hf	C	O	N	C	O	N
650078[b]	0.559/0.952 cm. (0.220/0.375 in.) Plate	1.39	Bal	8.1	0.9	245	50	12	240	10	<10
	0.318 (0.125 inch) Plate	1.39	Bal	8.1	0.9	300	70	<10	210	10	<10
	0.089 cm. (0.035 inch) Sheet	1.39	Bal	8.1	0.9	250	50	12	230	10	12
650068[b]	0.203 cm. (0.080 inch) Dia. Wire	1.34	Bal	8.4	0.9	280	70	18	-	-	-
Original Development Heat [c]		0.98	Bal	7.3	0.86	200	13	20	-	-	-
650056[d]	0.800 cm. (0.315 inch) Plate	1.17	Bal	8.1	0.9	240	60	20	-	-	-

(a) Metal analyses in weight percent ; interstitial analyses in weight ppm.
(b) Primary ASTAR-811C heat produced to Re specification 1.0 to 1.5 weight percent.
(c) Original development heat data from Reference (1).
(d) Additional heat with Re conforming to current limits of 0.8 to 1.2 weight percent. Plate from this heat also reduced to sheet for use as filler metal in plate welding to evaluate effect of lower Re level.

Heat [a]	Test Temp.		UTS		0.2% Y.S.		% Elongation	
	°F	°C	ksi	10^7 N/m^2	ksi	10^7 N/m^2	Unif.	Total
650078	- 320	- 196	182.9	126.1	166.5	114.8	18.2	24.9
3-2542	- 320	- 196	165.3	114.0	147.7	101.8	22.1	26.3
650078	RT	RT	117.5	81.0	98.1	67.6	15.3	27.3
3-2542	RT	RT	104.0	71.7	85.1	58.7	16.4	26.6
650078	2200	1205	58.8	40.5	36.3	25.0	15.4	29.1
3-2542	2200	1205	49.9	34.4	31.6	21.8	---	28.8
650078	3000	1649	23.5	16.2	22.1	15.2	1.4	87.4
3-2542	2800	1538	28.4	19.6	23.0	15.8	---	49.5
650078	3600	1982	10.3	7.1	10.1	7.0	0.6	112.7

(a) This program heat is Heat 650078.

Original development heat referenced as 3-2542 ; see Reference (1).

A constant 0.05 min^{-1} strain rate used throughout all tests.

TABLE 5 - Comparative Tensile Properties for Program ASTAR-811C and Original Development Heat.

4.0 RESULTS AND DISCUSSION

4.1 Plate Weld Studies

These studies were directed towards developing an understanding of the mechanism of underbead cracking in T-111 and ASTAR-811C multipass manual GTA plate welds. The results described below demonstrate that this problem ;

- Can be ameliorated utilizing certain procedural techniques for T-111,
- Can be eliminated with proper chemical and procedural control for ASTAR-811C, and,
- Should lend itself to a compositional solution with special filler wire selection for T-111.

This effort was conducted in sufficient depth to ascertain and demonstrate the basic mechanisms of the plate welding problem and the most important elements of its solution. Naturally, developing an understanding of the problem and defining its solution tend to proceed simultaneously. However, in the following discussion the mechanism of underbead cracking as now understood is described first for clarity of presentation. This is followed by a discussion of the experimental results obtained in this program which support this presentation and compares T-111 and ASTAR-811C.

4.1.1 The Mechanism of Underbead Cracking in T-111

The basic mode of underbead cracking observed in multipass GTA plate welds in T-111 is grain boundary fracture, Figure 7. Phenomenologically, this is a typical high temperature mode of failure in most metals. Grain boundary fracture at high temperatures occurs usually at low total strain although deformation adjacent to the grain boundaries may actually be quite extensive, Figure 8. This phenomenon is discussed and related to the behavior of T-111 and ASTAR-811C in detail in section 4.2.2 , "High Temperature Tensile Evaluation", of this report.

The source of strain in plate weldments is the thermal deformation which occurs in early passes of a multipass weldment as successive passes are applied. The thermal deformation results in compressive upsetting on the underside of the weldment. This upsetting is apparent in the typical plate weld shown in Figure 9.

21,257 50X

FIGURE 7 - Underbead Cracking in Root Fusion Pass and First Filler Pass of Multipass GTA Plate Weld in T-111. Weld Number B3.

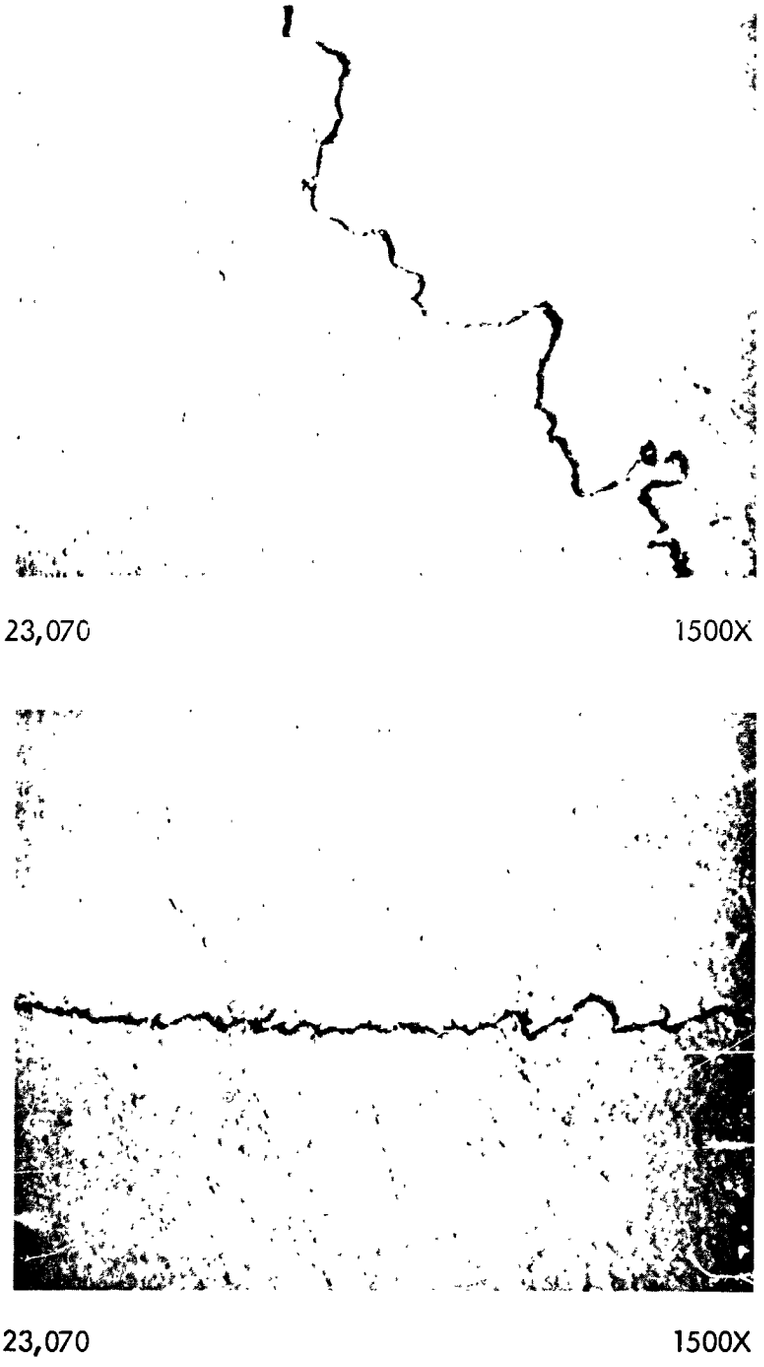

FIGURE 8 - Grain Boundaries in Unetched ASTAR-811C Multipass GTA Plate Weld Showing Extensive Deformation in Regions Adjacent to Them. Weld Number T4-A7.

20.295 5.5X

FIGURE 9 - ASTAR-811C Weld Number 4 Macrosection Showing Extensive Root Area Upsetting Which Occurs in Multipass GTA Plate Welds.

The basic tendency of metals to fracture at low total strain at high temperatures does not necessarily result in underbead cracking even though severe thermal strains invariably accompany plate welding. In fact, underbead cracking as displayed by T-111 must be considered as highly unusual. This implies that additional factors are involved in the case of T-111. These would appear to be both metallurgical and structural in nature. First, T-111 possesses good high temperature creep resistance, mainly as the result of solid solution strengthening of the matrix. Hence, the relative difference in the matrix and grain boundary strengths is somewhat more exaggerated than for some other refractory metal alloys at high temperatures. Secondly, lower melting alloying constituents, such as hafnium in T-111, tend to be concentrated at grain boundaries; hence weakening them at high temperatures. As a result, at temperatures which are high with respect to the normal use temperatures, the grain boundaries are relatively weak. The hafnium effect has been demonstrated by showing that the binary alloy Ta-10W does not display underbead cracking in multipass plate welds despite an equivalent high temperature creep strength[3]. As a further confirmation, underbead cracking was produced in a plate weld in FS-85. FS-85 is a high creep strength columbium-base alloy (Cb-27Ta-10W-1Zr) having metallurgical characteristics similar to T-111, with zirconium replacing hafnium as the reactive metal addition. The prediction and confirmation of underbead cracking in FS-85 and the absence thereof in Ta-10W furnishes definitive evidence for the mechanism of underbead cracking in T-111. It is important to understand that the reactive metals (i.e. Zr and Hf) in these alloy systems are essential for alkali metal corrosion resistance. They further provide a small increment of short time mechanical strength by dispersion strengthening. Hence, this problem cannot be solved simply by eliminating the reactive metal.

Along the same line of reasoning, however, the compromising effect of hafnium on creep strength was recognized during the development of ASTAR-811C. This alloy contains only half the hafnium content of T-111, contains rhenium as an additional strengthener and has a decided creep strength advantage over T-111 [1]. ASTAR-811C , then, by design has higher creep strength and , due to the lower hafnium than T-111, has an intuitively more favorable composition with respect to avoiding the underbead cracking problem. Demonstration of this difference in weld behavior was accomplished in this program.

An additional aspect of this problem deserves reemphasis. Reactive metal additions to refractory metal alloys only lead to underbead cracking in plate welds of the higher strength, creep resistant alloys. Alloys which have been optimized in composition for high temperature strength appaer to be susceptible whereas weaker alloys are not. Hence, to use advanced alloys in alkali metal systems requires the understanding of underbead cracking as described. Experimental verification of this interpretation is given below.

4.1.2 Experimental Results of the Plate Weld Studies

Experimental weldments were produced in small groups with changes incorporated as the evaluation of each successive weld or series of welds was completed. The test weldments produced are listed in Table 6 in a general chronological sequence. This sequence also defines basically the experimental plan pursued. Plate thickness was either 0.772/0.800 cm. (0.304/0.315 inches) or 0.952/0.978 cm. (0.375/0.385 inches). Joint configurations utilized are cross-referenced to Figure 2. The number of passes required to complete a weld varied depending on procedure although in general only two procedures were used. One procedure required 7 to 10 passes while the other required the use of 15 to 20 filler passes. Welding was done manually utilizing GTA welding, DCSP, with manual filler wire feed. This was modified somewhat for about half the welds which were traversed mechanically to achieve a welding speed of 25.4 cpm (10 ipm) versus a manual speed of about 7.62 cpm (3 ipm).

The first weldment produced using conventional procedures exhibited underbead cracking as expected. Subsequent welds in T-111 plate were made using ASTAR-811C filler wire as a first trial of that alloy. Three joint configurations were evaluated. None of these proved particularly beneficial. It was later surmised, and then proven, that a high rhenium content in the ASTAR-811C filler wire compromised these results. This stemmed from the fact the initial rhenium specification called for 1.0 to 1.5 weight percent. During the performance of this program that specification was modified to 0.8 to 1.2 weight percent. The bulk of the evaluation material was produced with approximately 1.4 weight percent rhenium. In this series, weld number 3 was produced by first buttering and remachining the faces of the T-111 plate. This preparation is shown in Figure 10. Although not beneficial in this test, buttering could well have merit if ASTAR-811C filler wire produced to current specifications were used.

Plate Weld Identification	Alloy		Heat Number		Plate Thkns.		Joint (i) Design	Number of (ii) Passes
	Plate	Wire	Plate	Wire	In.	Cm.		
T-111 Qualifier	T-111	T-111	650043	65059	0.305	0.775	a	8 (1,5)
1	T-111	ASTAR-811C	650043	650068	0.305	0.775	a	8 (1,5)
2	T-111	ASTAR-811C	650043	650068	0.305	0.775	b	7 (1,5)
3	T-111	ASTAR-811C	650043	650068	0.305	0.775	c	7 (1,5)
A1	T-111	T-111	650043	65080	0.305	0.775	a	10 (2,4)
A2	T-111	T-111	650043	65080	0.305	0.775	a	7 (2,3)
A3	T-111	T-111	650043	65080	0.305	0.775	a	15 (1,3,4)
A4	T-111	T-111	650043	65059	0.305	0.775	a	17 (1,3,6)
A5	T-111	T-111	650043	65059	0.304	0.772	a	17 (1,3,6)
B1	T-111	T-111	650024	65059	0.375	0.952	a	10 (2,3,5)
B2	T-111	T-111	650024	65059	0.375	0.952	a	10 (2,3,5)
B3	T-111	T-111	650024	65059	0.375	0.952	a	11 (2,3,5)
T4-A1	ASTAR-811C	ASTAR-811C	650078	650068	0.385	0.978	a	9 (1,4)
T4-A2	ASTAR-811C	ASTAR-811C	650078	650068	0.385	0.978	a	9 (1,3,4)
T4-A3	ASTAR-811C	ASTAR-811C	650056	650068	0.315	0.800	a	18 (1,3,5)
T4-A4	ASTAR-811C	ASTAR-811C	650078	650068	0.385	0.978	a	18 (1,3,6)
T4-A5	ASTAR-811C	ASTAR-811C	650078	650068	0.385	0.978	a	20 (1,3,6)
4	ASTAR-811C	ASTAR-811C	650056	650068	0.315	0.800	a	8 (1)
5	ASTAR-811C	ASTAR-811C	650056	650068	0.315	0.800	b	8 (1)
T4-A6	ASTAR-811C	ASTAR-811C	650078	650068	0.385	0.978	a	21 (1,3,6)
T4-A7	ASTAR-811C	ASTAR-811C	650056	650056	0.315	0.800	a	19 (1,3,5)

(i) Refers to Figure 2.

(ii) Numbers in parentheses as follows ; (1) Welding direction reversed each pass ; (2) Welding direction same each pass ; (3) Welding speed controlled at 25.4 cpm; (4) 5 min. cooling between passes (5) Black heat cool between passes (6) 2 min. cooling between passes

TABLE 6 – Plate Weld Records

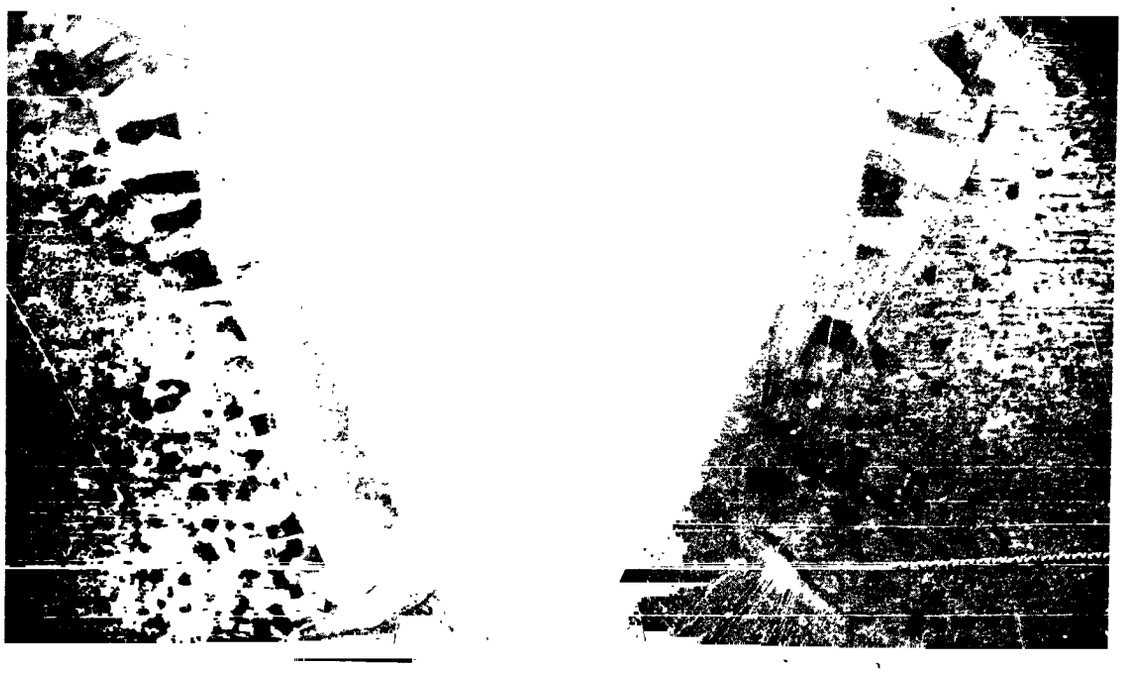

FIGURE 10 - T-111 Plate Weld Preparation for Joint Number 3 with Edges Pre-Buttered Using ASTAR-811C Filler Wire. Prepared as Shown in Figure 2c.

Subsequent trials in T-111 plate welding were designed to take advantage of the lower heat input which can be achieved with the use of higher welding speeds. A three to four fold decrease in unit weld length heat input is obtained by increasing welding speed from manual speeds which are about 7.62 cpm (3 ipm) to 25.4 cpm (10 ipm). This decrease stems primarily from the arc dwell time effect which is an inverse function of weld speed (i.e. minutes per inch). The number of passes in these welds was increased, significantly reducing the heat affected area per pass. Also, the welding direction was reversed each pass in an attempt to disrupt the epitaxial grain growth pattern in the weld. All of these changes were expected to be in the direction of less weld distortion and finer grain size. These procedural fixes seemed to offer some potential but were not in themselves adequate for eliminating underbead cracking.

The final series of weldments were made to evaluate ASTAR-811C. Initial trials showed ASTAR-811C program material with 1.4 percent rhenium to be superior to T-111 with respect to the underbead cracking problem. This can be seen in the dye penetrant results shown in Figure 11. A high sensitivity fluorescent penetrant, ZL 22, was used for these tests. Procedures were checked to a sensitivity standard of 2.54×10^{-5} cm. (1×10^{-5} inches). The defects apparent in Figure 11 have an average size of approximately that magnitude. The penetrant tests were performed on as-polished, unetched samples.

In Figure 11, the ASTAR-811C welds are seen to be considerably better than T-111 with regard to the underbead cracking as revealed by the dye penetrant. These results seem consistent with the relative strength concept for matrix versus grain boundary thermal deformation during welding. With its lower hafnium content ASTAR-811C would be expected to crack less than T-111. Proof of this interpretation was achieved by utilizing ASTAR-811C of lower rhenium content for additional weldments. These results are shown in Figure 12 where virtually no cracking is seen. The rationale for this effect is that rhenium is such a potent strengthener that even modest rhenium increases could result in a deleterious imbalance in relative matrix-grain boundary strengths. This in turn would cause excessive accommodation of thermal strain by the grain boundaries leading to grain boundary cracking.

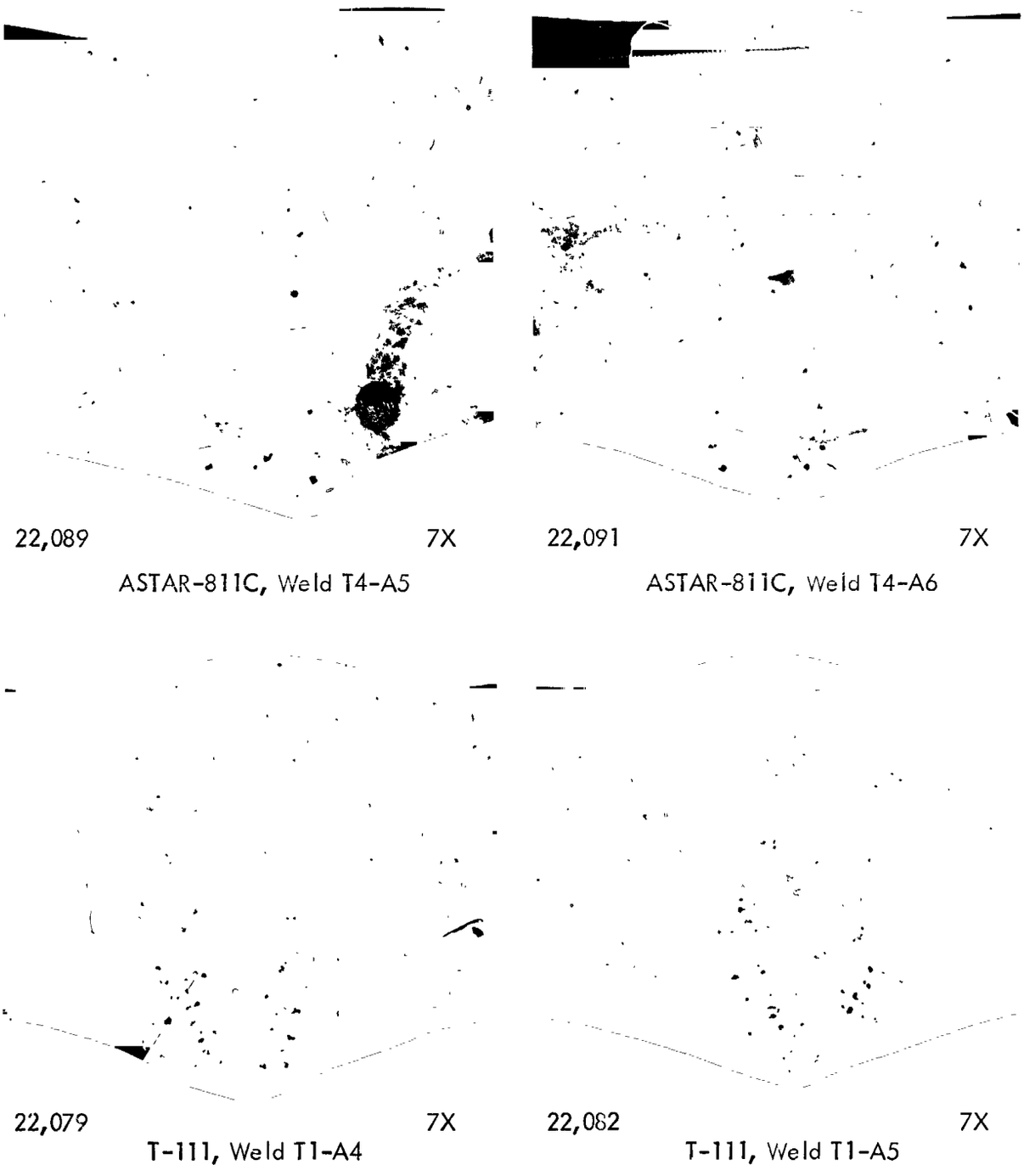

FIGURE 11 - High Sensitivity Fluorescent Penetrant Results for GTA Plate Welds. Indications of Cracking in ASTAR-811C Result From High Rhenium Content. See Figure 12 also.

21,862 7X

ASTAR-811C, Weld T4-A3

Plate - Heat Number 650056
Filler - Heat Number 650068

23,069 7X

ASTAR-811C, Weld T4-A7

Plate - Heat Number 650056
Filler - Heat Number 650056

Heat Number	Re Analysis, w/o
650056	1.17
650068	1.34

FIGURE 12 - High Sensitivity Fluorescent Penetrant Results for Two ASTAR-811C GTA Plate Welds Showing No Defects When Plate Only or Both Plate and Filler are Within Specification for Rhenium, 0.8 to 1.2 w/o.

The sensitivity to rhenium content was further confirmed in Varestraint testing as described in the Task II Final Report to this contract [5]. Varestraint data for the high rhenium heat had originally indicated T-111 and ASTAR-811C to be about equal in propensity for "hot cracking" during welding. Reevaluation using the low rhenium heat of ASTAR-811C resulted in a 70% decrease in cracking thereby confirming the plate weld results. At this level of Varestraint cracking other alloys show absolutely no tendency to hot crack in any way during welding. Hence, utilizing current rhenium specifications, ASTAR-811C should be weldable in multipass GTA plate welds without underbead cracking problems. An interesting aspect of this program is revealed in these results. Namely, the Varestraint test nominally measures propensity towards hot cracking in alloys having an excessively depressed solidus. With both T-111 and ASTAR-811C the Varestraint test appears to be sensitive to hot ductility limitations as well as the "hot short" condition usually associated with hot cracking.

Plate Weld Summary

Underbead cracking in T-111 occurs because of an unfavorable balance of matrix and grain boundary strengths during thermal deformation in multipass plate welds. The unfavorable balance results from the high temperature creep strength of the T-111 matrix coupled with the weakening of the grain boundaries by hafnium segregation. At normal application temperatures this type of cracking does not occur. At higher temperatures, as experienced in welding, a typical transition to grain boundary failure occurs which is exaggerated by the hafnium segregation.

In this respect ASTAR-811C, which contains half as much hafnium as T-111, is much more resistant to underbead cracking. Comparing ASTAR-811C of differing rhenium contents showed that matrix strengthening had the same relative effect in promoting underbead cracking as did grain boundary weakening.

Finally, these results demonstrate that the T-111 underbead cracking might be entirely eliminated through compositional modification. This could be accomplished by designing a special filler wire composition. An alternate approach to eliminating underbead cracking using weld procedural controls rather than chemistry modification did not seem to offer significant promise.

4.2 Fracture Toughness Evaluation

4.2.1 Notched Tensile Evaluation

The results of notched-unnotched tensile tests conducted on longitudinal weld specimens indicate T-111 and ASTAR-811C welds do not display notch sensitivity at temperatures as low as -196°C (-320°F) (liquid nitrogen). A wide range of pre-test thermal exposures were evaluated. These included:

- As welded
- As welded plus post-weld anneals of 1 hour at 1205°, 1316°, 1427°, 1538°, 1649°, 1760°, 1871° and 1982°C (2200°, 2400°, 2600°, 2800°, 3000°, 3200°, 3400°, and 3600°F).
- The above conditions followed by 1000 hour aging at 1149°C (2100°F) in ultra-high vacuum (< 1.33×10^{-6} N/m^2 (< 18^{-8} torr) pressure).

Test results are presented for T-111 and ASTAR-811C in Tables 7 and 8, respectively. All tests for which data are presented in Tables 7 and 8 were performed at -196°C (-320°F) (in liquid nitrogen) using a constant crosshead travel speed of 0.0127 cm/minute (0.005 inch/minute). The effect of strain rate on the notched tensile behavior was investigated by testing a set of aged T-111 welds at a crosshead travel speed of 1.27 cm/minute (0.5 inch/minute). The results of these tests, also performed at -196°C (-320°F), are presented in Table 9 and are quite similar to those for aged T-111 specimens reported in Table 7.

Initially the program goal was to determine the notched tensile transition temperature - i.e. the temperature below which the notch-strength-ratio (NSR) is less than unity - but this temperature appears to be below -196°C (-320°F), the lowest test temperature used. The extremely low values of tensile elongation seen for unnotched ASTAR-811C welds at -196°C (-320°F) prompted the determination of the notched-unnotched tensile properties of aged and unaged ASTAR-811C at -46°C (-50°F). These results are presented in Table 10. Comparison with the data of Table 8 reveals the tensile elongation has increased considerably and the NSR values are now more uniform. Nevertheless, the fact the -196°C (-320°F) values of the NSR are greater than unity indicates no true notch sensitivity exists at that temperature. The data of Tables 7 and 8 and observations regarding fracture mode are summarized as follows:

Test Condition [a]	Notched Specimens		Unnotched Specimens		NS(notched) / UTS(unnotched) [b]
	NS, ksi	K_t	UTS, ksi	% Elong.	
As Welded	180.8	3.8	151.2	15.6	1.20
As Welded + Aged	146.4	4.2	134.6	11.0	1.09
1 Hr.-2200°F PWA	171.7	3.8	142.0	16.5	1.21
" " + Aged	141.3	4.2	129.7	5.4	1.09
1 Hr.-2400°F PWA	168.7	3.8	144.7	18.4	1.17
" " + Aged	146.7	4.2	129.1	2.4	1.14
1 Hr.-2600°F PWA	163.8	4.2	143.2	20.5	1.14
" " + Aged	149.1		129.0	4.4	1.16
1 Hr.-2800°F PWA	162.8	4.2	140.6	18.9	1.16
" " + Aged	132.0	4.2	130.9	8.4	1.01
1 Hr.-3000°F PWA	162.5	4.2	137.6	13.0	1.18
" " + Aged	142.1	4.6	127.8	1.3	1.11
1 Hr.-3200°F PWA	168.2	3.8	138.9	18.9	1.21
" " + Aged	151.5	4.2	133.5	12.5	1.13
1 Hr.-3400°F PWA	168.5	3.8	139.8	18.9	1.21
" " + Aged	143.4	4.6	130.8	9.0	1.10
1 Hr.-3600°F PWA	162.1	3.8	131.9	15.3	1.23
" " + Aged	145.9	4.2	127.1	6.3	1.15

All tests at — 320°F using 0.005 inch/minute crosshead travel speed.

(a) All aging was for 1000 hours at 2100°F .

(b) Equivalent to the notch-strength ratio (NSR) .

TABLE 7 - Notched-Unnotched Tensile Data for Longitudinal GTA Welds in 0.089 cm (0.035 inch) T-111 Sheet.

Test Condition (a)	Notched Specimens		Unnotched Specimens		NS (notched) (b)
	NS, 10^7 N/m^2	K_t	UTS, 10^7 N/m^2	% Elong.	UTS (unnotched)
As Welded	124.7	3.8	104.2	15.6	1.20
As Welded + Aged	100.9	4.2	92.8	11.0	1.09
1 Hr.-1205°C PWA	118.4	3.8	97.9	16.5	1.21
" " + Aged	97.4	4.2	89.4	5.4	1.09
1 Hr.-1316°C PWA	116.3	3.8	99.8	18.4	1.17
" " + Aged	101.1	4.2	89.0	2.4	1.14
1 Hr.-1427°C PWA	112.9	4.2	98.7	20.5	1.14
" " + Aged	102.8	4.6	88.9	4.4	1.16
1 Hr.-1538°C PWA	112.2	4.2	96.9	18.9	1.16
" " + Aged	91.0	4.2	90.2	8.4	1.01
1 Hr.-1649°C PWA	112.0	4.2	94.9	13.0	1.18
" " + Aged	98.0	4.6	88.1	1.3	1.11
1 Hr.-1760°C PWA	116.0	3.8	95.8	18.9	1.21
" " + Aged	104.4	4.2	92.0	12.5	1.13
1 Hr.-1871°C PWA	116.2	3.8	96.3	18.9	1.21
" " + Aged	98.9	4.6	90.2	9.0	1.10
1 Hr.-1982°C PWA	111.8	3.8	90.9	15.3	1.23
" " + Aged	100.6	4.2	87.6	6.3	1.15

All tests at -196°C using 0.0127 cm./minute crosshead travel speed.

(a) All aging was for 1000 hours at 1149°C.

(b) Equivalent to the notch-strength ratio (NSR).

TABLE 7a - Notched-Unnotched Tensile Data for Longitudinal GTA Welds in T-111 0.089 cm. (0.035 inch) Sheet

Test Condition [a]	Notched Specimens		Unnotched Specimens		NS(notched) / UTS(unnotched) [b]
	NS, ksi	K_t	UTS, ksi	% Elong.	
As Welded	188.1	3.9	161.3	0.0	1.17
As Welded + Aged	172.6	3.9	141.1	0.9	1.22
1 Hr.-2200°F PWA	158.7	3.9	147.7	2.3	1.07
" " + Aged	155.1	3.9	142.4	0.6	1.09
1 Hr.-2400°F PWA	169.7	3.9	152.5	1.0	1.11
" " + Aged	165.5	3.9	143.7	1.0	1.15
1 Hr.-2600°F PWA	161.5	3.9	156.0	1.1	1.04
" " + Aged	168.1	3.9	140.6	1.1	1.20
1 Hr.-2800°F PWA	172.4	3.9	152.8	1.0	1.13
" " + Aged	153.6	3.9	142.3	0.5	1.08
1 Hr.-3000°F PWA	(c)	3.9	155.7	10.7	----
" " + Aged	167.4	3.9	146.5	2.9	1.14
1 Hr.-3200°F PWA	174.9	3.9	150.4	7.2	1.16
" " + Aged	143.7	3.9	142.2	1.9	1.01
1 Hr.-3400°F PWA	181.8	3.9	157.7	12.9	1.15
" " + Aged	161.5	3.9	139.9	1.4	1.15
1 Hr.-3600°F PWA	182.8	3.9	159.2	4.4	1.19
" " + Aged	136.1	3.9	135.9	0.4	1.00

All tests at — 320°F using 0.005 inch/minute crosshead travel speed except the as-welded specimens which were accidentally tested at 0.5 inch/minute.

(a) All aging was for 1000 hours at 2100 F.

(b) Equivalent to the notch-strength ratio (NSR).

(c) Specimen broke on loading.

TABLE 8 - Notched-Unnotched Tensile Data for Longitudinal GTA Welds in 0.089 cm (0.035 inch) ASTAR-811C Sheet.

Test Condition [a]	Notched Specimens		Unnotched Specimens		NS (notched) [b] / UTS (unnotched)
	NS, 10^7 N/m^2	K_t	UTS, 10^7 N/m^2	% Elong.	
As Welded	130.0	3.9	111.2	0.0	1.17
As Welded + Aged	119.0	3.9	97.3	0.9	1.22
1 Hr.-1205°C PWA	109.4	3.9	101.8	2.3	1.07
" " + Aged	106.9	3.9	98.2	0.6	1.09
1 Hr.-1316°C PWA	117.0	3.9	105.1	1.0	1.11
" " + Aged	114.1	3.9	99.1	1.0	1.15
1 Hr.-1427°C PWA	111.4	3.9	107.6	1.1	1.04
" " + Aged	115.9	3.9	96.9	1.1	1.20
1 Hr.-1538°C PWA	118.9	3.9	105.4	1.0	1.13
" " + Aged	105.9	3.9	98.1	0.5	1.08
1 Hr.-1649°C PWA	(c)	3.9	107.4	10.7	----
" " + Aged	115.4	3.9	101.0	2.9	1.14
1 Hr.-1760°C PWA	120.6	3.9	103.7	7.2	1.16
" " + Aged	99.1	3.9	98.0	1.9	1.01
1 Hr.-1871°C PWA	125.4	3.9	108.7	12.9	1.15
" " + Aged	111.4	3.9	96.5	1.4	1.15
1 Hr.-1982°C PWA	130.2	3.9	109.8	4.4	1.19
" " + Aged	93.8	3.9	93.7	0.4	1.00

All tests at -196°C using 0.0127 cm./minute crosshead travel speed except the as-welded specimens which were accidentally tested at 1.27 cm./minute.

(a) All aging was for 1000 hours at 1149°C.

(b) Equivalent to the notch-strength ratio (NSR).

(c) Specimen broke on loading.

TABLE 8a - Notched-Unnotched Tensile Data for Longitudinal GTA Welds in ASTAR-811C 0.089 cm. (0.035 inch) Sheet

Test Condition[a]	Notched Specimens		Unnotched Specimens		NS(notched)[b] / UTS (unnotched)
	NS, ksi	K_t	UTS, ksi	% Elong.	
As Welded	129.9	4.2	131.4	3.5	0.99
1 Hr.-2200°F PWA	150.7	4.2	135.8	1.2	1.11
1 Hr.-2400°F PWA	155.9	4.2	136.5	2.6	1.14
1 Hr.-2600°F PWA	151.1	4.2	132.9	3.4	1.14
1 Hr.-2800°F PWA	153.7	4.6	133.5	0.4	1.15
1 Hr.-3000°F PWA	159.6	4.2	132.3	0.5	1.21
1 Hr.-3200°F PWA	140.3	4.2	129.5	1.8	1.08
1 Hr.-3400°F PWA	149.9	4.2	129.1	0.3	1.16
1 Hr.-3600°F PWA	150.6	4.2	144.7	0.2	1.04

All tests at -320°F using 0.5 in/min crosshead travel speed.

(a) All specimens aged 1000 hours at 2100°F prior to testing.

(b) Equivalent to the notch-strength ratio (NSR).

TABLE 9 - High Strain Rate Notched-Unnotched Tensile Data for Longitudinal GTA Welds in 0.089 cm (0.035 inch) T-111 Sheet.

Test Condition[a]	Notched Specimens		Unnotched Specimens		NS(notched)[b] / UTS(unnotched)
	NS, 10^7 N/m^2	K_t	UTS, 10^7 N/m^2	% Elong.	
As Welded	89.6	4.2	90.6	3.5	0.99
1 Hr.-1205°C PWA	103.9	4.2	93.6	1.2	1.11
1 Hr.-1316°C PWA	107.5	4.2	94.1	2.6	1.14
1 Hr.-1427°C PWA	104.2	4.2	91.6	3.4	1.14
1 Hr.-1538°C PWA	106.0	4.6	92.0	0.4	1.15
1 Hr.-1649°C PWA	110.0	4.2	91.2	0.5	1.21
1 Hr.-1760°C PWA	96.7	4.2	89.3	1.3	1.08
1 Hr.-1871°C PWA	103.4	4.2	89.0	0.3	1.16
1 Hr.-1982°C PWA	103.8	4.2	99.8	0.2	1.04

All tests at - 196°C using 1.27 cm/ minute crosshead travel speed.

(a) All specimens aged 1000 hours at 1149°C prior to testing.

(b) Equivalent to the notch-strength ratio (NSR) .

TABLE 9a - High Strain Rate Notched-Unnotched Tensile Data for Longitudinal GTA Welds in 0.089 cm (0.035 inch) T-111 Sheet.

Test Condition (a)	Notched Specimens		Unnotched Specimens		NS(notched) / UTS(unnotched) (b)
	NS, ksi	K_t	UTS, ksi	% Elong.	
As Welded	161.9	3.9	136.8	6.0	1.18
As Welded + Aged	113.6	3.9	102.6	16.2	1.11
1 Hr.-2200°F PWA	124.6	3.9	117.2	18.3	1.16
" " + Aged	115.5	3.9	106.2	16.7	1.09
1 Hr.-2400°F PWA	124.2	3.9	106.0	15.1	1.17
" " + Aged	120.5	3.9	105.3	18.9	1.14
1 Hr.-2600°F PWA	128.4	3.9	109.0	11.2	1.18
" " + Aged	118.8	3.9	104.0	7.9	1.14
1 Hr.-2800°F PWA	123.5	3.9	111.8	10.8	1.10
" " + Aged	111.6	3.9	103.0	17.4	1.08
1 Hr.-3000°F PWA	127.6	3.9	111.1	19.0	1.15
" " + Aged	117.8	3.9	103.4	21.2	1.14
1 Hr.-3200°F PWA	124.3	3.9	113.7	19.9	1.20
" " + Aged	116.6	3.9	98.2	16.8	1.18
1 Hr.-3400°F PWA	131.4	3.9	110.4	11.8	1.19
" " + Aged	114.0	3.9	102.8	14.7	1.11
1 Hr.-3600°F PWA	134.5	3.9	110.3	16.2	1.22
" " + Aged	109.4	3.9	102.3	11.0	1.07

All tests at — 50°F using 0.005 inch/minute crosshead travel speed.

(a) All aging was for 1000 hours at 2100°F.

(b) Equivalent to the notch-strength ratio (NSR).

TABLE 10 - Notched-Unnotched Tensile Data for Longitudinal GTA Welds in 0.089 cm (0.035 inch) ASTAR-811C Sheet. All Tests at - 46°C (- 50°F).

Test Condition (a)	Notched Specimens		Unnotched Specimens		NS (notched) (b) / UTS (unnotched)
	NS, 10^7 N/m^2	K_t	UTS, 10^7 N/m^2	% Elong.	
As Welded	111.6	3.9	94.3	6.0	1.18
As Welded + Aged	78.3	3.9	70.7	16.2	1.11
1 Hr.-1205°C PWA	85.9	3.9	80.8	18.3	1.16
" " + Aged	79.6	3.9	73.2	16.7	1.09
1 Hr.-1316°C PWA	85.6	3.9	73.1	15.1	1.17
" " + Aged	83.1	3.9	72.6	18.9	1.14
1 Hr.-1427°C PWA	88.5	3.9	75.2	11.2	1.18
" " + Aged	81.9	3.9	71.7	7.9	1.14
1 Hr.-1538°C PWA	85.2	3.9	77.1	10.8	1.10
" " + Aged	76.9	3.9	71.0	17.4	1.08
1 Hr.-1649°C PWA	88.0	3.9	76.6	19.0	1.15
" " + Aged	81.2	3.9	71.3	21.2	1.14
1 Hr.-1760°C PWA	85.7	3.9	78.4	19.9	1.20
" " + Aged	80.4	3.9	67.7	16.8	1.18
1 Hr.-1871°C PWA	90.6	3.9	76.1	11.8	1.19
" " + Aged	78.6	3.9	70.9	14.7	1.11
1 Hr.-1982°C PWA	92.7	3.9	76.0	16.2	1.22
" " + Aged	75.4	3.9	70.5	11.0	1.07

All tests at -46°C using 0.0127 cm./minute crosshead travel speed.

(a) All aging was for 1000 hours at 1149°C.

(b) Equivalent to the notch-strength ratio (NSR).

TABLE 10a - Notched-Unnotched Tensile Data for Longitudinal GTA Welds in 0.089 cm. (0.035 inch) ASTAR-811 Sheet. All tests at -46°C (-50°F).

Alloy	Notch-strength-ratio		Unnotched Tensile Elongation	
	Aged	Unaged	Aged	Unaged
T-111	1.01 - 1.16	1.14 - 1.23	2 - 14%	13 - 20%
ASTAR-811C	1.00 - 1.22	1.04 - 1.19	0.4 - 3%	0 - 13%

For both alloys the tensile strength decreased following aging at 1149°C (2100°F). Notched specimens failed at the notches in all cases. A significant decrease in the tensile elongation of the unaged weld specimens resulted from the aging. Despite this fact the notch-strength-ratio values were relatively unchanged for either alloy after aging. Values of the notch-strength-ratio of T-111 welds agree well with the 1.15 value found by Ammon and Begley using notched tensile tests on base metal of the original development heats of T-111[7]. Estimates of the reduction in area of the notched and unnotched specimens are virtually impossible due to the very coarse, oriented grain structure of the GTA weld specimens.

The only significant variation in behavior between T-111 and ASTAR-811C welds was the fracture mode. Fractures in T-111 appear to have been the result of shear processes. Unaged T-111 welds invariably failed by transgranular shear while in aged specimens intergranular shear was more prominent. Fractures in ASTAR-811C welds were predominantly cleavage-type in appearance. Interestingly, the higher elongation specimens, tested at -46°C (-50°F) (Table 10), displayed transgranular shear as the dominant failure mode.

An obvious and important conclusion can be inferred from these results. Despite the varied post-weld thermal exposures, some of which produced significant microstructural changes, T-111 and ASTAR-811C demonstrate a remarkable resistance to notch sensitivity to temperatures at least as low as -196°C (-320°F). Details of the microstructural responses observed will be deferred to a later section of this report. It is particularly worthwhile to note that despite quite low tensile elongations of several of the ASTAR-811C welds the notch-strength-ratios were still greater than unity. Hence, even at temperatures where relatively little tensile ductility is retained the alloy is not notch sensitive.

Several aspects of the test data make a completely tractable explanation or discussion of the results somewhat difficult. The bulk of our knowledge regarding the loss of ductility in body-centered-cubic metals at low temperatures has been derived from efforts to understand the factors responsible for brittle fracture. The "non-brittle" failures , particularly those of T-111, do not lend themselves to direct application of this knowledge. General consideration of some of these factors does, however, allow certain observations and conclusions to be made.

The occurrence of cleavage as the primary fracture mode is not an immutable feature of the crystalline lattice. Three basic factors known to contribute to or promote the occurrence of brittle cleavage-type fractures [8]. They are :

i - a triaxial state of stress
ii - low test temperatures
iii - a high strain (or loading) rate

All three factors need not be present simultaneously to produce brittle fracture. Brittle fractures in service are most often induced by a combination of (i) and (ii). The presence of a notch results in multiaxial stresses (more probably biaxial than triaxial for the sheet specimens employed in this study) and steep stress gradients ; hence, notched tensile tests are widely used to determine whether or not a material is notch-sensitive and thereby likely to be prone to brittle failure. For commonality or convenience the condition when the notch-strength-ratio becomes less than unity is taken to be the point at which the material becomes notch sensitive.

Our knowledge of brittle failure in metals establishes reasonably well that Griffith-type flaws (i.e. of a pre-existing nature) are not the source of cleavage cracks, except possibly where the grain boundaries are extremely weak. Equally well established is the fact even extremely brittle metals exhibit some measure of slip or twinning prior to fracture. Both of these observations enforce a Zener-type model based on the pileup of dislocations as providing the stress concentrations necessary for the initiation and propagation of cleavage. Detailed consideration of the atomistics of the various models and their refinements are not germane to this discussion and will not be pursued further. The interested reader is referred to the recent

review by Rosenfield, et al [9]. Of the consequences of the dislocation pileup model for the initiation and propagation of cleavage, one important feature is the prediction that the critical stress required is inversely proportional to the average grain diameter. This effect appears related to the mean free slip length. Hence, large grain size , implying large uninterrupted slip distances, would be expected to lead to relatively low values for the cleavage stress and greater probability for crack nucleation. Hence, in this respect welds represent a more severe test condition per se than base metal.

The concept of transition temperature and the utilization of this concept depend critically on the criteria by which one measures or defines ductility. The notch toughness of a material should really be considered in terms of two distinct transition temperatures [8,10]. These are :

Ductility Transition Temperature (DTT) - normally defined for notch tensile tests as the temperature at which the reduction in area decreases to one-half its typical or maximum value, and,

Fracture Appearance Transition Temperature (FATT) - the temperature at which the mode of failure changes from predominant separation along shear planes to predominant cleavage.

Dieter [8] points out the DTT is related to the fracture-initiation tendencies of the material while the FATT is more intimately related to its fracture-propagation characteristics. (While these comments relate primarily to fractures during notch-impact testing, since the cleavage stress is only weakly dependent on strain rate they should apply equally well to any other test involving notch-fracture relationships.) In the region between the DTT and the FATT fractures may be difficult to initiate but once initiated are expected to propagate easily.

In terms of the above definitions it appears we can say with a reasonable degree of certainty that both the fracture appearance- and ductility-transition temperatures of GTA welds in T-111 sheet are well below -196°C (-320°F). Further, the data strongly suggests the fracture appearance transition temperature of GTA sheet welds in ASTAR-811C is well above -196°C (-320°F) but the ductility transition temperature is probably below that temperature. -46°C (-50°F) is clearly above both transition temperatures for ASTAR-811C welds. In fairness

to the ASTAR-811C results it should be pointed out that the ductility transition temperature is usually more pertinent to service performance, because if it is difficult to initiate a crack, then it becomes rather unnecessary to worry about its propagation[8].

Simply stated in summary, no notch sensitivity has been found in as-welded post-weld annealed, or aged GTA welds in T-111 or ASTAR-811C sheet at temperatures as low as -196°C (-320°F).

4.2.2 High Temperature Tensile Evaluation

The results of the room temperature and elevated temperature tensile tests on sheet weld specimens of T-111 and ASTAR-811C are presented in tabular form in Tables 11 and 12, respectively. The stress-strain curves revealed yield point effects in the unaged T-111 welds tested at room temperature and 538°C (1000°F) as well as displaying Portevin-LeChatelier discontinuous yielding at 982°C (1800°F). Yield point effects were not detected for unaged ASTAR-811C weld specimens but discontinuous yielding was observed in the 982°C (1800°F) tests. With regard to the thermal exposure variables, post-weld annealing and aging, the data of Tables 11 and 12 can be summarized as follows:

Post-weld Annealing Effects

- Post-weld annealing lowered the room temperature and 538°C (1000°F) tensile strength of unaged T-111 and ASTAR-811C. This may be due to a reduction of the carbon supersaturation in the rapidly cooled sheet welds. The effect is much more pronounced in the higher-carbon ASTAR-811C than in T-111.
- The effects noted are independent of the particular post-weld annealing temperature employed.
- There appears to be no effect on either the uniform or total elongation values of either alloy.
- No influence was noted on the fracture mode of either alloy. This varied only as a function of test temperature and is discussed separately in a later section.
- Microstructural effects, per se, are discussed separately in a later section of this report.

Test Condition	Test Temp.(°F)	UTS, ksi		0.2% Y.S., ksi		% Unif. Elongation		% Total Elongation	
		Unaged	Aged	Unaged	Aged	Unaged	Aged	Unaged	Aged
As Welded	R.T.	93.9	83.8	74.3	73.1*	12.4	18.4	24.8	24.9
	1000	58.4	55.8	37.3	39.3	14.2	16.6	24.3	23.2
	1800	58.6	53.2	35.8	32.6	11.3	13.6	16.9	19.7
	2100	49.4	44.0	33.9	31.1	6.2	9.2	10.2	13.6
	2400	35.3	34.4	26.9	26.4	5.6	3.4	7.6	5.9
	2600	29.2	29.5	25.9	23.8	2.9	3.1	5.6	4.1
1 Hr.-2200°F PWA	R.T.	88.4	85.8	75.8*	74.0*	12.9	19.3	22.8	27.4
	1000	57.0	55.0	43.9	39.3	14.0	16.8	21.6	22.2
	1800	57.8	52.8	37.8	32.2	12.4	14.7	17.2	17.6
	2100	45.5	42.4	33.0	29.1	6.3	7.4	9.3	9.5
	2400	34.2	36.2	26.8	29.0	4.1	3.8	7.2	6.3
	2600	28.4	30.1	23.0	23.9	2.5	3.4	5.1	4.5
1 Hr.-2400°F PWA	R.T.	87.9	86.2	76.4*	74.3*	12.8	15.2	22.9	22.4
	1000	61.0	54.8	52.9*	38.3	15.1	15.3	25.8	22.7
	1800	55.5	53.2	33.1	32.3	15.4	13.6	21.6	18.6
	2100	48.5	43.9	32.3	30.5	13.1	7.9	15.8	11.2
	2400	35.1	36.3	28.6	27.6	4.0	4.0	6.5	[illegible]
	2600	28.8	29.8	24.8	25.0	2.6	2.8	4.8	5.2
1 Hr.-2600°F PWA	R.T.	88.8	86.5	76.9*	74.1*	13.6	18.4	23.3	26.0
	1000	56.4	54.2	43.3*	38.7	20.6	14.4	26.1	21.8
	1800	57.9	53.2	33.0	32.7	16.3	14.2	21.2	16.6
	2100	47.9	44.6	31.6	30.0	13.5	9.9	20.6	13.0
	2400	35.4	33.8	27.7	27.1	4.5	4.3	7.6	5.8
	2600	27.6	30.0	22.7	25.1	3.0	2.8	5.1	4.1
1 Hr.-2800°F PWA	R.T.	88.3	85.5	73.3*	73.4*	14.8	17.1	25.4	24.7
	1000	58.9	57.0	46.9*	39.3*	20.4	19.2	29.8	26.2
	1800	57.4	51.8	32.8	30.6	15.8	13.0	21.6	15.9
	2100	46.9	41.8	29.2	28.8	13.2	9.0	18.2	10.6
	2400	32.4	36.0	27.3	27.8	5.1	5.0	8.2	5.8
	2600	27.9	28.0	22.4	24.0	3.3	2.7	5.6	4.2

All aging was 1000 hrs. - 2100°F at $< 10^{-8}$ torr pressure.

* Upper yield stress

0.05 min^{-1} strain rate used throughout all elevated temperature tests. Room temperature tests conducted at 0.005 min^{-1} to 0.6% strain, then 0.05 min^{-1} to fracture.

TABLE 11 - Tensile Test Data for Longitudinal GTA Welds in 0.089 cm (0.035 inch) T-111 Sheet in the Aged and Unaged Conditions.

Test Condition	Test Temp.(°F)	UTS, ksi		0.2% Y.S., ksi		% Unif. Elong.		% Total Elong.	
		Unaged	Aged	Unaged	Aged	Unaged	Aged	Unaged	Aged
1 Hr.-3000°F PWA	R.T.	85.8	85.5	72.1*	70.2	13.8	15.5	21.1	22.8
	1000	54.8	55.5	42.1	38.1	19.5	17.2	28.1	22.0
	1800	57.7	52.4	32.2	31.1	14.7	13.4	22.4	17.4
	2100	47.2	42.1	29.4	29.2	13.6	8.5	17.5	11.1
	2400	33.9	34.3	25.2	27.8	4.9	3.7	7.2	5.3
	2600	26.9	28.8	22.3	24.6	3.4	4.1	6.1	5.8
1 Hr.-3200°F PWA	R.T.	85.1	83.9	70.7*	73.5*	13.8	15.6	22.4	21.0
	1000	58.2	57.0	43.0	41.0*	16.7	19.4	24.8	25.3
	1800	55.9	53.0	30.4	30.4	13.6	15.9	17.6	20.1
	2100	45.1	43.3	26.8	28.5	11.3	10.2	16.0	13.5
	2400	34.2	34.1	24.8	27.5	6.0	3.6	9.1	4.8
	2600	26.7	27.3	21.5	21.7	3.3	3.7	5.4	6.3
1 Hr.-3400°F	R.T.	83.5	85.0	69.8*	72.8*	12.5	18.7	19.6	26.8
	1000	57.5	55.6	42.4	38.3*	18.4	19.8	30.5	24.4
	1800	52.1	52.1	27.8	29.8	15.1	16.6	22.7	20.6
	2100	45.8	40.8	27.0	27.4	10.4	9.2	14.6	12.0
	2400	33.9	34.1	24.9	26.2	6.5	3.8	8.6	5.6
	2600	28.4	27.9	21.8	22.0	4.8	4.1	7.2	5.5
1 Hr.-3600°F PWA	R.T.	80.2	82.6	69.3*	71.7*	13.6	17.8	20.6	23.2
	1000	51.4	55.0	36.5	37.5*	17.8	19.0	25.1	28.4
	1800	53.0	46.4	28.7	26.5	16.8	12.1	22.0	17.2
	2100	43.0	42.7	26.1	26.7	8.4	8.6	12.8	11.6
	2400	34.3	34.6	25.0	26.0	6.0	4.4	8.9	5.3
	2600	28.5	28.5	22.9	21.6	3.7	3.4	5.1	5.6

All aging was 1000 hours - 2100°F at $< 10^{-8}$ torr pressure.

* Upper yield stress

0.05 min^{-1} strain rate used throughout all elevated temperature tests. Room temperature tests conducted at 0.005 min^{-1} to 0.6% strain, then 0.05 min^{-1} through fracture.

TABLE 11(Cont.) - Tensile Test Data for Longitudinal GTA Welds in 0.089 cm (0.035 inch) T-111 Sheet in the Aged and Unaged Conditions.

Test Condition	Test Temp.(°C)	UTS, 10^7 N/m^2		0.2% Y.S., 10^7 N/m^2		% Unif. Elong.		% Total Elong.	
		Unaged	Aged	Unaged	Aged	Unaged	Aged	Unaged	Aged
As Welded	R.T.	64.7	57.8	51.2	50.4*	12.4	18.[illegible]	24.8	24.9
	538	40.3	38.5	25.7	27.1	14.2	16.6	24.3	23.2
	982	40.4	36.7	24.7	22.5	11.3	13.6	16.9	19.7
	1149	34.1	30.3	23.4	21.4	6.2	9.2	10.2	13.6
	1316	24.3	23.7	18.5	18.2	5.6	3.4	7.6	5.9
	1427	20.1	20.3	17.8	16.4	2.9	3.1	5.6	4.1
1 Hr.-1205°C PWA	R.T.	61.0	59.2	52.3*	51.0*	12.9	19.3	22.8	27.4
	538	39.3	37.9	30.3	27.1	14.0	16.8	21.6	22.2
	982	39.8	36.4	26.1	22.2	12.4	14.7	17.2	17.6
	1149	31.4	29.2	22.8	20.1	6.3	7.4	9.3	9.5
	1316	23.6	24.9	18.5	20.0	4.1	3.8	7.2	6.3
	1427	19.6	20.8	15.8	16.5	2.5	3.4	5.1	4.5
1 Hr.-1316°C PWA	R.T.	60.6	59.4	52.7*	51.2*	12.8	15.2	22.9	22.4
	538	42.1	37.8	36.5*	26.4	15.1	15.3	25.8	22.7
	982	38.3	36.7	22.8	22.3	15.4	13.6	21.6	18.6
	1149	33.4	30.3	22.3	21.0	13.1	7.9	15.8	11.2
	1316	24.2	25.0	19.7	19.0	4.0	4.0	6.5	6.2
	1427	19.8	20.5	17.1	17.2	2.6	2.8	4.8	5.2
1 Hr.-1427°C PWA	R.T.	61.2	59.6	53.0*	51.1*	13.6	18.4	23.3	26.0
	538	38.9	37.4	29.8*	26.7	20.6	14.4	26.1	21.8
	982	39.9	36.7	22.8	22.5	16.3	14.2	21.2	16.6
	1149	33.0	30.8	21.8	20.7	13.5	9.9	20.6	13.0
	1316	24.4	23.3	19.1	18.7	4.5	4.3	7.6	5.8
	1427	19.0	20.7	15.6	17.3	3.0	2.8	5.1	4.1
1 Hr.-1538°C PWA	R.T.	60.9	59.0	50.5*	50.6*	14.8	17.1	25.4	24.7
	538	40.6	39.3	32.3*	27.1*	20.4	19.2	29.8	26.2
	982	39.6	35.7	22.6	21.1	15.8	13.0	21.6	15.9
	1149	32.3	28.8	20.1	19.8	13.2	9.0	18.2	10.6
	1316	22.3	24.8	18.8	19.2	5.1	5.0	8.2	5.8
	1427	19.2	19.3	15.4	16.5	3.3	2.7	5.6	4.2

All aging was 1000 hrs. 1149°C at < 2.33×10^{-6} N/m^2 pressure.

*Upper yield stress

0.05 min^{-1} strain rate used throughout all elevated temperature tests. Room temperature tests conducted at 0.005 min^{-1} to 0.6% strain, then 0.05 min^{-1} to fracture.

TABLE 11a - Tensile Test Data for Longitudinal GTA Welds in 0.089 cm. (0.035 inch) T-111 Sheet in the Aged and Unaged Conditions.

Test Condition	Test Temp.(°C)	UTS, 10^7 N/m^2		0.2% Y.S., 10^7 N/m^2		% Unif. Elong.		% Total Elong.	
		Unaged	Aged	Unaged	Aged	Unaged	Aged	Unaged	Aged
1 Hr.-1649°C PWA	R.T.	59.2	59.0	49.7*	48.4	13.8	15.5	21.1	22.8
	538	37.8	38.3	29.0	26.3	19.5	17.2	28.1	22.0
	982	39.8	36.1	22.2	21.4	14.7	13.4	22.4	17.4
	1149	32.5	29.0	20.3	20.1	13.6	8.5	17.5	11.1
	1316	23.4	23.6	17.4	19.2	4.9	3.7	7.2	5.3
	1427	18.5	19.8	15.4	16.5	3.4	3.1	6.1	5.8
1 Hr.-1760°C PWA	R.T.	58.7	57.8	48.7*	50.7*	13.8	15.6	22.4	21.0
	538	40.1	39.3	29.6	28.3*	16.7	19.4	24.8	25.3
	982	38.5	36.5	21.0	21.0	13.6	15.9	17.0	20.1
	1149	31.1	29.9	18.5	19.7	11.3	10.2	16.0	13.5
	1316	23.6	23.5	17.1	19.0	6.0	3.6	9.1	4.8
	1427	18.4	18.8	14.8	15.0	3.3	3.7	5.4	6.3
1 Hr.-1871°C	R.T.	57.6	58.6	48.1*	50.2*	12.5	18.7	19.6	26.8
	538	39.6	38.3	29.2	26.4*	18.4	19.8	30.5	24.4
	982	35.9	35.9	19.2	20.5	15.1	16.6	22.7	20.6
	1149	31.6	28.1	18.6	18.9	10.4	9.2	14.6	12.0
	1316	23.4	23.5	17.2	18.1	6.5	3.8	8.6	5.6
	1427	19.6	19.2	15.0	15.2	4.8	4.1	7.2	5.5
1 Hr.-1982°C PWA	R.T.	55.3	57.0	47.8*	49.4*	13.6	17.8	20.6	23.2
	538	35.4	37.9	25.2	27.2*	15.8	19.0	25.1	28.4
	982	36.5	32.0	19.8	18.3	16.8	12.1	22.0	17.2
	1149	29.6	29.4	18.0	18.4	8.4	8.6	12.8	11.6
	1316	23.6	23.8	17.2	17.9	6.0	4.4	8.9	5.3
	1427	19.6	19.6	15.8	14.9	3.7	3.4	5.1	5.6

All aging was 1000 hours - 1149°C at $< 2.33 \times 10^{-6}$ N/m^2 pressure.

*Upper yield stress

0.05 min^{-1} strain rate used throughout all elevated temperature tests. Room temperature tests conducted at 0.005 min^{-1} to 0.6% strain, then 0.05 min^{-1} through fracture.

TABLE 11a (Cont.) - Tensile Test Data for Longitudinal GTA Welds in 0.089 cm. (0.035 inch) T-111 Sheet in the Aged and Unaged Conditions.

Test Condition	Test Temp.(°F)	UTS, ksi		0.2% Y.S., ksi		% Unif. Elong.		%Total Elong.	
		Unaged	Aged	Unaged	Aged	Unaged	Aged	Unaged	Aged
As Welded	R.T.	126.0	102.1	110.6	82.9	12.2	13.7	14.8	16.4
	1000	118.0	62.3	78.7	43.2	11.1	14.5	14.6	19.5
	1800	77.9	57.6	43.7	37.5	13.4	12.2	16.1	15.1
	2100	67.5	50.0	49.9	36.1	13.3	13.7	16.5	23.6
	2400	47.4	43.2	34.5	35.5	7.4	8.6	19.2	21.7
	2600	41.8	37.6	33.7	33.2	5.8	4.2	17.1	9.0
1 Hr.-2200°F PWA	R.T.	105.0	101.8	84.1	83.7	15.6	14.9	21.2	15.3
	1000	70.4	63.4	43.2	43.2	12.8	17.0	13.7	21.1
	1800	74.6	57.5	42.0	37.8	14.9	12.0	17.6	15.1
	2100	60.1	50.3	36.7	36.4	12.8	11.9	15.6	19.5
	2400	47.0	43.0	34.1	35.2	9.2	7.5	24.3	18.2
	2600	39.4	38.2	34.9	31.9	6.1	4.0	11.5	6.6
1 Hr.-2400°F PWA	R.T.	105.0	102.3	85.8	82.3	14.5	14.4	18.8	18.9
	1000	72.2	64.9	45.7	43.2	10.6	15.9	14.4	22.0
	1800	74.7	58.6	38.2	37.1	13.8	15.0	15.2	17.8
	2100	58.1	51.5	38.5	36.8	12.3	12.8	15.5	18.6
	2400	45.0	43.9	35.0	35.1	8.3	7.8	19.7	17.2
	2600	39.0	38.7	33.1	33.4	6.7	5.2	14.0	11.6
1 Hr.-2600°F PWA	R.T.	103.4	98.6	87.7	81.1	7.9	8.6	11.4	8.6
	1000	71.4	63.5	47.5	43.8	9.7	16.2	13.0	19.5
	1800	74.9	58.4	38.1	36.8	14.3	13.2	18.3	16.8
	2100	62.4	50.7	39.4	35.0	13.1	11.4	16.8	21.2
	2400	45.6	42.4	34.1	33.3	9.3	8.2	21.0	18.8
	2600	39.0	38.2	32.0	33.3	6.2	5.3	11.5	11.4
1 Hr.-2800°F PWA	R.T.	108.9	100.1	86.9	81.1	12.3	15.7	17.0	19.4
	1000	70.7	63.0	45.3	43.0	10.9	17.1	16.4	22.1
	1800	74.7	58.9	40.0	36.3	15.1	15.1	18.7	19.3
	2100	62.1	49.4	35.7	34.9	12.7	11.9	14.6	19.9
	2400	52.8	42.0	34.4	32.4	9.8	8.8	19.3	18.2
	2600	38.0	38.4	31.5	34.0	7.8	5.0	15.9	13.5

All aging was 1000 hours - 2100°F at $< 10^{-8}$ torr pressure.

0.05 min^{-1} strain rate used throughout all elevated temperature tests. Room temperature tests conducted at 0.005 min^{-1} to 0.6% strain, then 0.05 min^{-1} to fracture.

TABLE 12 - Tensile Test Data for Longitudinal GTA Welds in 0.089 cm (0.035 in.) ASTAR-811C Sheet in the Aged and Unaged Conditions.

Test Condition	Test Temp.(°F)	UTS , ksi		0.2% Y.S. , ksi		% Unif. Elong.		% Total Elong.	
		Unaged	Aged	Unaged	Aged	Unaged	Aged	Unaged	Aged
1 Hr.-3000°F PWA	R.T.	105.5	99.9	79.2	81.4	13.9	15.9	18.4	22.6
	1000	73.9	62.3	42.7	40.0	10.4	16.1	14.6	21.9
	1800	73.1	58.7	38.1	36.2	13.7	15.7	16.6	18.2
	2100	65.0	50.4	38.5	35.5	12.6	13.5	17.8	19.0
	2400	47.2	43.0	33.4	34.0	11.2	10.5	21.8	19.0
	2600	41.7	38.5	33.4	33.9	7.8	5.4	20.0	17.1
1 Hr.-3200°F PWA	R.T.	109.0	99.3	81.9	81.1	14.6	13.6	18.6	13.6
	1000	67.9	62.8	39.9	42.3	9.5	17.0	12.3	21.2
	1800	74.2	57.9	38.6	35.1	14.2	15.2	16.6	17.4
	2100	64.3	50.2	35.9	34.9	13.2	14.7	17.3	21.0
	2400	47.9	42.1	35.6	32.4	9.9	9.7	21.8	24.2
	2600	41.4	37.9	34.9	33.1	5.9	5.2	13.9	19.9
1 Hr.-3400°F PWA	R.T.	107.9	99.3	82.7	80.8	13.8	15.9	19.1	19.6
	1000	70.1	61.1	41.0	41.6	10.8	16.4	13.6	18.2
	1800	73.9	57.6	38.2	34.7	13.8	15.4	16.1	19.1
	2100	62.8	49.4	36.8	32.9	14.1	16.0	16.0	23.7
	2400	45.4	42.1	32.7	32.9	10.8	9.9	18.0	22.8
	2600	40.5	37.6	34.7	31.7	7.2	7.9	15.3	21.5
1 Hr.-3600°F PWA	R.T.	105.3	94.3	82.0	79.6	13.6	7.7	19.7	7.9
	1000	71.0	59.4	42.4	38.4	9.1	14.6	12.6	17.8
	1800	70.1	56.7	36.2	32.9	13.4	14.8	14.0	17.2
	2100	62.9	49.3	36.1	34.3	12.8	14.7	15.3	18.3
	2400	46.1	40.6	32.8	31.1	10.6	9.4	17.6	21.1
	2600	38.2	36.6	32.0	31.1	6.7	5.9	15.8	19.5

All aging was 1000 hours - 2100°F at $< 10^{-8}$ torr pressure.

0.05 min^{-1} strain rate used throughout all elevated temperature tests. Room temperature tests conducted at 0.005 min^{-1} to 0.6% strain, then 0.05 min^{-1} to fracture.

TABLE 12 (Cont.) - Tensile Test Data for Longitudinal GTA Welds in 0.089 cm (0.035 inch) ASTAR-811C Sheet in the Aged and Unaged Conditions.

Test Condition	Test Temp.(°C)	UTS, 10^7 N/m^2		0.2% Y.S., 10^7 N/m^2		% Unif. Elong.		% Total Elong.	
		Unaged	Aged	Unaged	Aged	Unaged	Aged	Unaged	Aged
As Welded	R.T.	86.9	70.4	76.2	57.2	12.2	13.7	14.8	16.4
	538	81.4	43.0	54.3	29.8	11.1	14.5	14.6	19.5
	982	53.7	39.7	30.1	25.9	13.4	12.2	16.1	15.1
	1149	46.5	34.5	34.4	24.9	13.3	13.7	16.5	23.6
	1316	32.7	29.8	23.8	24.5	7.4	8.6	19.2	21.7
	1427	28.8	25.9	23.2	22.9	5.8	4.2	17.1	9.0
1 Hr.-1205°C PWA	R.T.	72.4	70.2	58.0	57.7	15.6	14.9	21.2	15.3
	538	48.5	43.7	29.8	29.8	12.8	17.0	13.7	21.1
	982	51.4	39.6	29.0	26.1	14.9	12.0	17.6	15.1
	1149	41.4	34.7	25.3	25.1	12.8	11.9	15.6	19.5
	1316	32.4	29.6	23.5	24.3	9.2	7.5	24.3	18.2
	1427	27.2	26.3	24.1	22.0	6.1	4.0	11.5	6.6
1 Hr.-1316°C PWA	R.T.	72.4	70.5	59.2	56.7	14.5	14.4	18.8	18.9
	538	49.8	44.7	31.5	29.8	10.6	15.9	14.4	22.0
	982	51.5	40.4	26.3	25.6	13.8	15.0	15.2	17.8
	1149	40.1	35.5	26.5	25.4	12.3	12.8	15.5	18.6
	1316	31.0	30.3	24.1	24.2	8.3	7.8	19.7	17.2
	1427	26.9	26.7	22.8	23.0	6.7	5.2	14.0	11.6
1 Hr.-1427°C PWA	R.T.	71.3	68.0	60.5	55.9	7.9	8.6	11.4	8.6
	538	49.2	43.8	32.8	30.2	9.7	16.2	13.0	19.5
	982	51.6	40.3	26.3	25.4	14.3	13.2	18.3	16.8
	1149	43.0	35.0	27.2	24.1	13.1	11.4	16.8	21.2
	1316	31.4	29.2	23.5	23.0	9.3	8.2	21.0	18.8
	1427	26.9	26.3	22.9	23.0	6.2	5.3	11.5	11.4
1 Hr.-1538°C PWA	R.T.	75.1	69.0	59.9	55.9	12.3	15.7	17.0	19.4
	538	48.7	43.4	31.2	29.6	10.9	17.1	16.4	22.1
	982	51.5	40.6	27.6	25.0	15.1	15.1	18.7	19.3
	1149	42.8	34.1	24.6	24.1	12.7	11.9	14.6	19.9
	1316	36.4	29.0	23.7	22.3	9.8	8.8	19.3	18.2
	1427	26.2	26.5	21.7	23.4	7.8	5.0	15.9	13.5

All aging was 1000 hours - 1149°C at $< 2.33 \times 10^{-6}$ N/m^2 pressure.

0.05 min^{-1} strain rate used throughout all elevated temperature tests. Room temperature tests conducted at 0.005 min^{-1} to 0.6% strain, then 0.05 min^{-1} to fracture.

TABLE 12a - Tensile Test Data for Longitudinal GTA Welds in 0.089 cm. (0.035 inch) ASTAR-811C in the Aged and Unaged Conditions.

Test Condition	Test Temp.(°C)	UTS, 10^7 N/m^2		0.2% Y.S., 10^7 N/m^2		% Unif. Elong.		% Total Elong.	
		Unaged	Aged	Unaged	Aged	Unaged	Aged	Unaged	Aged
1 Hr.-1649°C PWA	R.T.	72.7	68.9	54.6	56.1	13.9	15.9	18.4	22.6
	538	51.0	43.0	29.4	27.6	10.4	16.1	14.6	21.9
	982	50.4	40.5	26.3	25.0	13.7	15.7	16.6	18.2
	1149	44.8	34.8	26.5	24.5	12.6	13.5	17.8	19.0
	1316	32.5	29.6	23.0	23.4	11.2	10.5	21.8	19.0
	1427	28.8	26.5	23.0	23.4	7.8	5.4	20.0	17.1
1 Hr.-1760°C PWA	R.T.	75.2	68.5	56.5	55.9	14.6	13.6	18.6	13.6
	538	46.8	43.3	27.5	29.2	9.5	17.0	12.3	21.2
	982	51.2	39.9	26.6	24.2	14.2	15.2	16.6	17.4
	1149	44.3	34.6	24.8	24.1	13.2	14.7	17.3	21.0
	1316	33.0	29.0	24.5	22.3	9.9	9.7	21.8	24.2
	1427	28.5	26.1	24.1	22.8	5.9	5.2	13.9	19.9
1 Hr.-1871°C PWA	R.T.	74.4	68.5	57.0	55.7	13.8	15.9	19.1	19.6
	538	48.3	42.1	28.3	28.7	10.8	16.4	13.6	18.2
	982	51.0	39.7	26.3	23.9	13.8	15.4	16.1	19.1
	1149	43.3	34.1	25.4	22.7	14.1	16.0	16.0	23.7
	1316	31.3	29.0	22.5	22.7	10.8	9.9	18.0	22.8
	1427	27.9	25.9	23.9	21.9	7.2	7.9	15.3	21.5
1 Hr.-1982°C PWA	R.T.	72.6	65.0	56.5	54.9	13.6	7.7	19.7	7.9
	538	49.0	41.0	29.2	26.5	9.1	14.6	12.6	17.8
	982	48.3	39.1	25.0	22.7	13.4	14.8	14.0	17.2
	1149	43.4	34.0	24.9	23.6	12.8	14.7	15.3	18.3
	1316	31.8	28.0	22.6	21.4	10.6	9.4	17.6	21.1
	1427	26.3	25.2	22.1	21.4	6.7	5.9	15.8	19.5

All aging was 1000 hours - 1149°C at < 2.33×10^{-6} N/m^2 pressure.

0.05 min^{-1} strain rate used throughout all elevated temperature tests. Room temperature tests conducted at 0.005 min^{-1} to 0.6% strain, then 0.05 min^{-1} to fracture.

TABLE 12a (Cont.) - Tensile Test Data for Longitudinal GTA Welds in 0.089 cm. (0.035 inch) ASTAR-811C Sheet in the Aged and Unaged Conditions.

Aging Effects (1000 Hours at 1149°C (2100°F))

- Aging eliminated the strain aging effects (i.e. discontinuous yielding) noted in the stress-strain curves of the unaged specimens.
- A slight improvement was seen in the tensile elongation values for test temperatures to 982°C (1800°F).
- Aging had no significant effect on the fracture mode of either alloy.
- Aging had essentially no effect on the tensile strength properties of T-111 or on the yield strength of ASTAR-811C. However, a significant decrease was observed in the ultimate tensile strength of the aged ASTAR-811C.
- As for the post-weld annealing effects, details of the microstructural response to aging will be deferred to a later section of this report.

The different response of the tensile strength of T-111 and ASTAR-811C to aging is seen by comparison of Figures 13 and 14 where the tensile strength of aged and unaged welds is plotted as a function of test temperature. The data of Figures 13 and 14 are for tests on welds given a 1 hour 1649°C (3000°F) post-weld anneal. This condition was selected arbitrarily; reference to Table 12 indicates any condition except as-welded could be used equally well. The variation noted in the ultimate tensile strength behavior of the aged and unaged ASTAR-811C welds is apparently due to a difference in the apparent work-hardening rate. Figure 15 shows typical engineering stress-strain curves of ASTAR-811C weld specimens for the various thermal exposure conditions. A notable decrease in the flow (yield) stress is seen to occur on post-weld annealing. However, no further decrease occurs on aging at 1149°C (2100°F). The apparent work-hardening rate is quite similar after aging to that of the as-welded condition while for the post-weld annealed but unaged condition it is somewhat greater.

The exact nature of the strengthening mechanisms operative in ASTAR-811C are not known. Nevertheless the experimental observations outlined above can be understood in terms of the following sequence of events.

1. During the very rapid cooling of the solidified weld metal the precipitation of Ta_2C begins. There is evidence that, at least during the initial stages of the precipitation

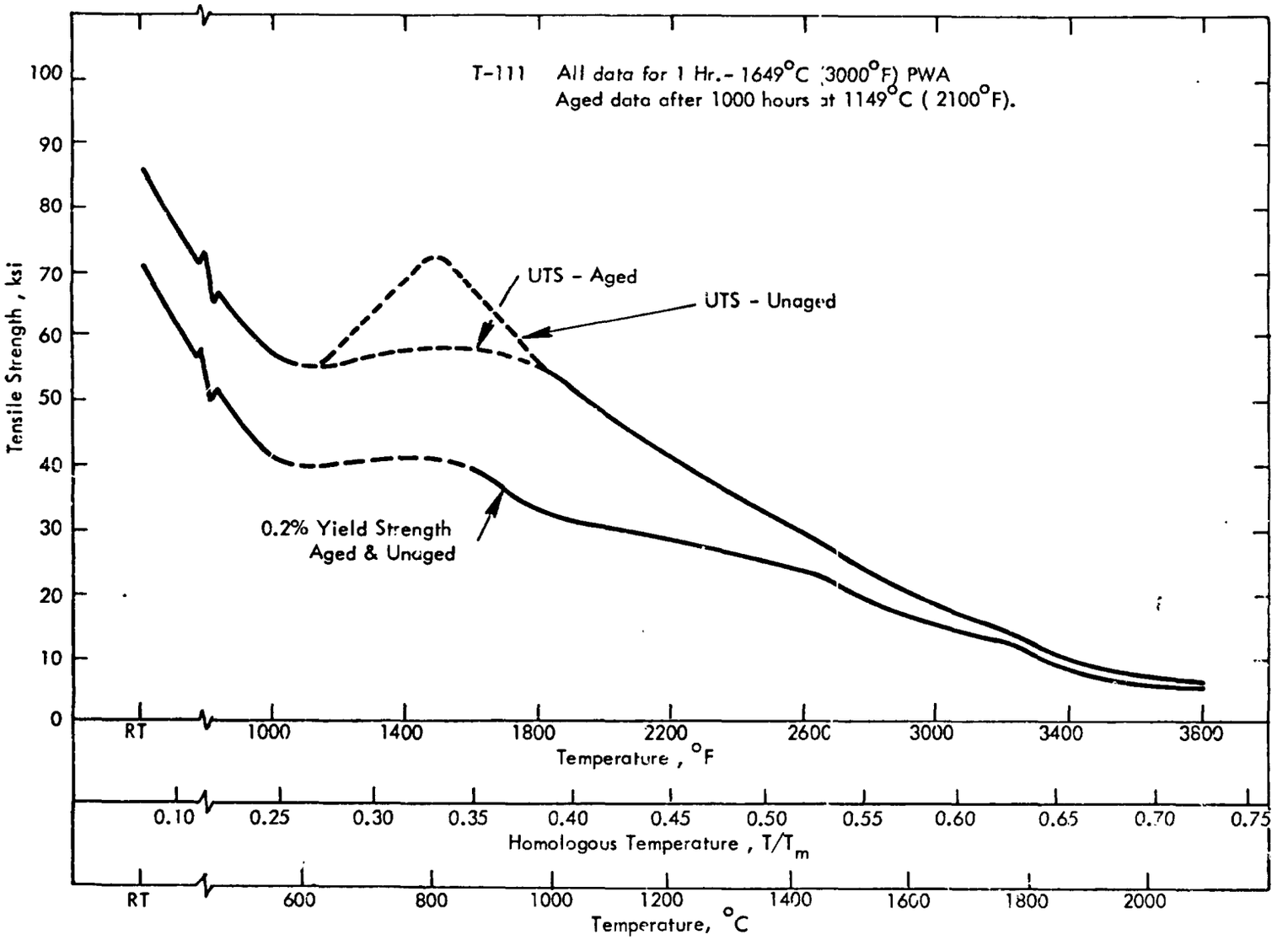

FIGURE 13 - Tensile Properties vs. Test Temperature for Longitudinal GTA Welds in 0.089 cm (0.035 inch) T-111 Sheet.

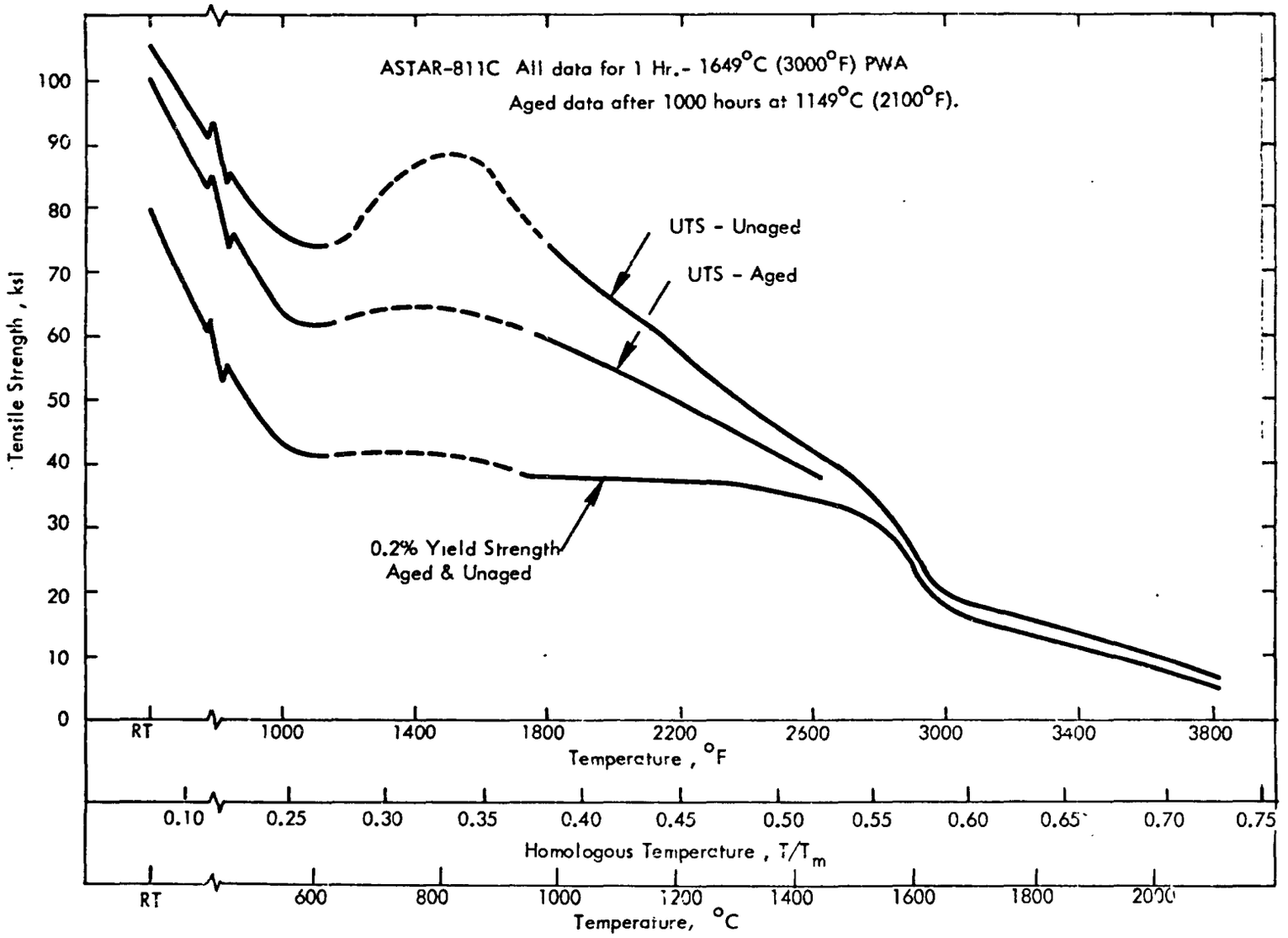

FIGURE 14 - Tensile Properties vs. Test Temperature for Longitudinal GTA Welds in 0.089 cm (0.035 inch) ASTAR-811C Sheet.

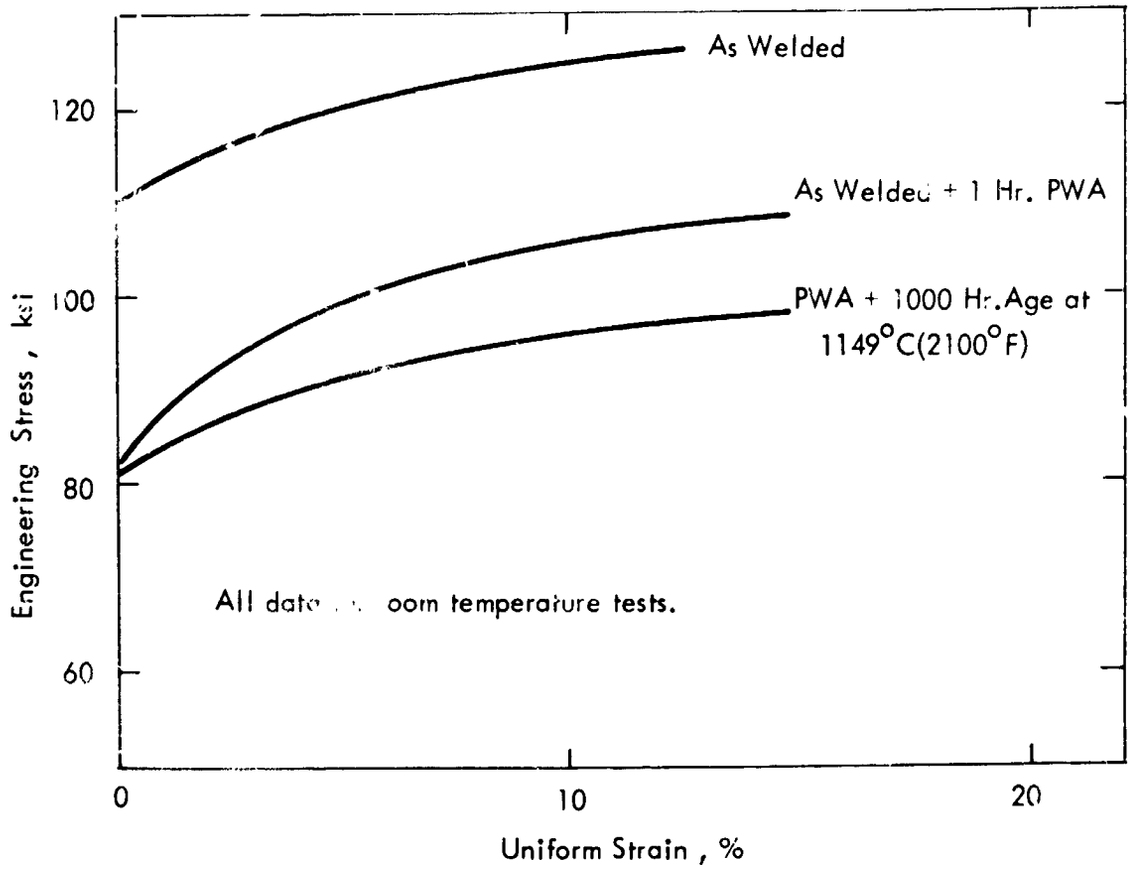

FIGURE 15 - Engineering Stress-Strain Behavior for Tensile Tests on GTA Welds in 0.089 cm (0.035 inch) ASTAR-811C Sheet as a Function of Post Weld Thermal History.

process, some measure of coherency exists between the Ta_2C and the matrix [1].

2. During the short time post-weld anneals the Ta_2C precipitates grow and lose coherency with the matrix. For the higher temperature post-weld anneals at least some of the smaller precipitates (or clusters) may actually be put back into solution but due to the relatively slow cooling rate following the post-weld annealing are re-precipitated and coarsen.
3. Aging 1000 hours at 1149°C (2100°F) results in continued precipitate growth, apparently reaching the stage where the precipitates are too coarse to have any significant effect on the mechanical strength.

The first stage would account for the yield stress and work-hardening rate of the as-welded specimens. It is well established that during the plastic deformation of metals containing closely-spaced, coherent particles the particles are cut by the dislocations as they move on their glide planes [11-13]. As a result the energy , and hence the flow stress, required to initiate plastic deformation is substantially higher than that required to deform the matrix. However, once bulk plastic flow is established the observed work-hardening rate is essentially the same as that of the matrix.

Continued precipitate growth and loss of coherency , such as in stage 2 above , results in a condition whereby plastic flow is achieved by either the Orowan mechanism or by cross-slip of the dislocations out of their glide planes. For either mechanism the flow stress is approximately equivalent and somewhat less than that required for the "particle shear" mechanism. As deformation proceeds dislocation loops are left around the particles. Concurrent with the decrease in yield stress the rate of work-hardening increases due to the high density of dislocation loops or interface dislocations produced since these resist the passage of further slip [11,14]. These observations and expected behavior are in general agreement with the behavior of ASTAR-811C welds following post-weld annealing. The strength and work-hardening observed after aging correspond well to that expected if the precipitates have coarsened appreciably. So long as particle spacing does not change greatly the yield stress would be expected to remain reasonably constant since it is independent of particle size [11].

Ductility and Fracture

Ductility, or rather the loss of it, was the primary concern of most aspects of this program. Hence, it is particularly interesting to review the tensile elongation data. Figures 16 and 17 present the uniform and total elongation data for weld specimens of T-111 and ASTAR-811C, respectively, as a function of test temperature from room temperature through 2093°C (3800°F). In addition to the data of Tables 11 and 12 these plots include the results of additional high temperature tests on unaged sheet weld specimens, Tables 13 and 14. These latter tests were performed to allow more complete determination of the ductility minimum implied by the 1316° and 1427°C (2400° and 2600°F) results. Reference to Figures 16 and 17 attests to their success in that respect.

The ductility behavior displayed in Figures 16 and 17 is in no way peculiar to these alloys but is rather a general feature of the ductility-temperature curves of nearly all metals. Rhines and Wray [15] conducted a comprehensive study of this phenomenon in monel. Their conclusions were ;

- At temperatures below the temperature of minimum or decreased ductility deformation proceeds as the net result of intracrystalline slip ; hence, the ductility is high or "normal".
- At higher temperatures, where grain boundary shearing may be a dominant mode of deformation, fissures or cracks appear and grow along grain boundaries until they meet, thereby completing the fracture at low overall elongation. This is the region of minimum or decreased ductility.
- At still higher temperatures softening processes such as recovery and/or recrystallization occur during deformation. The nucleation and growth of new grains (and hence new, crack-free grain boundaries) serves to alleviate the growth of the grain boundary fissures and high ductility is restored.

Modifications are of course required to the above arguments in the case of more complex alloys. Nevertheless certain guidelines are established which provide some appreciation of the factors involved.

Comparison of Figures 16 and 17 reveals the minimum in tensile elongation occurs at approximately the same temperature range for T-111 and ASTAR-811C - between 1539° (2800°)

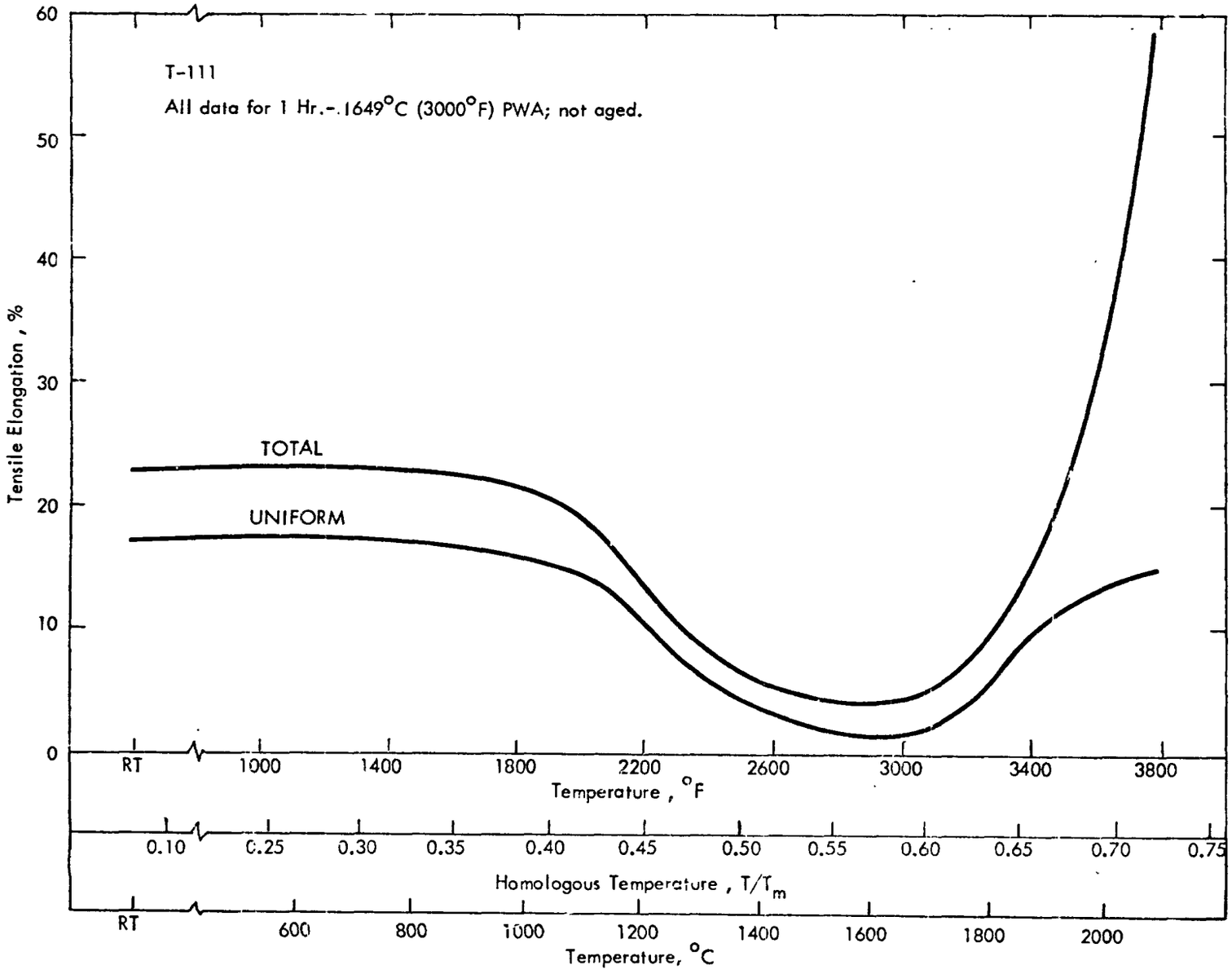

FIGURE 16 - Tensile Elongation vs. Test Temperature for Unaged Longitudinal GTA Welds in 0.089 cm (0.035 inch) T-111 Sheet.

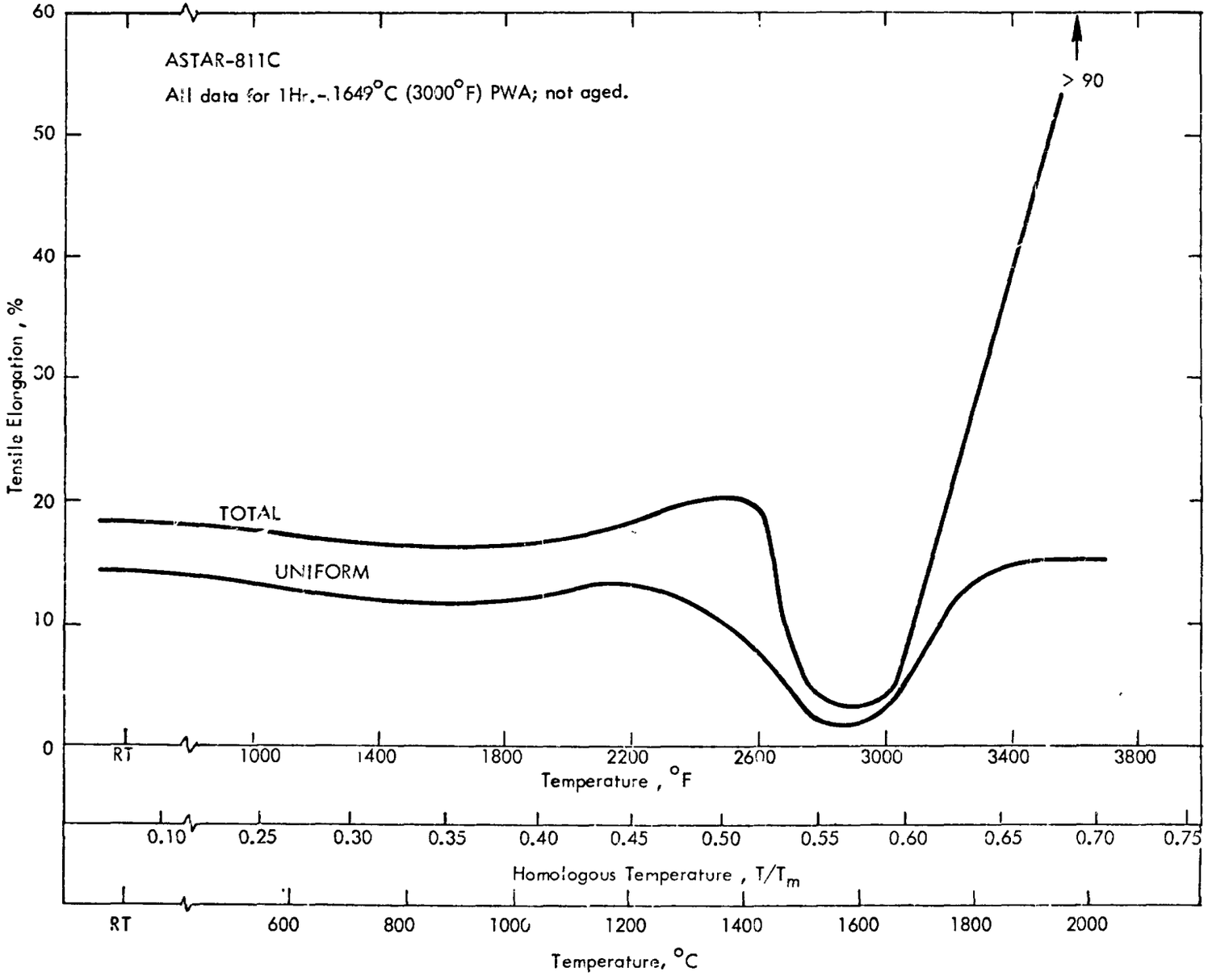

FIGURE 17 - Tensile Elongation vs. Test Temperature for Unaged Longitudinal GTA Welds in 0.089 cm (0.035 inch) ASTAR-811C Sheet.

Pre-Test Thermal History	Test Temp. (°F)	UTS ksi	0.2% Y.S. ksi	% Unif. Elong.	% Total Elong.
As Welded	3000	16.6	13.4	1.6	4.4
1 Hr.-2200°F PWA	3200	14.1	13.1	3.5	6.7
1 Hr.-3400°F PWA	3300	10.6	9.7	6.2	18.2
1 Hr.-2400°F PWA	3400	9.0	5.3	10.1	16.3
1 Hr.-2600°F PWA	3600	7.0	6.0	12.2	27.2
1 Hr.-2800°F PWA	3800	5.6	5.3	15.2	70.0
1 Hr.-3000°F PWA	4000	5.2	4.1	14.1	110.6
1 Hr.-3200°F PWA	4200	4.0	4.0[a]	22.2	> 126[b]

(a) Load drop.

(b) No fracture - limit of crosshead travel.

0.05 min^{-1} strain rate used throughout all tests.

TABLE 13 - Tensile Test Data for High Temperature Tests on GTA Welds in 0.089 cm. (0.035 inch) T-111 Sheet.

Pre-Test Thermal History	Test Temp. (°C)	UTS 10^7 N/m^2	0.2% Y.S. 10^7 N/m^2	%Unif. Elong.	% Total Elong.
As Welded	1649	11.4	9.2	1.6	4.4
1 Hr.-1205°C PWA	1760	9.7	9.0	3.5	6.7
1 Hr.-1871°C PWA	1816	7.3	6.7	6.2	18.2
1 Hr.-1316°C PWA	1871	6.2	3.6	10.1	16.3
1 Hr.-1427°C PWA	1982	4.8	4.1	12.2	27.2
1 Hr.-1538°C PWA	2093	3.9	3.6	15.2	70.0
1 Hr.-1649°C PWA	2205	3.6	2.8	14.1	110.6
1 Hr.-1760°C PWA	2316	2.7	2.7(a)	22.2	>126(b)

(a) Load Drop.

(b) No fracture - reached limit of crosshead travel.

0.05 min^{-1} strain rate used throughout all tests.

TABLE 13a - Tensile Test Data for High Temperature Tests on GTA Welds in 0.089 cm. (0.035 inch) T-111 Sheet.

Pre-Test Thermal History	Test Temp. (^{o}F)	UTS ksi	0.2% Y.S. ksi	% Unif. Elong.	% Total Elong.
1 Hr.-2600^{o}F PWA	2800	33.1	31.4	1.5	3.3
1 Hr.-2800^{o}F PWA	3000	18.4	16.6	1.8	2.6
1 Hr.-3000^{o}F PWA	3200	16.8	11.7	10.4	19.5
1 Hr.-3200^{o}F PWA	3400	13.1	8.8	14.7	25.2
1 Hr. -3400^{o}F PWA	3600	10.0	9.0	15.0	96.4
1 Hr.-3600^{o}F PWA	3800	6.9	5.9	10.5	92.8

0.05 min^{-1} strain rate used throughout all tests.

TABLE 14 - Tensile Test Data for High Temperature Tests on GTA Welds in 0.089 cm. (0.035 in.) ASTAR-811C Sheet.

Pre-Test Thermal History	Test Temp.(°C)	UTS 10^7 N/m^2	0.2% Y.S. 10^7 N/m^2	% Unif. Elong.	% Total Elong.
1 Hr.-1427°C PWA	1538	22.8	21.6	1.5	3.3
1 Hr.-1538°C PWA	1649	12.7	11.4	1.8	2.6
1 Hr.-1649°C PWA	1760	11.6	8.1	10.4	19.5
1 Hr.-1760°C PWA	1871	9.0	6.1	14.7	25.2
1 Hr.-1871°C PWA	1982	6.9	6.2	15.0	96.4
1 Hr.-1982°C PWA	2093	4.8	4.1	10.5	92.8

0.05 min^{-1} strain rate used throughout all tests.

TABLE 14a - Tensile Test Data for High Temperature Tests on GTA Welds in 0.089 cm. (0,035 inch) ASTAR-811C Sheet.

and just over 1649°C (3000°F). However, an important difference exists between the two alloys with respect to the temperature range over which the ductility is seen to be reduced. With regard to the conclusions of Rhines and Wray[15] this implies intracrystalline deformation remains the dominant role in ASTAR-811C to temperatures where grain boundary shear is already dominant in the deformation of T-111. Such behavior would be promoted by the presence of a dispersed phase such as the dimetal carbide known to exist in ASTAR-811C at the temperatures of interest. The kinetics of the softening processes in ASTAR-811C must be such that the ductility is able to recover at temperatures below that required for a similar recovery in T-111. The fact this occurs at temperatures slightly below the carbon solvus for ASTAR-811C suggests the carbide precipitates may be serving as nucleation sites and therby promoting dynamic recovery or recrystallization during testing.

A review of the fracture behavior of T-111 and ASTAR-811C as a function of test variables revealed neither post-weld annealing nor aging had a significant effect on the fracture appearance of either alloy, the appearance being essentially dependent only on the test temperature.

T-111

- Specimens tested at RT, 538° and 982°C (1000° and 1800°F) exhibited transgranular shear failures with very high reduction in area values.
- Specimens tested at 1316° through about 1760°C (2400° through 3200°F) appeared to have failed by separation along the fusion zone grain boundaries with quite low reductions in areas.
- Tests at 1149°, 1816° and 1871°C (2100°, 3300° and 3400°F) resulted in fractures having both of the above characteristics.
- Tests above 1871°C (3400°F) resulted in very fibrous-appearing transgranular shear failures; reduction in area values approached 100%.

ASTAR-811C

- Tests at all temperatures through 1427°C (2600°F) resulted in transgranular shear fractures having very good reductions in area.
- 1538° and 1649°C (2800° and 3000°F) tests resulted in fractures very much like those in T-111 tested at the same temperatures.
- Tests above 1760°C (3200°F) resulted in very high reduction in area, fibrous-appearing fractures.

Superposition of the fracture behavior reviewed above with the ductility-temperature results of Figures 16 and 17 demonstrates excellent agreement. We may conclude in summary that :

- A high temperature region of decreased tensile ductility exists for weld specimens of T-111 and ASTAR-811C. This is in no way unique to these alloys and does not reflect a peculiarity of either tantalum-base alloys or body-centered-cubic metals in general.
- The width of the ductility "trough" in the elongation-temperature plots is significantly greater for T-111 than for ASTAR-811C. This appears to be related to the presence of a carbide precipitate in ASTAR-811C.

4.2.3 Bend Ductility Response

A summary of the 1t, 2t and 4.5t bend test results on aged welds in T-111 and ASTAR-811C is presented in Tables 15 and 16 , respectively. Included in Table 16 are the results of 1t bend tests on specimens of ASTAR-811C welds in the as-welded and as-welded plus one hour 1649°C (3000°F) post-weld annealed conditions. These tests were performed to permit more meaningful interpretation of the results on the aged ASTAR-811C welds. The individual bend data plots which are summarized in these tables are presented in the Appendix. A review of the data of Tables 15 and 16 shows the following:

T-111

- No trend was observed which could be related to the selection of post-weld annealing temperature.
- The bend DBTT's are approximately the same for all three bend radii.
- The bend DBTT's fall within the narrow range of -101° to -157°C (-150° to -250°F) for all conditions evaluated. This includes both longitudinal and transverse bend tests.

The results of these tests on aged T-111 welds are markedly different from those previously determined under identical welding, aging and testing conditions [2]. In the previous study of the response of T-111 welds to long-time elevated temperature aging, 1t bend transition temperatures were in the vicinity of 0°F. This is 83° to 139°C (150° to 250°F) higher than

1 H.. PWA Temp.	Bend DBTT, °F					
	1t		2t		4.5 t	
	Long.	Transv.	Long.	Transv.	Long.	Transv.
2200°F	-200	-250	-250	-200	-225	-200
2400°F	-225	-175	-250	-175	-250	-175
2600°F	-250	-200	-250	-200	-250	-150
2800°F	-200	<-150	-175	-150	-200	-175
3000°F	-200	-175	-225	-200	-175	-250
3200°F	-200	-200	-225	-200	-225	-200
3400°F	-200	-250	-225	-225	-225	-175
3600°F	-200	-250	-150	-150	-200	-250

TABLE 15 - Summary of Bend Ductile-Brittle Transition Temperature Results for GTA Welds in 0.089 cm (0.035 inch) T-111 Sheet. All Welds Aged 1000 hours at 1149°C (2100°F) Prior to Testing.

1 Hr. PWA Temp.	Bend DBTT, °C					
	1t		2t		4.5t	
	Long.	Transv.	Long.	Transv.	Long.	Transv.
1205°C	- 129	- 157	- 157	- 129	- 143	- 129
1316°C	- 143	- 115	- 157	- 115	- 157	- 115
1427°C	- 157	- 129	- 157	- 129	- 157	- 101
1538°C	- 129	<- 101	- 115	- 101	- 129	- 115
1649°C	- 129	- 115	- 143	- 129	- 115	- 157
1760°C	- 129	- 129	- 143	- 129	- 143	- 129
1871°C	- 129	- 157	- 143	- 143	- 143	- 115
1982°C	- 129	- 157	- 101	- 101	- 129	- 157

TABLE 15a - Summary of Bend Ductile-Brittle Transition Temperature Results for GTA Welds in 0.089 cm (0.035 inch) T-111 Sheet. All Welds Aged 1000 hours at 1149°C (2100°F) Prior to Testing.

1 Hour P W A Temp.	Bend DBTT, °F					
	1t		2t		4.5 t	
	Longit.	Transv.	Longit.	Transv.	Longit.	Transv.
2200°F	150	175	150	200	75	150
2400°F	175	175	125	200	125	175
2600°F	150	175	100	150	125	200
2800°F	150	150	175	200	100	175
3000°F	100	175	150	175	<25	100
3200°F	100	125	100	150	< 0	125
3400°F	150	125	150	200	100	125
3600°F	200	175	250	225	150	175
None[a]	125	125				
3000°F[a]	125	< 50				

(a) Not aged prior to testing.

TABLE 16 - Summary of Bend Ductile-Brittle Transition Temperature Results for GTA Welds in 0.089 cm (0.035 inch) ASTAR-811C Sheet. All Welds Aged 1000 hours at 1149°C (2100°F) Prior to Testing Except as Indicated.

1 Hr. PWA Temp.	Bend DBTT, °C					
	1t		2t		4.5 t	
	Long.	Transv.	Long.	Transv.	Long.	Transv.
1205°C	66	79	66	93	24	66
1316°C	79	79	52	93	52	79
1427°C	66	79	38	66	52	93
1538°C	66	66	79	93	38	79
1649°C	38	79	66	79	<-4	38
1760°C	38	52	38	66	<-18	52
1871°C	66	52	66	93	38	52
1982°C	93	79	121	107	66	79
None[(a)]	52	52				
1649°C	52	<10				

(a) Not aged prior to testing.

TABLE 16a - Summary of Bend Ductile-Brittle Transition Temperature Results for GTA Welds in 0.089 cm (0.035 inch) ASTAR-811C Sheet. All Welds Aged 1000 hours at 1149°C (2100°F) Prior to Testing Except as Indicated.

the present results. A possible explanation for this difference in behavior is the slightly higher carbon content of the earlier heat since this would tend to strengthen the grain volumes relative to the grain boundaries. Such an effect might likely lead to the grain boundary failures seen, since the higher the matrix strength the more aggravated the condition; hence, the alleviation of this behavior would be postponed to somewhat higher temperatures.

ASTAR-811C

- As for T-111, selection of the post-weld annealing temperature did not seem to have any effect on the results.
- The slight variations in bend DBTT observed did not show a strong correlation with bend radius.
- The range of bend transition temperatures for all tests, including longitudinal and transverse bends, was from -18° to 121°C (0° to 250°F).

The lack of extensive prior experience with the bend ductility of ASTAR-811C indicated the need to more completely define the response in the program heat. It was for this reason the 1t bend DBTT was determined for the as-welded and the as-welded plus post-weld annealed conditions. To provide some perspective on these data a general comparison is provided below for the 1t bend performance of the development heat of ASTAR-811C (data from Reference 4) and that of the program heat (Heat 650078) ;

Development Heat [4]	Condition	Heat 650078
< -196°C (< -320°F)	Base Metal	-157°C (-250°F)
-157°C (-250°F)	As GTA Welded	52°C (125°F)
-73°C (-100°F)	1000 hours 982°C (1800°F)	----
----	1000 hours 1149°C (2100°F)	66°C (150°F) approx.

All values listed above are the 1t bend DBTT's.

The development heat displays a clear superiority in performance to that of the program material. The most likely reason for this is the greater W and Re contents, and hence greater matrix strength, of Heat 650078. The similarity of the transition behavior before and after aging implies the aging itself is not playing a dominant role.

Failures in both alloys are better described as ductile grain boundary tears than brittle cleavage-type fractures. In many cases fractures which initiated in the weld fusion zone were arrested by the base metal or the heat affected zone. Figure 18 shows a typical failure in T-111. The "tears" along the fusion zone grain boundaries are evident.

The problems associated with making more quantitative conclusions based on bend tests are mainly related to the fact the state of stress is less well defined than in most other ductile-brittle tests. The elementary theory of bending considers only the circumferential (or outer fiber) strain. However, experiments have shown that the distribution of strain in the bending of sheet is not truly amenable to such a simple analysis[8]. The distribution of strain in the outer fibers depends significantly on the method of bending ; three-point bending such as that used in bend ductile-brittle transition temperature tests produces a rather non-uniform distribution of strain. An attempt has been made to predict the minimum bend radius for a given sheet thickness from a knowledge of its tensile properties [16]. This analytical treatment predicts a minimum bend radius (R) for a sheet of thickness t according to the expression ,

$$\frac{R}{t} = \frac{50}{\%\ \text{elong.}} - \frac{1}{2}$$

where (% elong.) refers to the engineering fracture strain in a tensile test at the temperature of interest. This expression fails utterly for the case of T-111 and ASTAR-811C welds since it demands a tensile elongation of 33% if a 1t minimum bend radius is ever to be satisfied. Reference to the tensile data of the preceding section (4.2.2) shows that for neither alloy does the tensile elongation reach this value below 1649°C (3000°F). The failure of this expression is most probably related to its basic assumption of [16] "homogeneous and isotropic materials", neither condition of which are satisfied by the GTA weld structures being evaluated.

The approximate equivalence of the 1t, 2t and 4.5t bend transition temperatures was totally unexpected. For T-111 welds this would not appear to be cause for concern due to the quite low temperatures involved. The results for ASTAR-811C , however, with bend transition temp-

10X

Post-Weld Annealed 1 Hr.- 1649°C (3000°F)

Aged 1000 Hrs.-1149°C (2100°F)

FIGURE 18 - Typical Bend Test Fracture in Aged T-111 GTA Weld Specimen.

eratures slightly above room temperature, merit future consideration and attention. The fact no similar indications were provided by the other engineering tests discussed previously tends to suggest the large, highly oriented grain structures of the GTA weld specimens to be particularly, and perhaps uniquely, susceptible to premature failure due to very high localized straining during bend testing.

In conclusion, the modest increase in the bend DBTT noted for T-111 in the present study appears to be the result of the large, oriented grain structure of the weld specimens. In ASTAR-811C the bend test results more likely reflect the combined influence of the grain size effect and the very high matrix strength of ASTAR-811C at the temperatures of interest.

4.3 Microstructural Response to Thermal Exposures

T-111

The microstructural response of GTA welds in T-111 to various post-weld thermal exposures has been characterized during the performance of a previous NASA-sponsored program[2]. The results of that program showed that aging at temperatures from 982° through 1149°C (1800° through 2100°F) resulted in the appearance of both grain boundary and interdendritic precipitates in the weld fusion zones. Post-weld annealing at elevated temperatures had virtually no effect on the observed aging reaction. The results of the present program concur with those results except for the fact grain boundary precipitates were not observed for any of the conditions evaluated in the present work. If this is due to the slightly lower carbon content (30-40 ppm) of the present T-111 relative to that evaluated previously (about 50-60 ppm), a rather tenuous balance is suggested for the appearance or non-appearance of the grain boundary precipitates.

Figure 19 shows the effect of aging 1000 hours at 1149°C (2100°F) on the as-welded microstructure. The interdendritic precipitates are seen to form primarily at the junction of two or more dendrites. The effects of 1 hour post-weld anneals from 1205° through 1538°C (2200°F through 2800°F) were relatively minor, being mainly confined to producing a well defined interdendritic precipitate. In general, the effect of the 1149°C (2100°F) aging on specimens

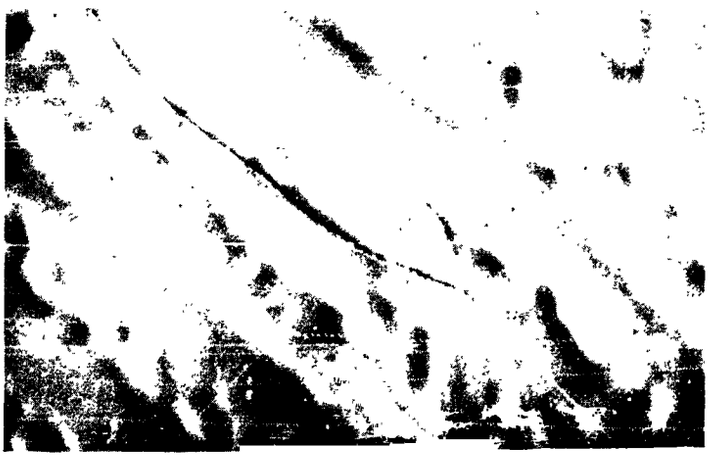

20,275 WELD 1500X

As Welded

20,276 WELD 1500X

Aged 1000 Hrs.-1149°C (2100°F)

FIGURE 19 - Microstructure of GTA Weld Specimen in T-111 Sheet.

post-weld annealed in this temperature range was insignificant. A typical microstructure resulting from post-weld annealing plus aging in this range is shown in Figure 20. Post-weld annealing at 1649° and 1760°C (3000° and 3200°F) began to effect local homogenization of the fusion zone microstructure. Figure 21 shows the microstructure of a specimen post-weld annealed 1 hour at 1649°C (3000°F) and aged 1000 hours at 1149°C (2100°F). Comparison of Figures 20 and 21 reveals the pronounced segregation in the fusion zone is being alleviated.

One hour post-weld anneals at 1871° and 1982°C (3400° and 3600°F) effected complete homogenization of the weld fusion zones and resulted in extensive grain growth. Aging of the resulting microstructures for 1000 hours at 1149°C (2100°F) had no further effect. Figure 22 shows the fusion zone microstructure following 1982°C (3600°F) post-weld annealing and 1149°C (2100°F) aging.

The results of this investigation of the microstructural response of GTA sheet welds in T-111 to aging suggests the previously observed ductility impairment implied by the bend test results[2] on aged T-111 welds may be due to the slightly higher carbon content of that material relative to the present material. The observation of Ta_2C grain boundary precipitates may be only coincidental since no direct observation has been made connecting their presence and the fracture behavior except that it tends to be grain boundary in character. It appears more likely that the carbon remaining in solution, or present as sub-microscopic intragranular precipitates, imparts additional matrix strengthening requiring proportionately greater strain accommodation at the fusion zone grain boundaries during bending. The modest increase observed in the bend DBTT noted in the present study is more likely due simply to the large, oriented grain structure of the GTA weld specimens and in that respect represents a more intrinsic feature of the alloy.

ASTAR-811C

The effect of 1000 hour aging at 1149°C (2100°F) on the as-welded microstructure of ASTAR-811C is shown in Figure 23. The as-welded, unaged weld fusion zone is seen to be exceptionally

20,278 WELD 1500X

Post-Weld Annealed 1 Hr.-1427°C(2600°F)
Aged 1000 Hrs.-1149°C (2100°F)

FIGURE 20 - Microstructure of GTA Weld Specimen in T-111 Sheet.

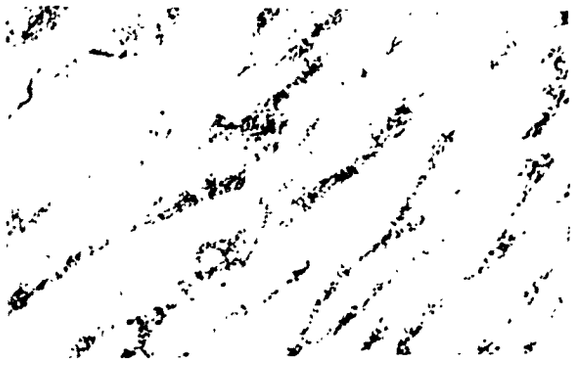

20,280 WELD 400X

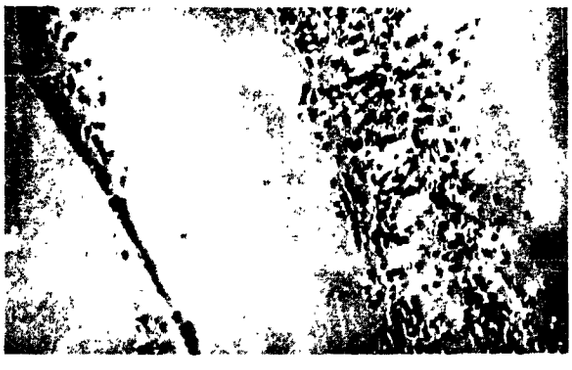

20,280 WELD 1500X

Post-Weld Annealed 1 Hr.-1649°C (3000°F)
Aged 1000 Hrs.-1149°C (2100°F)

FIGURE 21 - Microstructure of GTA Weld Specimen in T-111 Sheet.

20,282 WELD 400X

20.282 WELD 1500X

Post-Weld Annealed 1 Hr.-1982°C (3600°F)
Aged 1000 Hrs.-1149°C (2100°F)

FIGURE 22 - Microstructure of GTA Weld Specimen in T-111 Sheet.

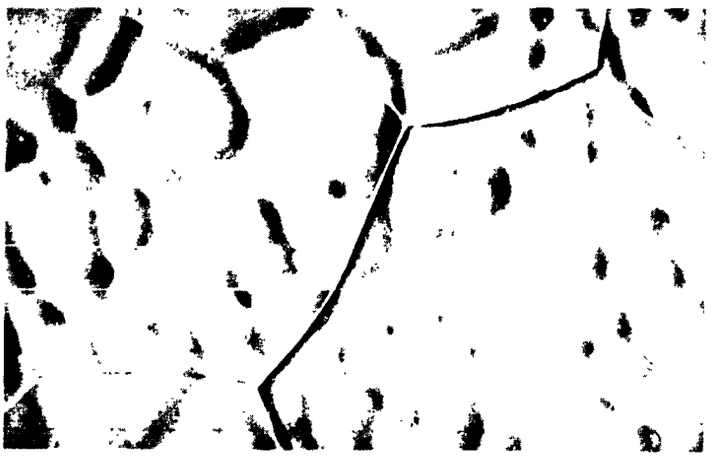

22,155 WELD 1500X

As Welded

22,337 W/HAZ 400X

22,156 WELD 1500X

Aged 1000 Hrs.-1149°C (2100°F)

FIGURE 23 - Microstructure of GTA Weld Specimens in ASTAR-811C Sheet.

"clean". Aging has caused two distinct changes in the microstructure. Similar to T-111 an interdendritic precipitate is seen to develop in the cored weld zone. However, completely unlike T-111, grain boundary precipitates are found throughout the weld, heat affected zone, and base metal. In addition, a fine intragranular precipitate has developed in the heat-affected zone. The grain boundary precipitate is a general feature of all the aged specimens, being present in two somewhat different morphologies. The most frequently observed of these is the blocky, cellular precipitate which displayed a tendency to grow preferentially into one or the other of the two adjacent grain volumes rather than into both equally. Also observed, but less frequently, the grain boundary precipitate developed as a semi-continuous thin film on the boundary.

One hour post-weld anneals at 1205° through 1538°C (2200° through 2800°F) produced only precipitation of the interdendritic phase in the weld fusion zones. Subsequent aging at 1149°C (2100°F) for 1000 hours resulted in weld and heat-affected zone microstructures similar to those of the as-welded plus aged specimens shown in Figure 23. Typical heat-affected zone and weld zone microstructures are shown for specimens aged after 1205° and 1427°C (2200° and 2600°F) post-weld anneals in Figures 24 and 25, respectively.

Post-weld annealing at 1649°C (3000°F) for one hour resulted in the appearance of carbide precipitates both at the grain boundaries and within the grain volumes of the weld fusion zone (Top, Figure 26). This marked the first appearance of the carbide precipitates prior to aging. Subsequent aging for 1000 hours at 1149°C (2100°F) resulted in extensive cellular precipitation and coarsening of the intragranular carbides present in the heat-affected zone and base metal (Bottom, Figure 26). A one hour post-weld anneal at 1760°C (3200°F) began to effect localized homogenization in the weld fusion zone.

One hour anneals at 1871° and 1982°C (3400° and 3600°F) resulted in considerable grain growth throughout the weld zone and base metal. The appearance of the precipitates, Figure 27, suggested the carbides had dissolved on annealing and re-precipitated on cooling. In many cases the fusion zone precipitation had occurred on the low-angle sub-boundaries

22,184 HAZ 1500X

22,184 WELD 1500X

Post-Weld Annealed 1 Hr.-1205°C (2200°F)

Aged 1000 Hrs.-1149°C (2100°F)

FIGURE 24 - Microstructure of GTA Weld Specimens in ASTAR-811C Sheet.

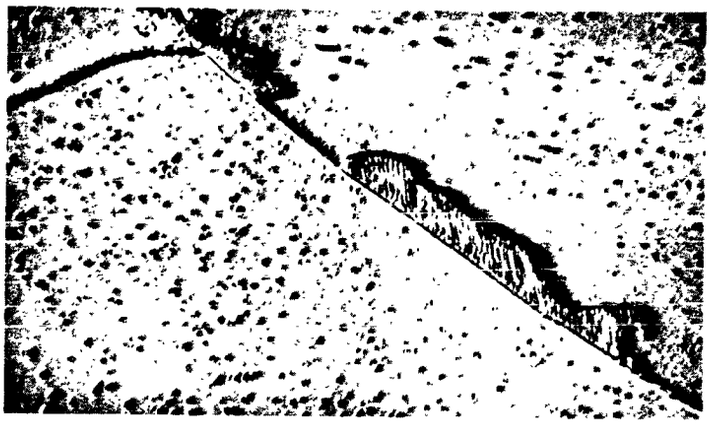

22,185 HAZ 1500X

22,185 WELD 1500X

Post-Weld Annealed 1 Hr.-1427°C (2600°F)
Aged 1000 Hrs.-1149°C (2100°F)

FIGURE 25 - Microstructure of GTA Weld Specimens in ASTAR-811C Sheet.

22,157 WELD 1500X

Post-Weld Annealed 1 Hr.-1649°C (3000°F)

No Age

22,186 W/HAZ 400X

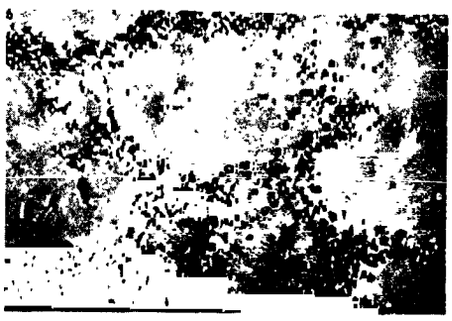

22,158 WELD 1500X

22,186 HAZ 1500X

Post-Weld Annealed 1 Hr.-1649°C (3000°F)

Aged 1000 Hrs.-1149°C (2100°F)

FIGURE 26 - Microstructure of GTA Weld Specimens in ASTAR-811C Sheet.

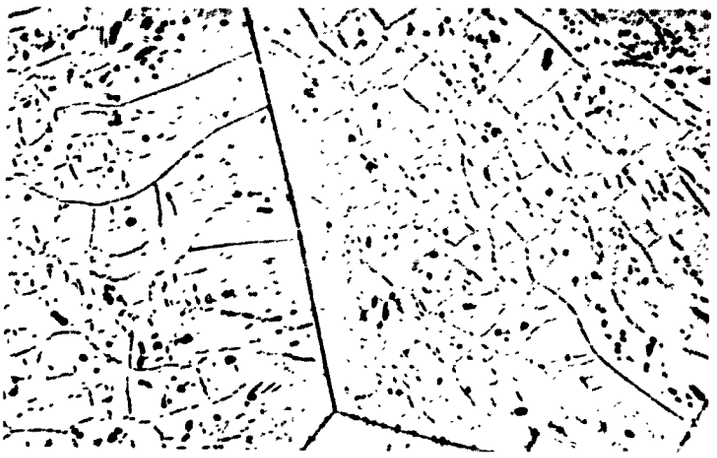

22,159 WELD 400X

22,159 WELD 1500X

Post-Weld Annealed 1 Hr.-1982°C (3600°F)

No Age

FIGURE 27 - Microstructure of GTA Weld Specimen in ASTAR-811C Sheet.

formed by polygonization-like dislocation rearrangements within the fusion zone grain volumes. Subsequent 1000 hour aging at 1149°C (2100°F) resulted in little change within the weld fusion zone except for the development of the cellular precipitates along the grain boundaries, Figure 28. Also shown in Figure 28 is a narrow precipitation-free zone adjacent to the grain boundaries in the aged base metal. This is typically observed in alloys where the nucleation and growth kinetics of the precipitation process are controlled by vacancy supersaturation since on cooling the grain boundaries serve as ready vacancy sinks and relieve the supersaturation local to them. Note also the lack of dislocation substructure in the base metal.

No evidence was found which suggested the cellular precipitate plays a significant role in the mechanical behavior of ASTAR-811C with regard to either the strength or fracture properties. However, the pearlite-like appearance of several of the larger, more easily resolved colonies prompted a closer look. Chromium shadowed carbon replicas were prepared from several of the metallographic specimens and examined by transmission electron microscopy. An electron micrograph of such an area is shown in Figure 29 for a specimen which had been post-weld annealed at 1205°C (2200°F) prior to aging. As the temperature of the post-weld anneal was increased the cellular precipitate was seen to occur as narrower colonies than that seen in Figure 29, and tended to lie adjacent to a higher fraction of the grain boundary length. Some evidence of this can be seen by comparing Figures 25, 26, and 28. In general, when two or more colonies were present in a common grain the orientation of their lamella was quite similar, suggesting a possible orientation relationship between precipitate and matrix. No evidence was obtained which allowed inference of the possible driving force for the reaction leading to this precipitate morphology.

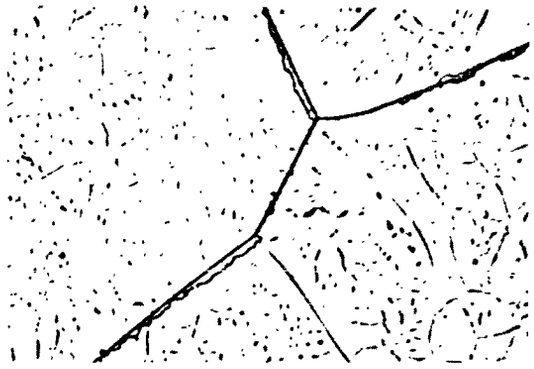

22,187 WELD 400X

22,187 WELD 1500X

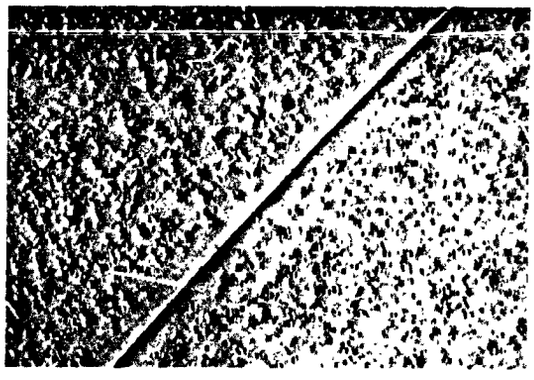

22,187 BASE METAL 1500X

Post-Weld Annealed 1 Hr.-1982°C (3600°F)

Aged 1000 Hrs.-1149°C (2100°F)

FIGURE 28 - Microstructure of GTA Weld Specimen in ASTAR-811C Sheet.

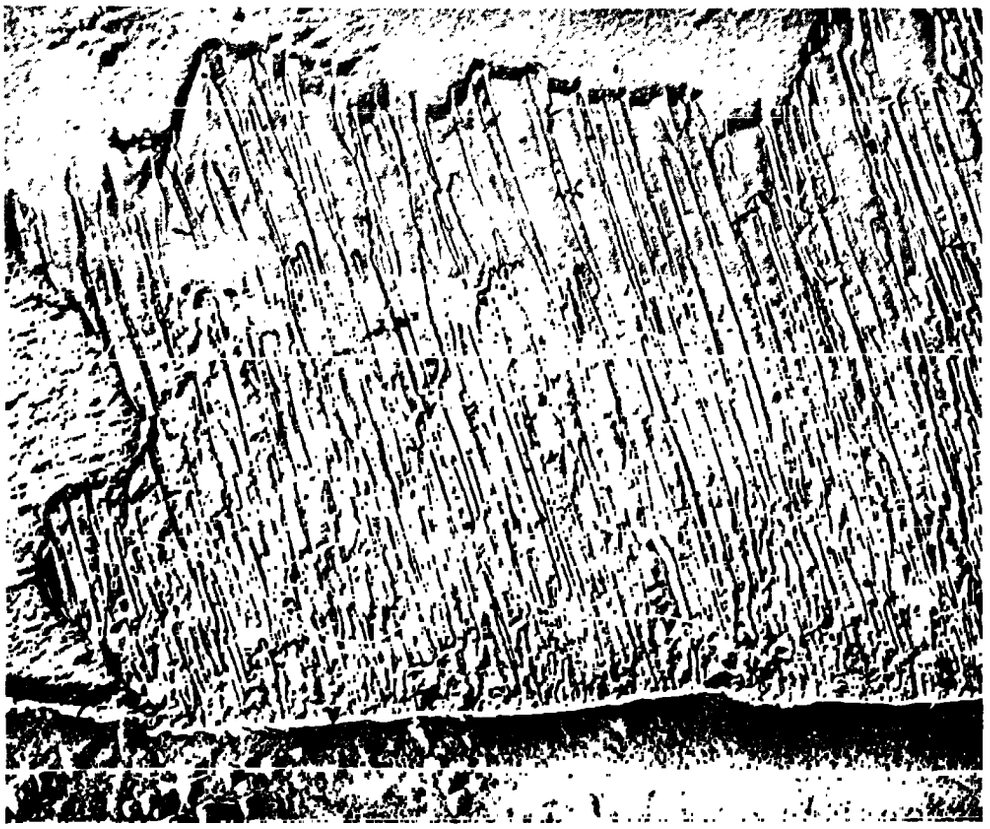

22,184 6000X

Post-Weld Annealed 1 Hr.-1205°C (2200°F)

Aged 1000 Hrs.-1149°C (2100°F)

FIGURE 29 - Transmission Electron Micrograph of a Carbon Replica of a Cellular Precipitate in an Aged GTA Weld in ASTAR-811C Sheet.

5.0 CONCLUSIONS

Underbead Cracking in Multipass GTA Plate Welds

1. Although this problem is the rule rather than the exception in T-111, ASTAR-811C displays virtually no tendency toward this behavior.
2. Underbead cracking is peculiar to high creep strength alloys designed for resistance to liquid alkali metal corrosion. Alloys of lower creep strength or alloys free of reactive metals (corrosion inhibition) do not display underbead cracking.
3. Underbead cracking results from the manner in which weld thermal strains are accommodated in multipass welding. An imbalance in grain boundary versus matrix strengths at high temperatures can cause grain boundaries to strain to failure. An imbalance within the critical temperature range occurs either by strengthening the matrix or by weakening the grain boundaries. The results of each were demonstrated in this program.
4. Since the effects of alloy additions on the factors which generally affect matrix and grain boundary strengths are known, elimination of underbead cracking should lend itself to a chemical solution. This can be achieved, for example, by using a modified filler wire composition. Results of welding ASTAR-811C confirm this approach to be promising.

Fracture Toughness of T-111 and ASTAR-811C Sheet Welds

5. GTA welds in T-111 and ASTAR-811C sheet are not notch sensitive to temperatures as low as -196°C (-320°F).
6. The low temperature notch-tensile properties of GTA welds in T-111 and ASTAR-811C sheet are affected only slightly by thermal exposures to 1982°C (3600°F) for one hour or by 1000 hour aging at 1149°C (2100°F).
7. One hour post-weld anneals to 1982°C (3600°F) and 1000 hour aging at 1149°C (2100°F) had little effect on the room and elevated temperature tensile properties of GTA welds in T-111 and ASTAR-811C sheet.
8. A high temperature region (between 0.45 and 0.65 T_m) of reduced tensile ductility was observed for both T-111 and ASTAR-811C GTA sheet weld specimens.

9. The width of the ductility "trough" in the elongation-temperature data is significantly greater for T-111 than for ASTAR-811C. This appears to be related to the presence of a carbide precipitate in ASTAR-811C.
10. The 1t, 2t, and 4.5t bend transition temperatures of aged GTA sheet welds of T-111 fall in the range -101° to -157°C (-150° to -250°F) and are unaffected by one hour post-weld anneals to 1982°C (3600°F). These results are significantly better (i.e. the bend DBTT's are lower for the present program welds) than had been found previously using similar aging treatments. This difference is believed due to a slight improvement in purity of the present T-111. Metallographic results tend to support this conclusion.
11. The 1t, 2t, and 4.5t bend transition temperatures of aged GTA sheet welds of ASTAR-811C fall in the range -18° to 121°C (0° to 250°F) and, like T-111, are unaffected by one hour post-weld anneals to 1982°C (3600°F). These values are considerably higher than previous dererminations on similarly aged and tested ASTAR-811C. This difference in behavior is believed due to the higher W and Re contents of the program heat (Heat 650078).

6.0 REFERENCES

1. Buckman, R. W. Jr., and Goodspeed, R.C., "Development of Precipitation Strengthened Tantalum Base Alloy, ASTAR-811C", Work done under Contract NAS 3-2542, Summary Topical Report, WANL-PR-(Q)-016, (1968).

2. Lessmann, G.G. and Gold, R. E., "Long-Time Elevated Temperature Stability of Refractory Metal Alloys", Part II of "Determination of Weldability and Elevated Temperature Stability of Refractory Metal Alloys", NASA-CR-1608, September, 1970.

3. Stoner, D. R., Work performed at Westinghouse Astronuclear Laboratory on Contract NAS 3-10602, "Development of Large Diameter T-111 Tubing".

4. Buckman, R. W. Jr., and Goodspeed, R. C., "Development of Precipitation Strengthened Tantalum Base Alloys", Final Report on Contract NAS 3-2542, WANL-PR-(Q)-017, (1968).

5. Lessmann, G. G. and Gold, R. E., "The Varestraint Test for Refractory Metals", WANL-PR(VVV)-002, NASA CR-72828 , November, 1970

6. Gold, R. E. and Begley, R. T., "Investigation of High Temperature Fracture of T-111 and ASTAR-811C", WANL-PR(VVV)-003, NASA CR-72859 , April, 1971

7. Ammon, R. L. and Begley, R. T., Summary Phase Report on "Pilot Production and Evaluation of Tantalum Alloy Sheet", WANL-PR-M-004, June 15, 1963 (Westinghouse Astronuclear Laboratory).

8. Dieter, G. E., Mechanical Metallurgy, McGraw-Hill (1961).

9. Rosenfield, A. R., Votava, E. and Hahn, G. T., "Dislocations and the Ductile-Brittle Transition", Chapter 3 in Ductility, ASM (1968)

10. Imgram A. G., Holden, F. C., Ogden, H. R. and Jaffee, R. I., "Notch Sensitivity of Refractory Metals", WADD-TR-60-278, (April, 1960).

11. Kelly, A. and Nicholson, R. B., "Precipitation Hardening", Progress in Materials Science, 10, No. 3, MacMillan (1963).

12. Fine, M. E., "Precipitation Hardening", Chapter 4 in The Strengthening of Metals (edited by D. Peckner), Reinhold Publishing (1964).

13. Parker, E. R., "Strain Hardening", Chapter 2 in The Strengthening of Metals (edited by D. Peckner), Reinhold Publishing (1964).

14. Fisher, J. C., Hart, E. W. and Pry, R. H., Acta Met, 1, p. 336 (1953).

15. Rhines, F. N. and Wray, P. J., "Investigation of the Intermediate Temperature Ductility Minimum in Metals", ASM Trans. Quarterly, 54, No. 2, pp. 117 - 128, June, 1961.

16. Datsko, J. and Yang, C. T., "Correlation of Bendability of Materials with their Tensile Properties", Trans ASME, Series B, 82, pp. 309 - 314, 1960.

APPENDIX - BEND TEST DATA COMPILATION

APPENDIX (CONTINUED)

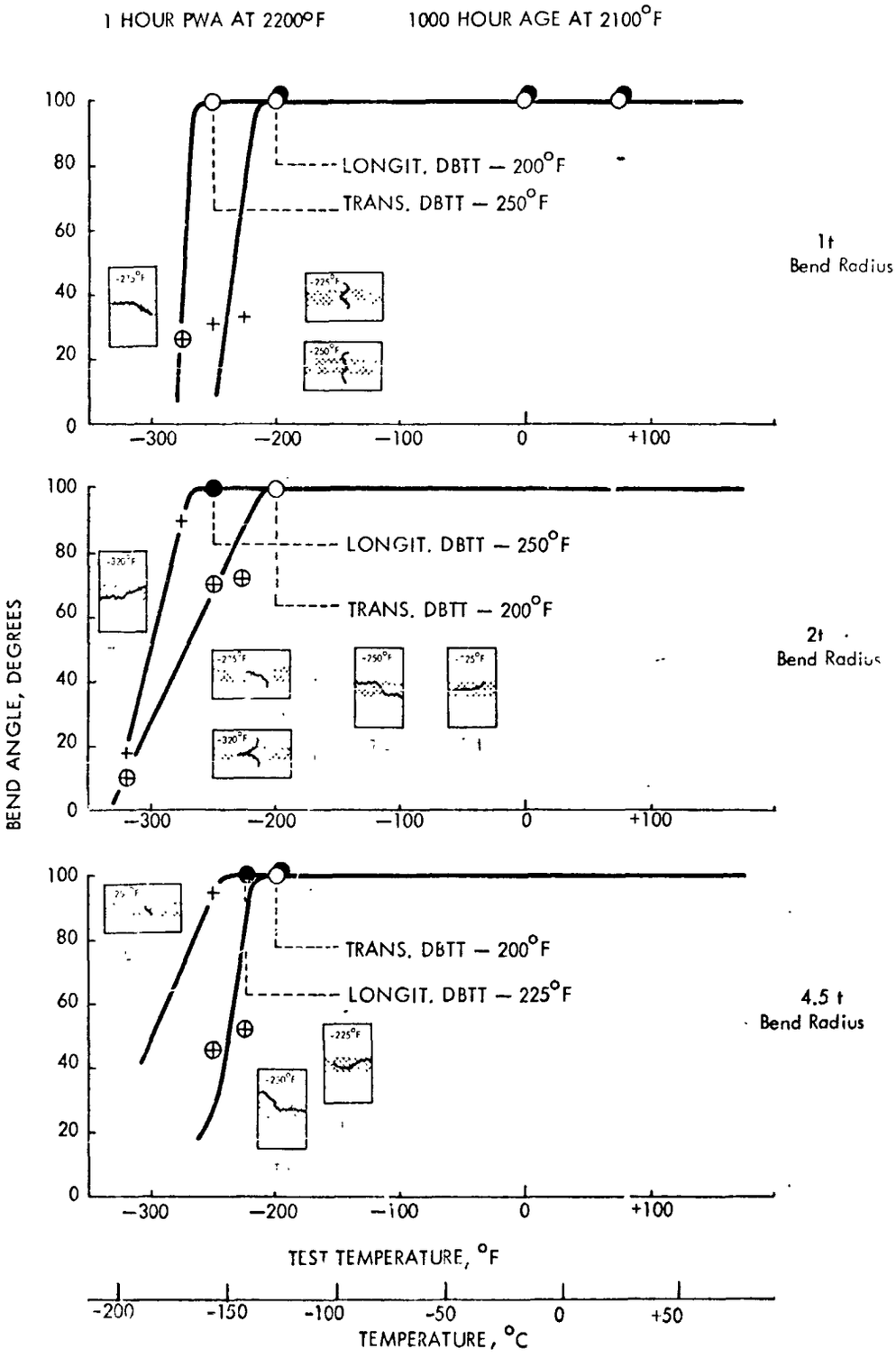

Figure A1. Bend Test Data for GTA Welds in 0.089 cm. (0.035 inch) T-111 Sheet. 1 Hour PWA at 1205°C (2200°F). Aged 1000 Hours at 1149°C (2100°F).

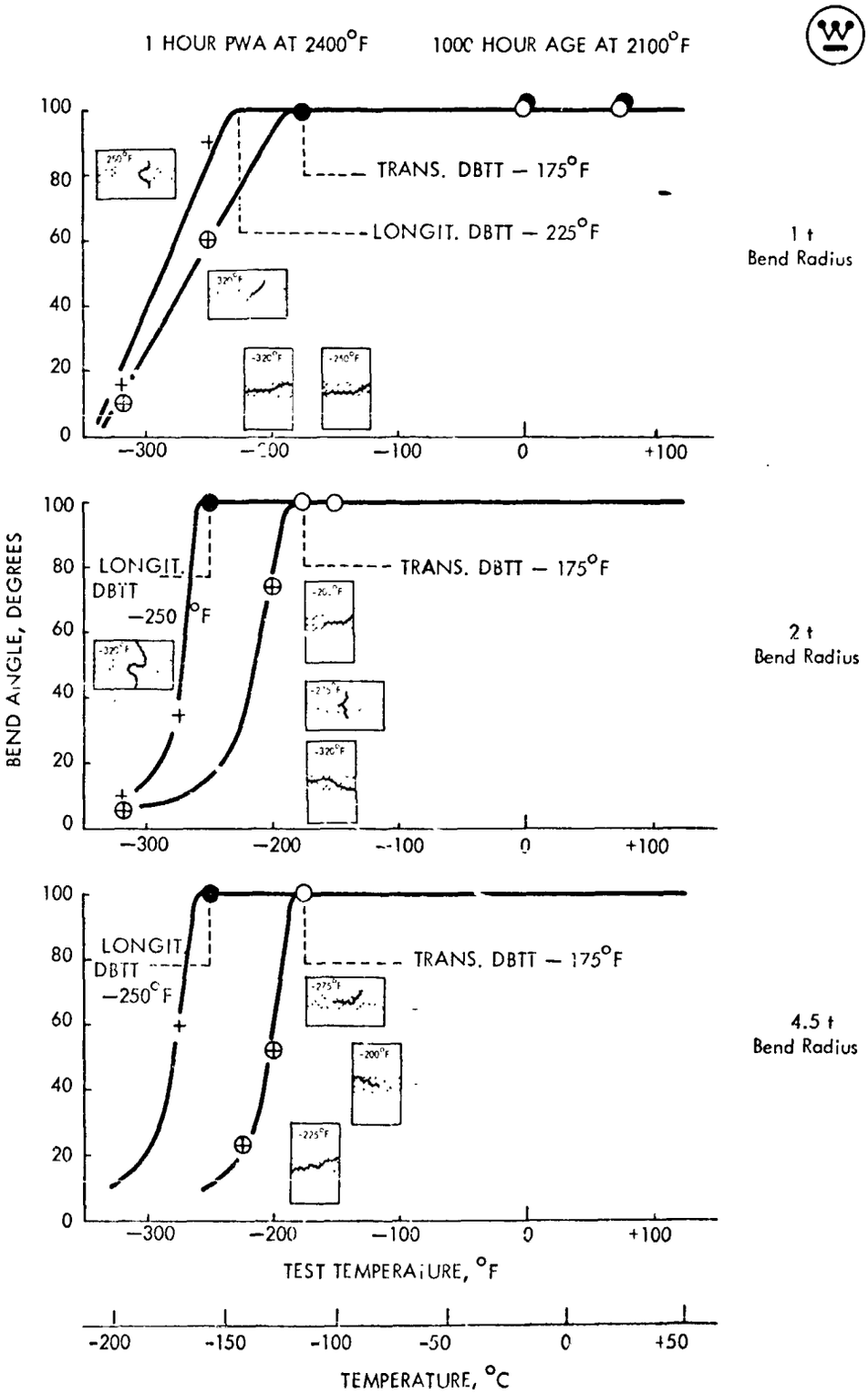

Figure A2. Bend Test Data for GTA Welds in 0.089 cm. (0.035 inch) T-111 Sheet. 1 Hour PWA at 1316°C (2400°F). Aged 1000 Hours at 1149°C (2100°F).

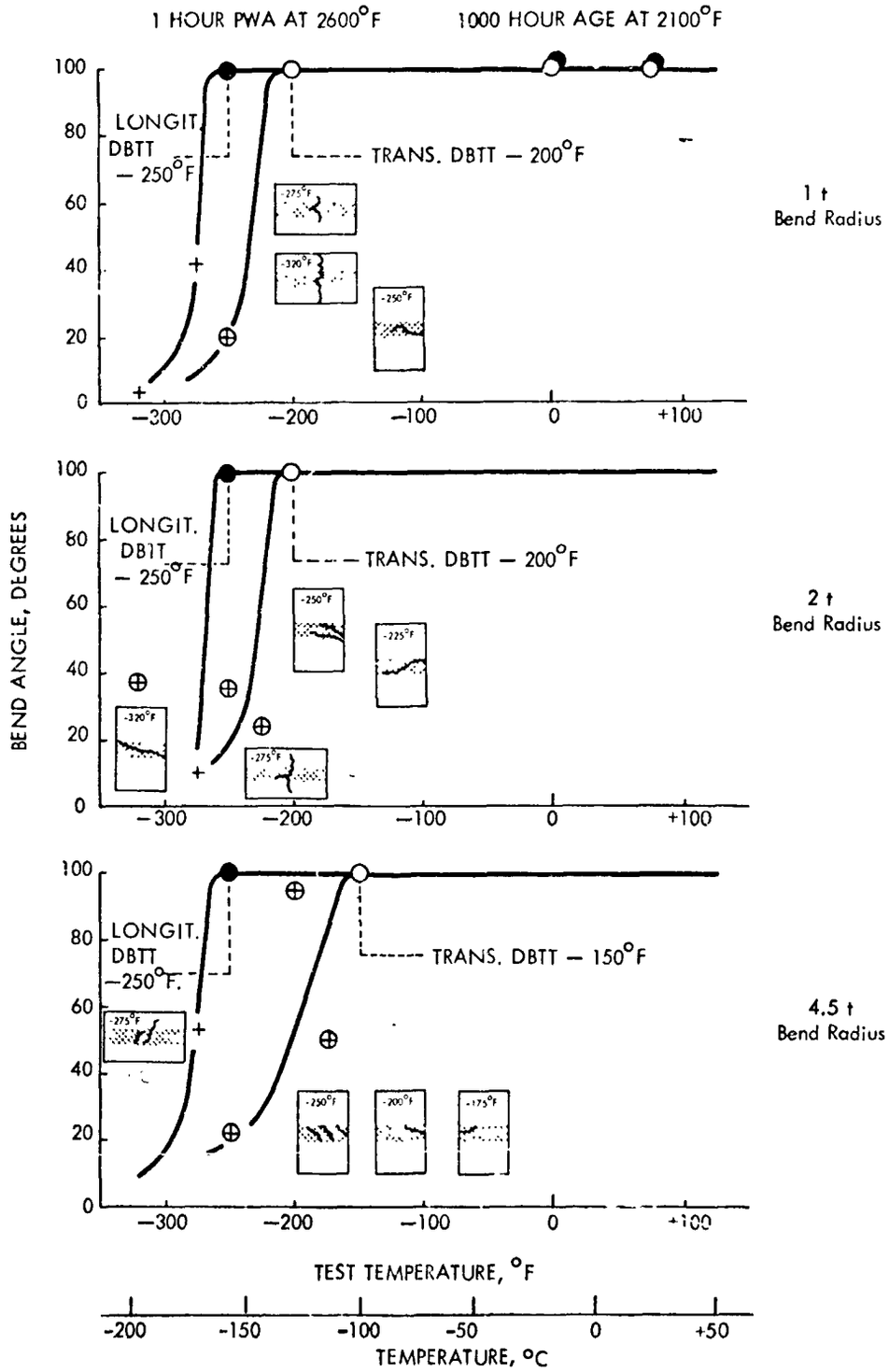

Figure A3. Bend Test Data for GTA Welds in 0.089 cm. (0.035 inch) T-111 Sheet. 1 Hour PWA at 1427°C (2600°F). Aged 1000 Hours at 1149°C (2100°F).

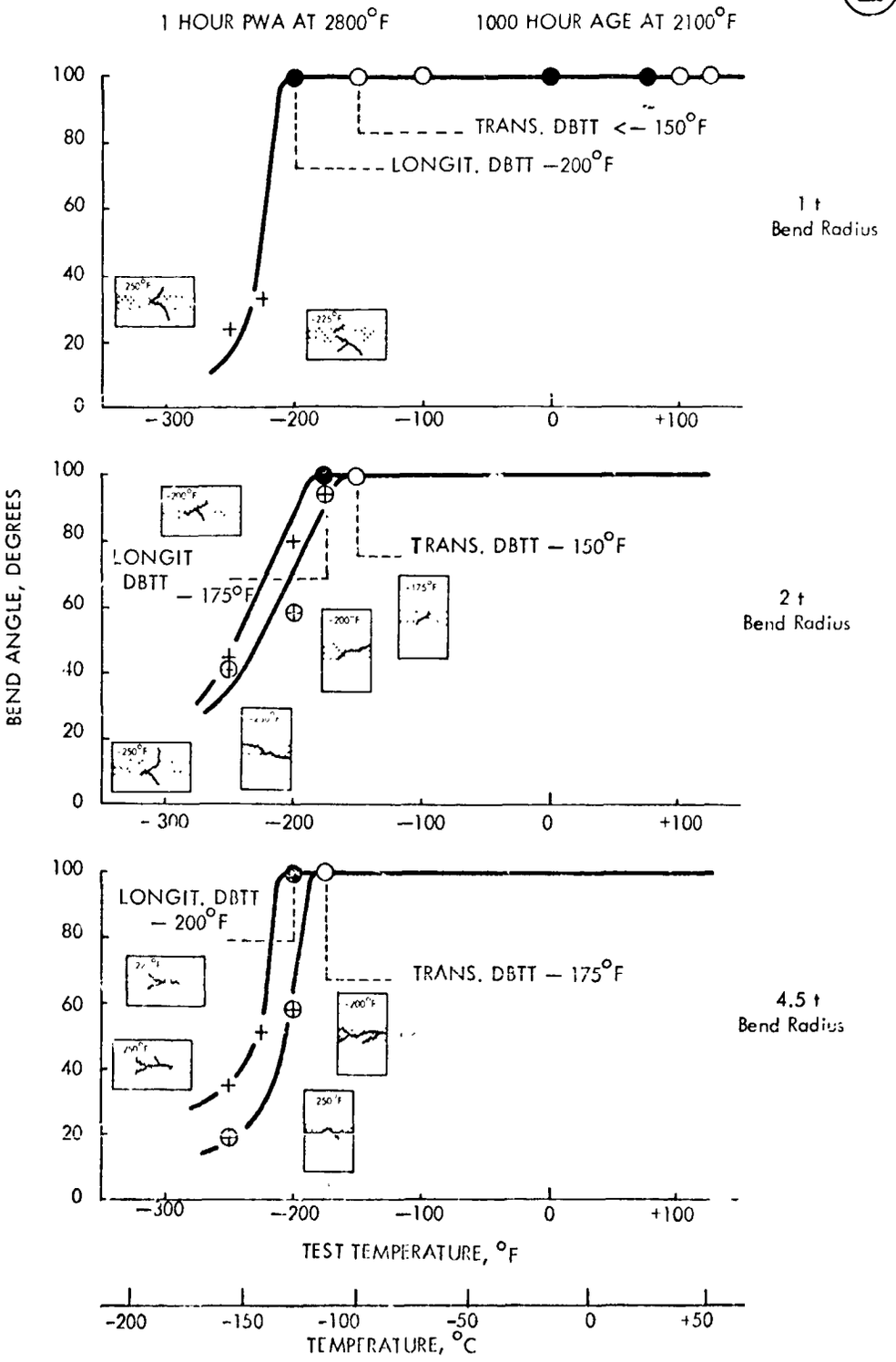

Figure A4. Bend Test Data for GTA Welds in 0.089 cm. (0.035 inch) T-111 Sheet. 1 Hour PWA at 1538°C (2800°F). Aged 1000 Hours at 1149°C (2100°F).

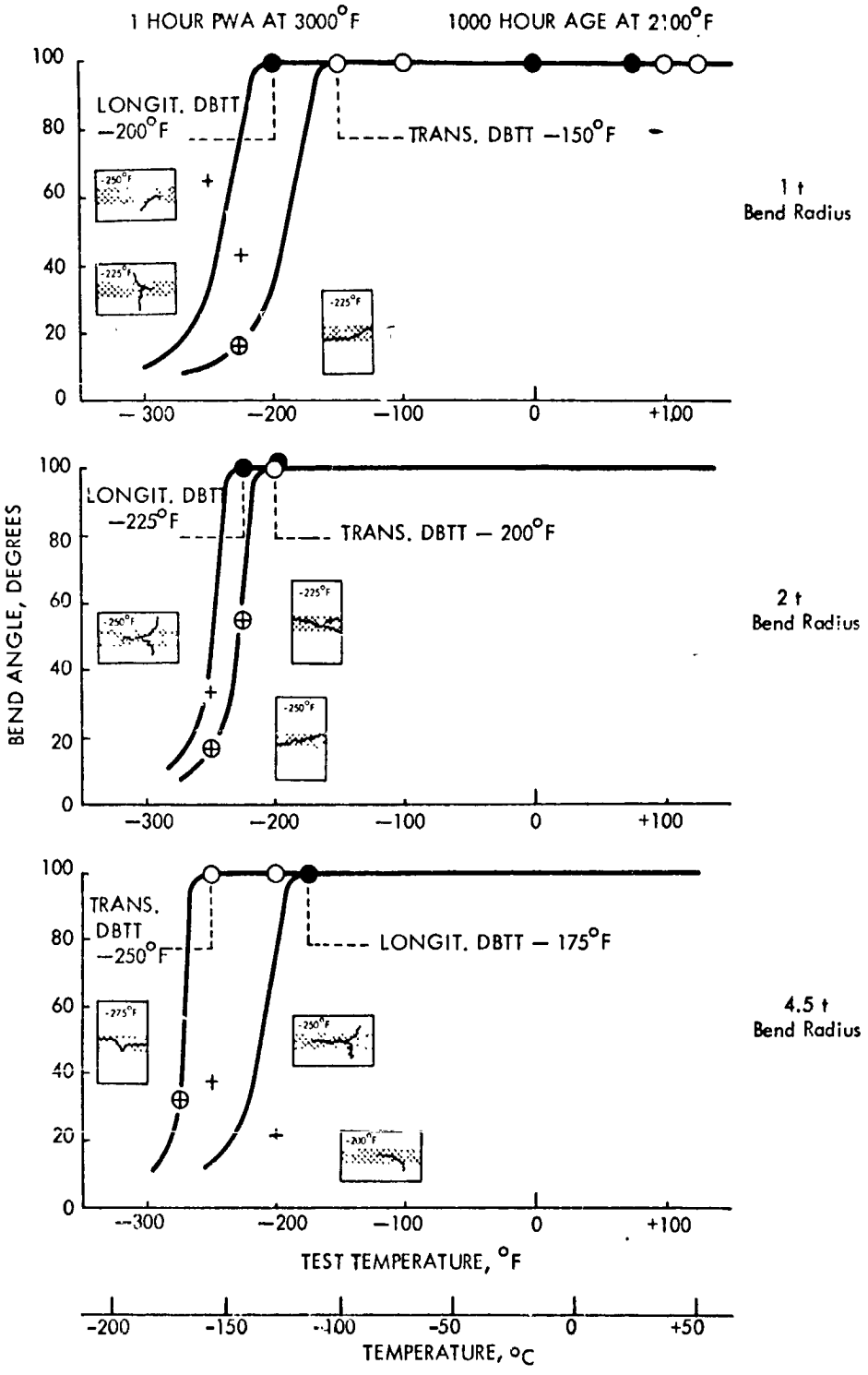

Figure A5. Bend Test Data for GTA Welds in 0.089 cm. (0.035 inch) T-111 Sheet. 1 Hour PWA at 1649°C (3000°F). Aged 1000 Hours at 1149°C (2100°F).

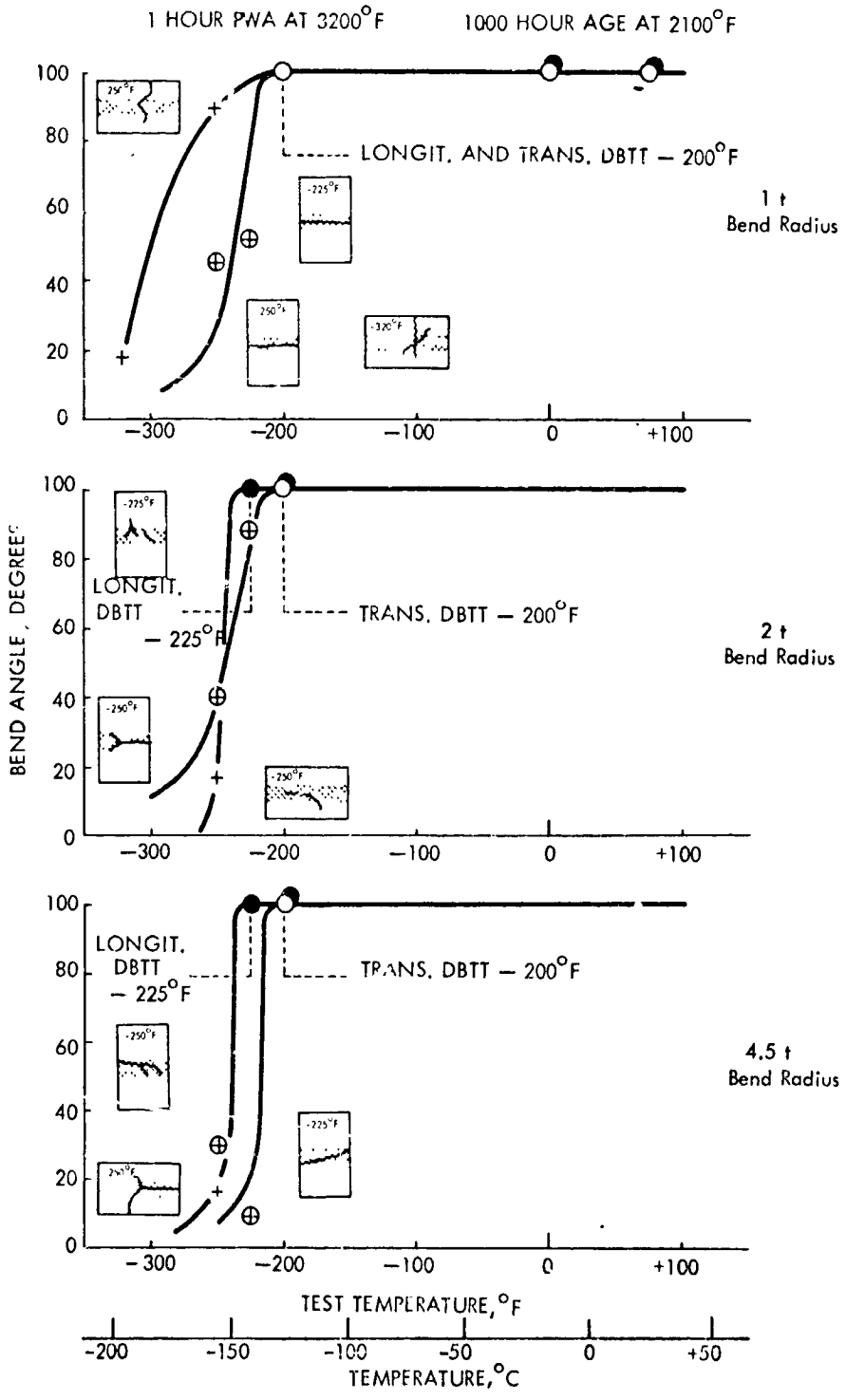

Figure A6. Bend Test Data for GTA Welds in 0.089 cm. (0.035 inch) T-111 Sheet. 1 Hour PWA at 1760°C (3200°F). Aged 1000 Hours at 1149°C (2100°F).

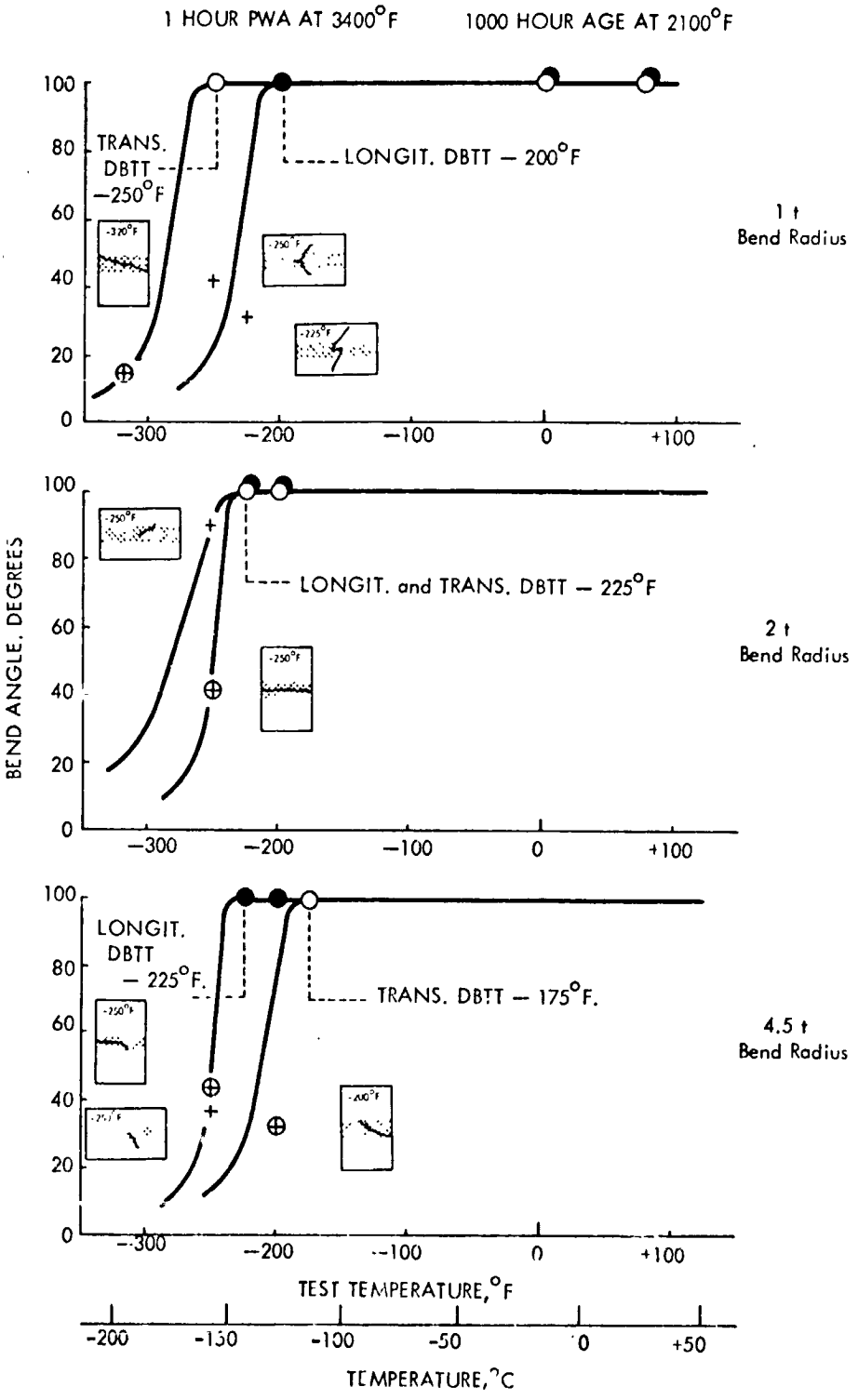

Figure A7. Bend Test Data for GTA Welds in 0.089 cm. (0.035 inch) T-111 Sheet. 1 Hour PWA at 1871°C (3400°F). Aged 1000 Hours at 1149°C (2100°F).

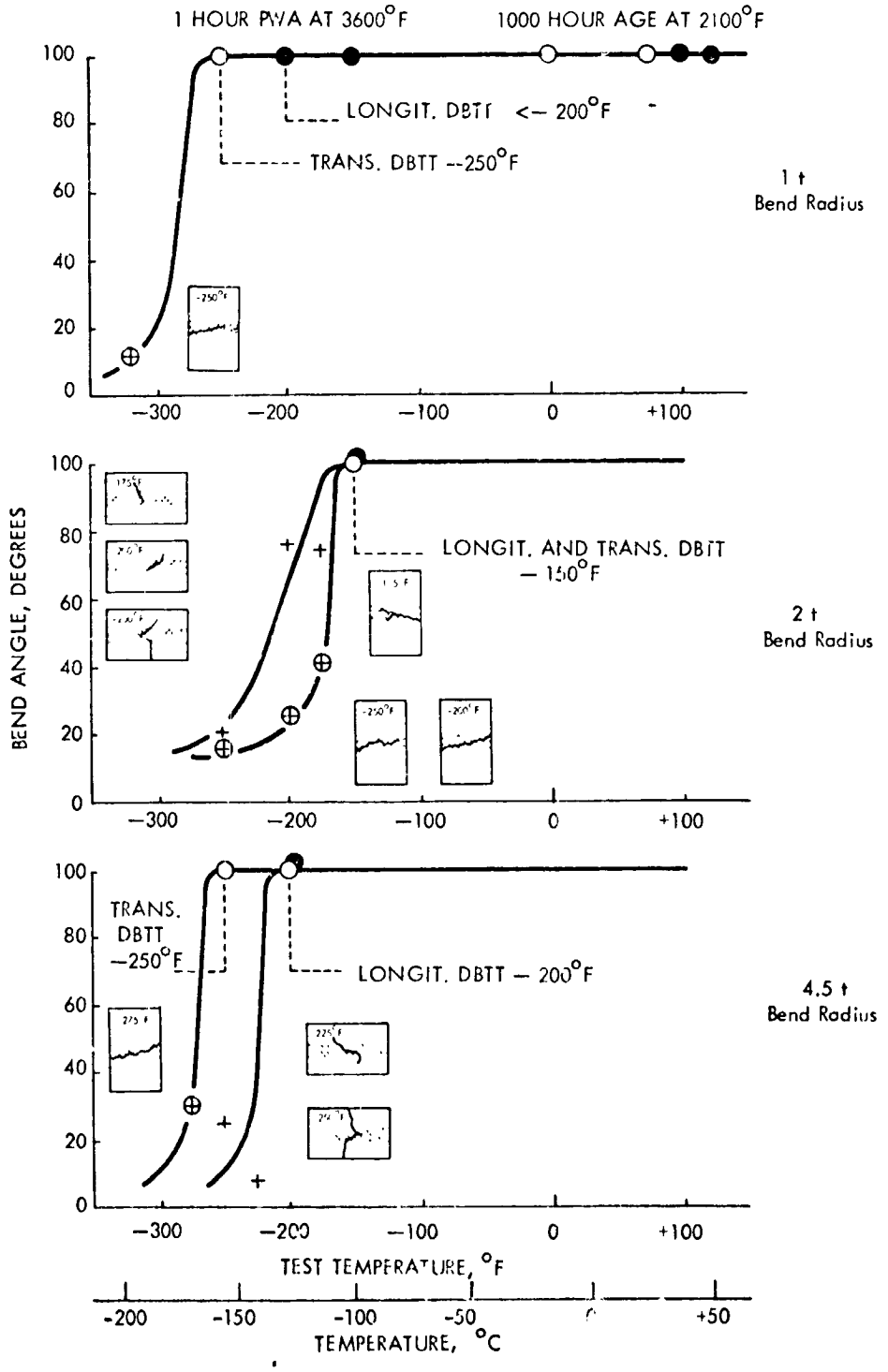

Figure A8. Bend Test Data for GTA Welds in 0.089 cm. (0.035 inch) T-111 Sheet. 1 Hour PWA at 1982°C (3600°F). Aged 1000 Hours at 1149°C (2100°F).

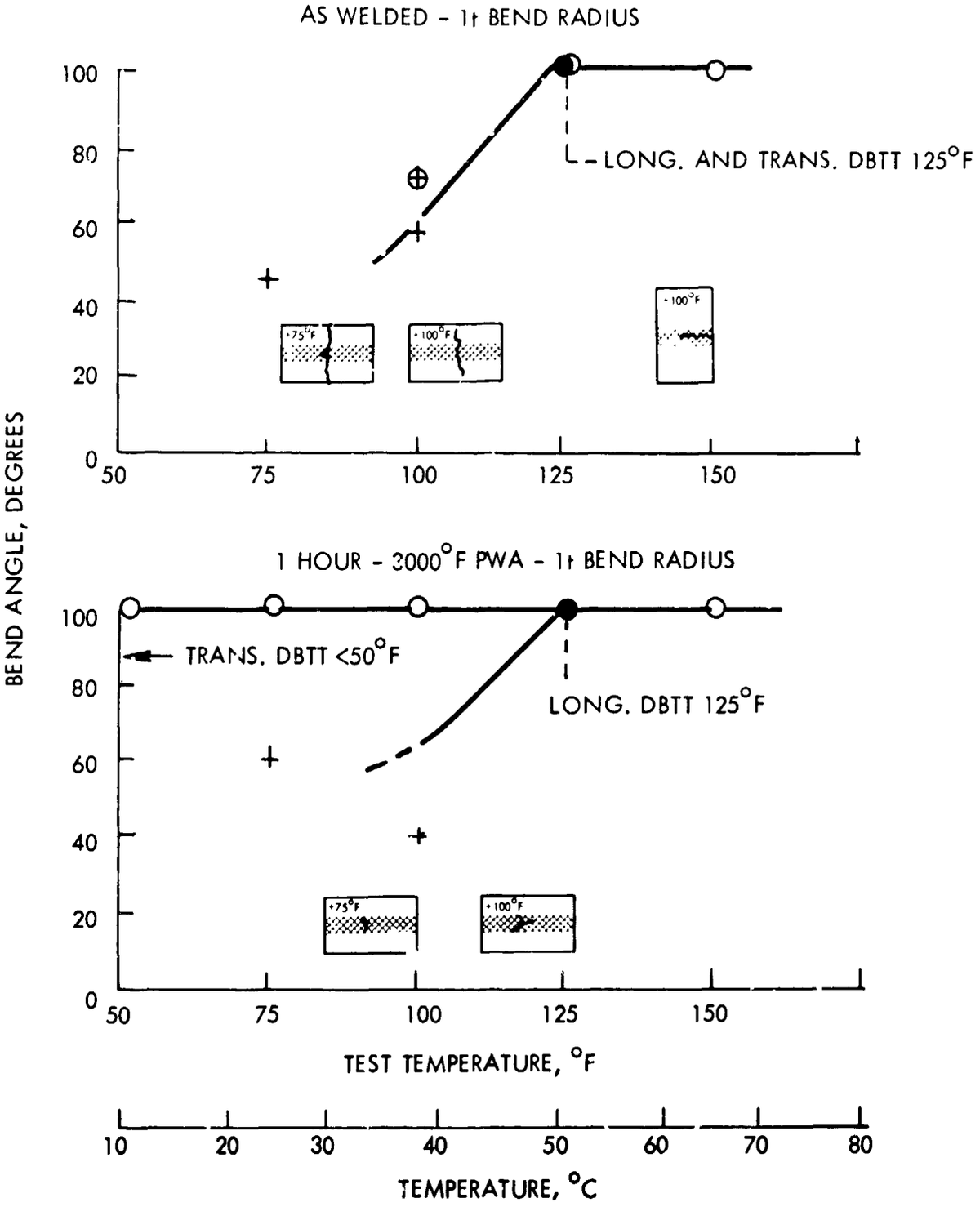

Figure A9. Bend Test Data for GTA Welds in 0.089 cm. (0.035 inch) ASTAR-811C Sheet. Pre-Test Thermal History as Indicated. 1t Bend Radius.

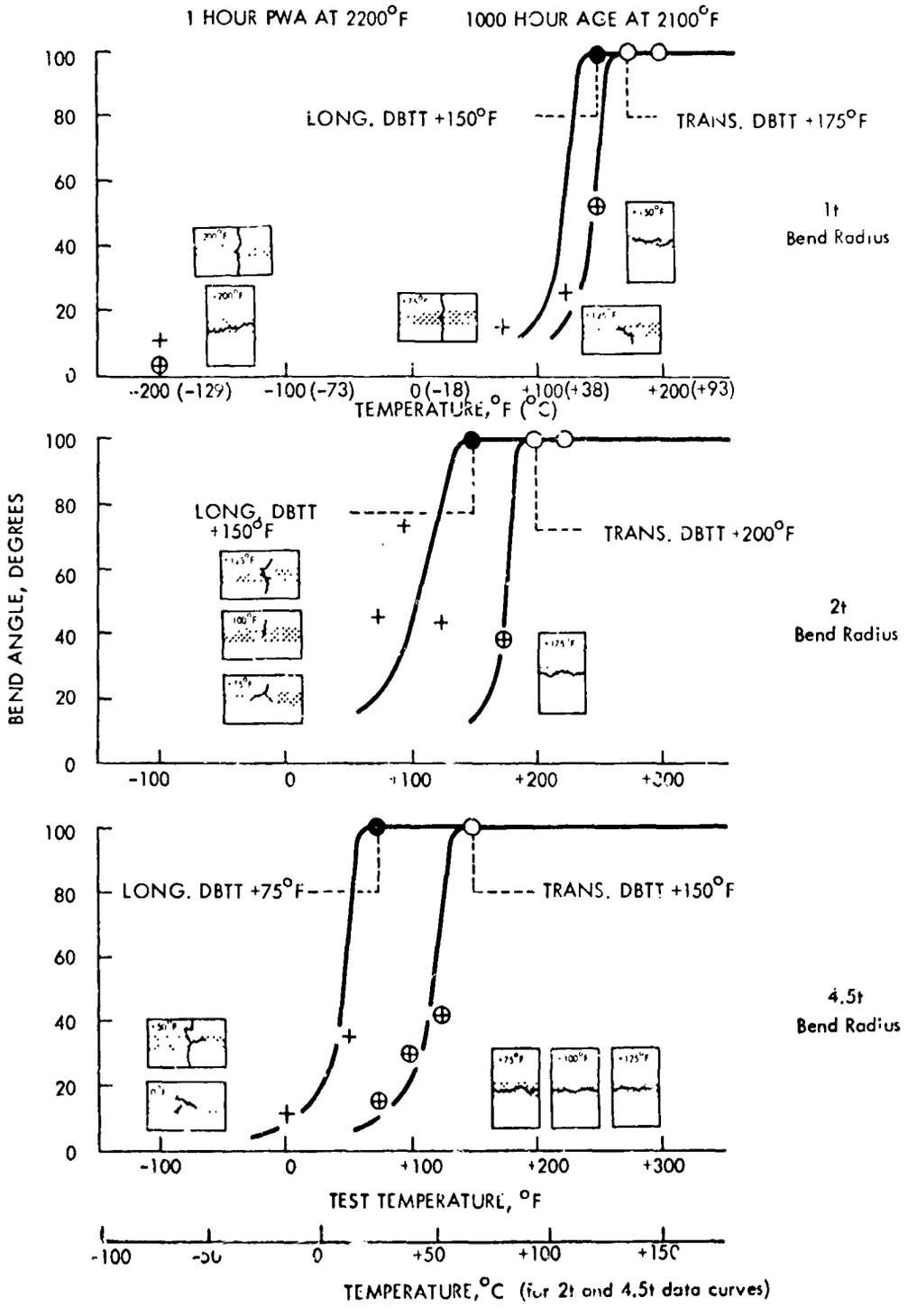

Figure A10. Bend Test Data for GTA Welds in 0.089 cm. (0.035 inch) ASTAR-811C Sheet. 1 Hour PWA at 1205°C (2200°F). Aged 1000 Hours at 1149°C (2100°F).

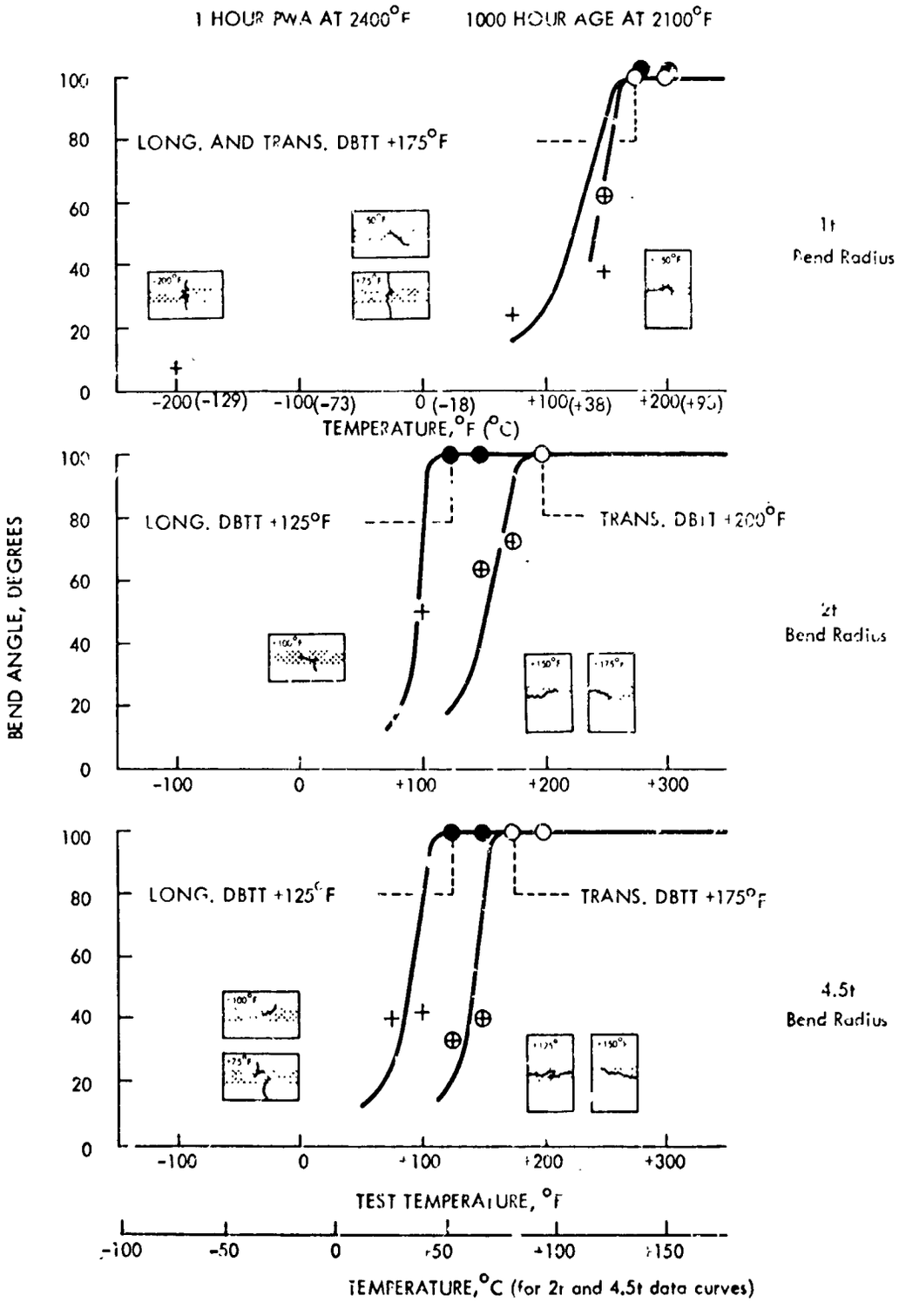

Figure A11. Bend Test Data for GTA Welds in 0.089 cm (0.035 inch) ASTAR-811C Sheet. 1 Hour at 1316°C (2400°F) PWA. Aged 1000 Hours at 1149°C (2100°F).

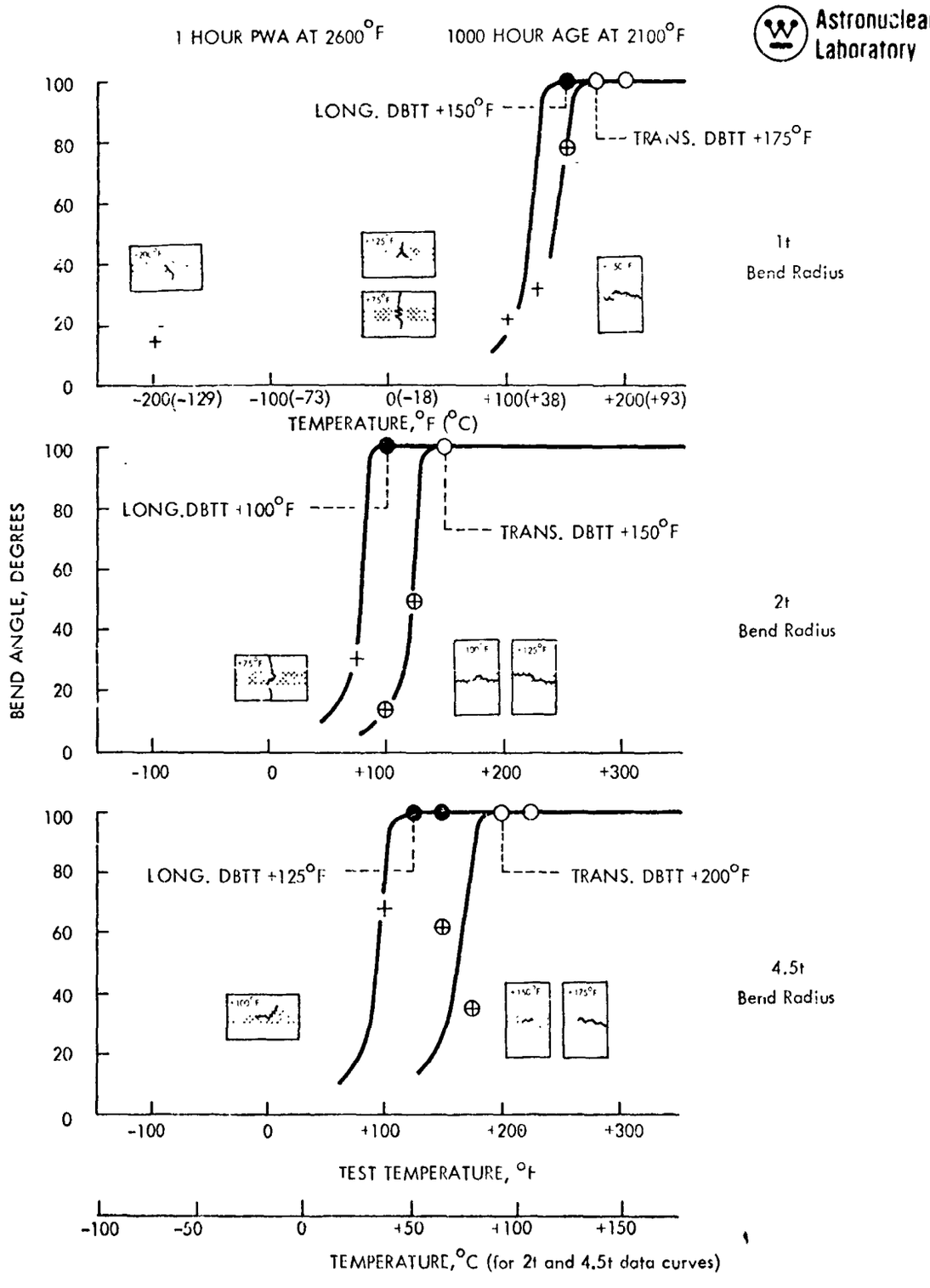

Figure A12. Bend Test Data for GTA Welds in 0.089 cm (0.035 inch) ASTAR-811C Sheet. 1 Hour PWA at 1427°C (2600°F). Aged 1000 Hours at 1149°C (2100°F).

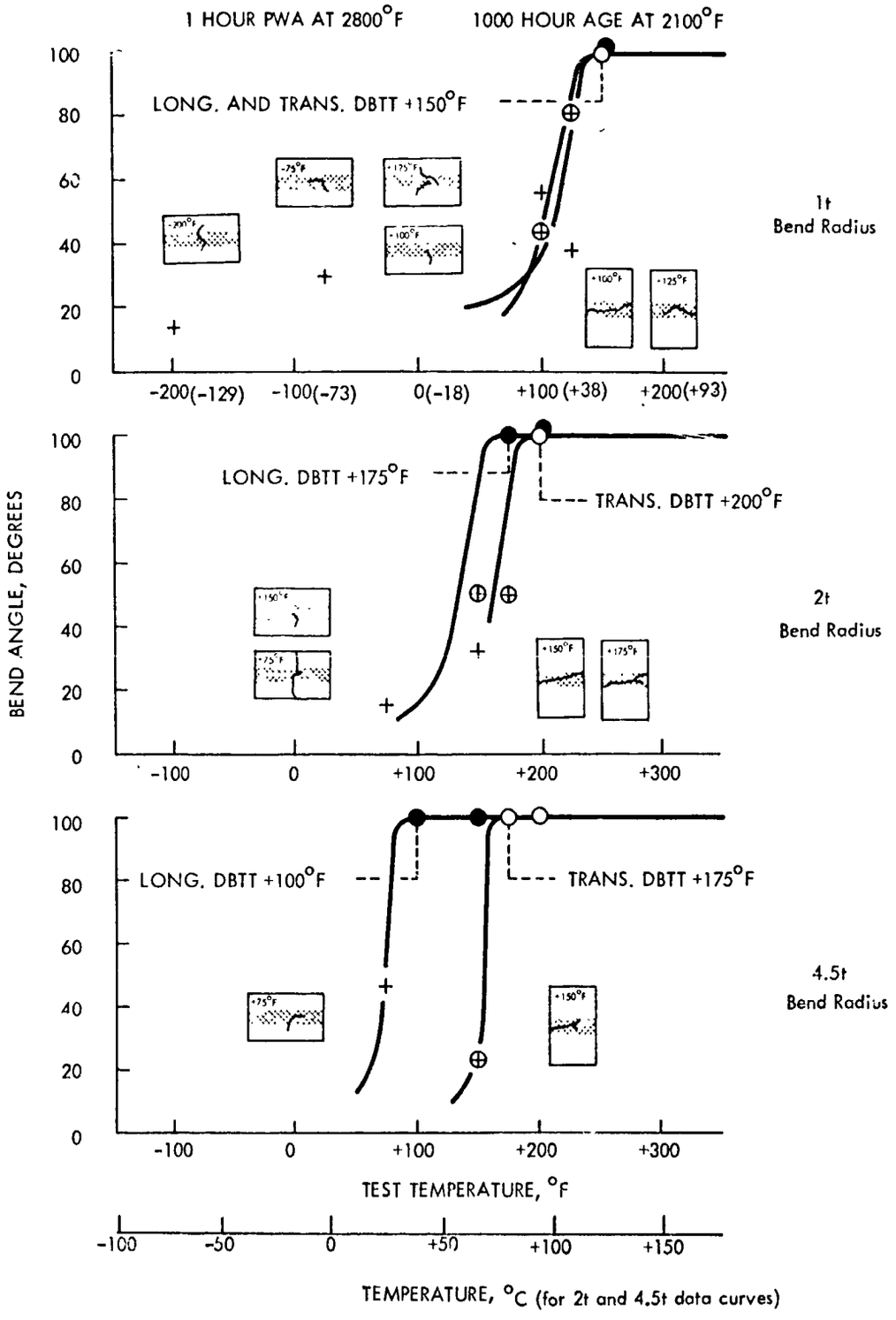

Figure A13. Bend Test Data for GTA Welds in 0.089 cm (0.035 inch) ASTAR-811C Sheet. 1 Hour PWA at 1538°C (2800°F). Aged 1000 Hours at 1149°C (2100°F).

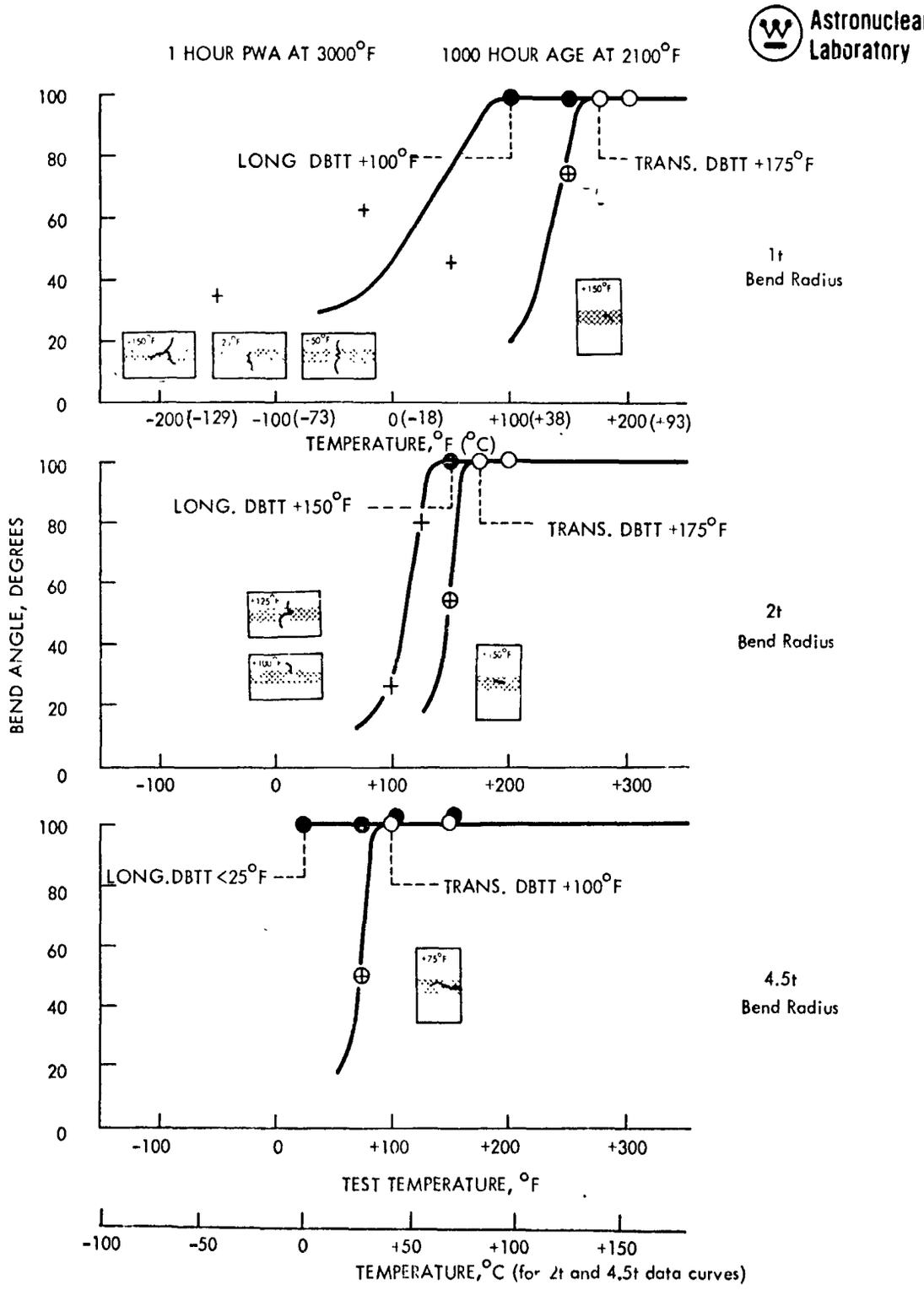

Figure A14. Bend Test Data for GTA Welds in 0.089 cm (0.035 inch) ASTAR-811C Sheet. 1 Hour PWA at 1649°C (3000°F). Aged 1000 Hours at 1149°C (2100°F).

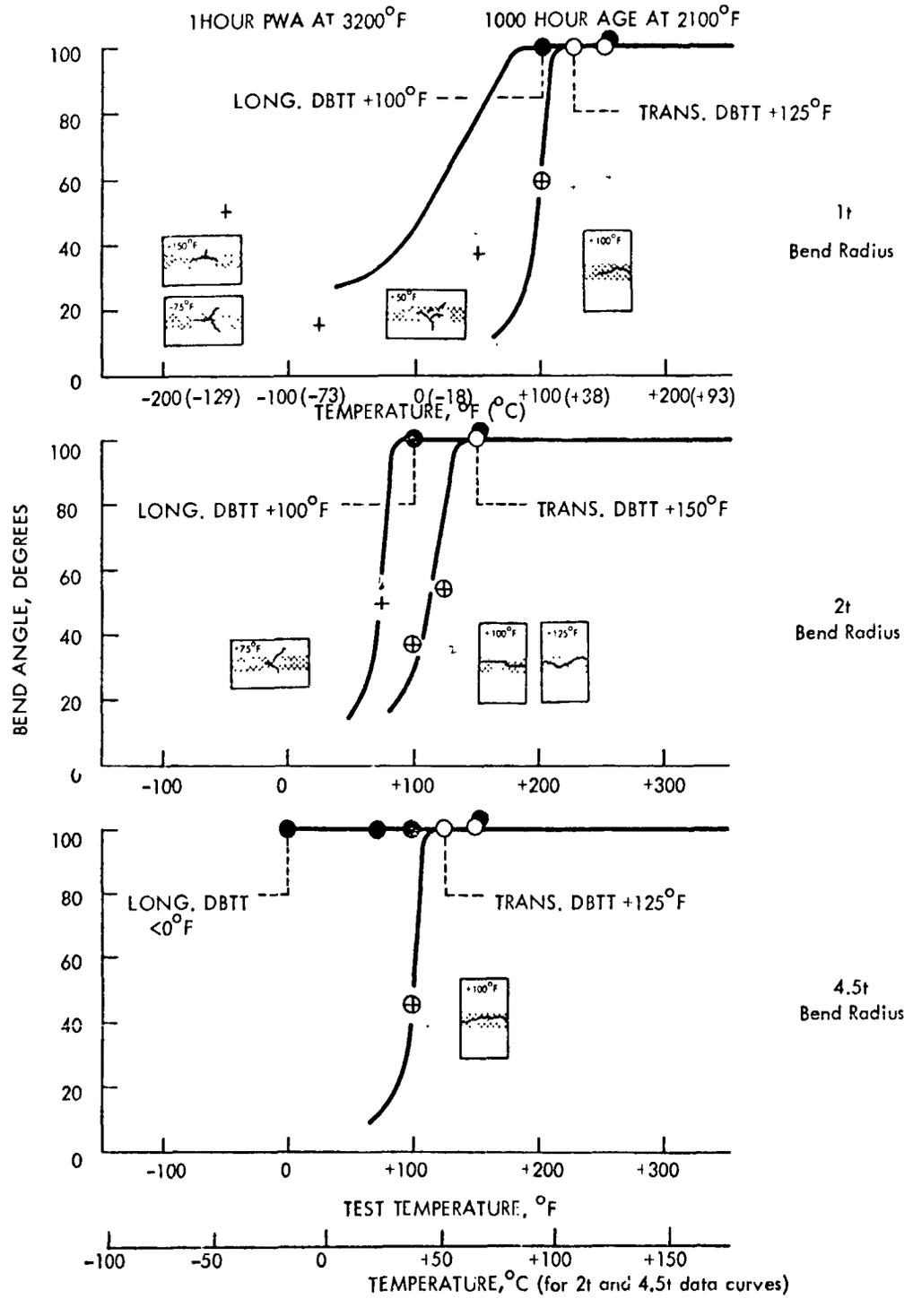

Figure A15. Bend Test Data for GTA Welds in 0.089 cm (0.035 inch) ASTAR-811C Sheet, 1 Hour PWA at 1760°C (3200°F). Aged 1000 Hours at 1149°C (2100°F).

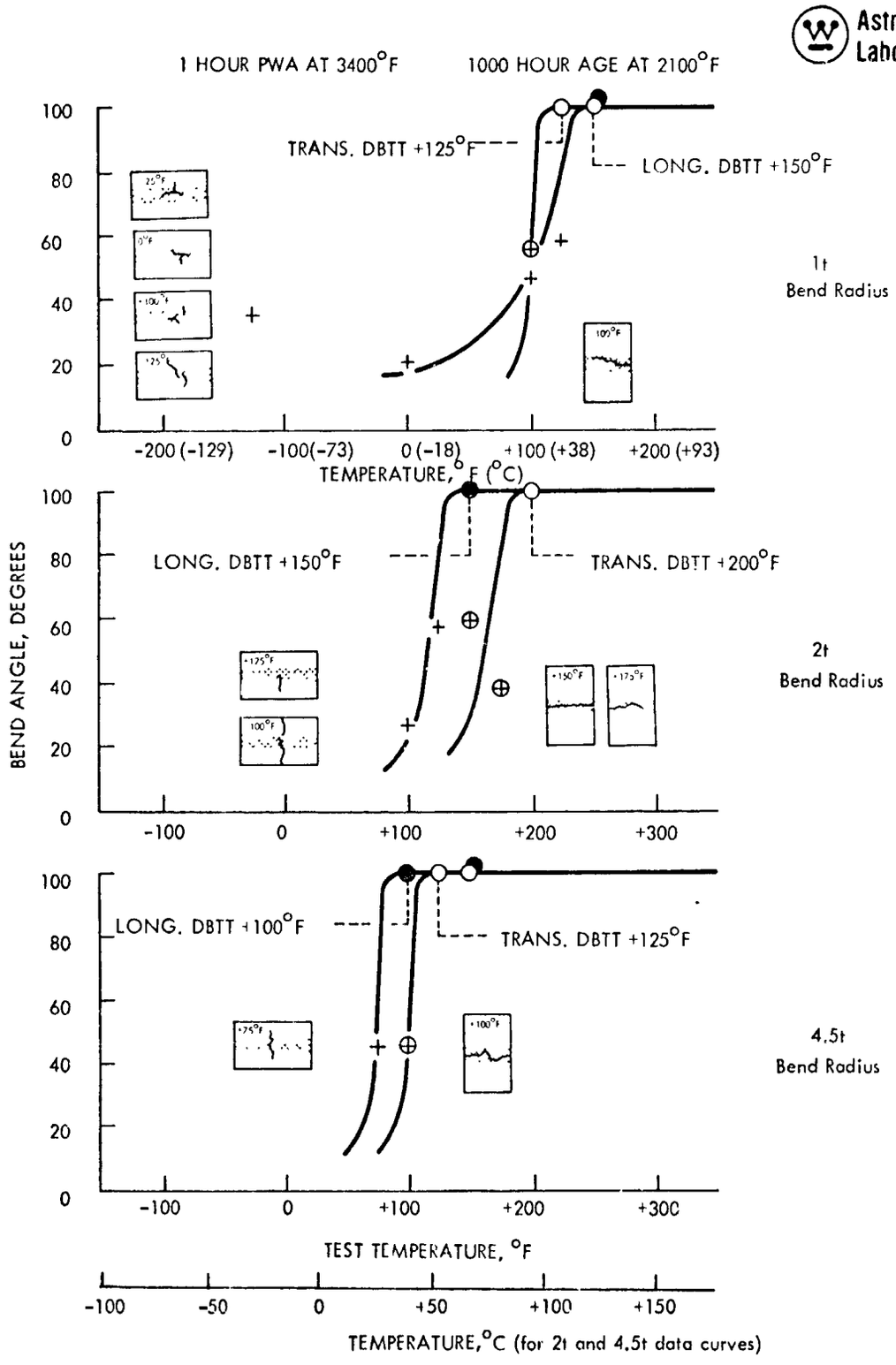

Figure A16. Bend Test Data for GTA Welds in 0.089 cm (0.035 inch) ASTAR-811C Sheet. 1 Hour PWA at 1871°C (3400°F). Aged 1000 Hours at 1149°C (2100°F).

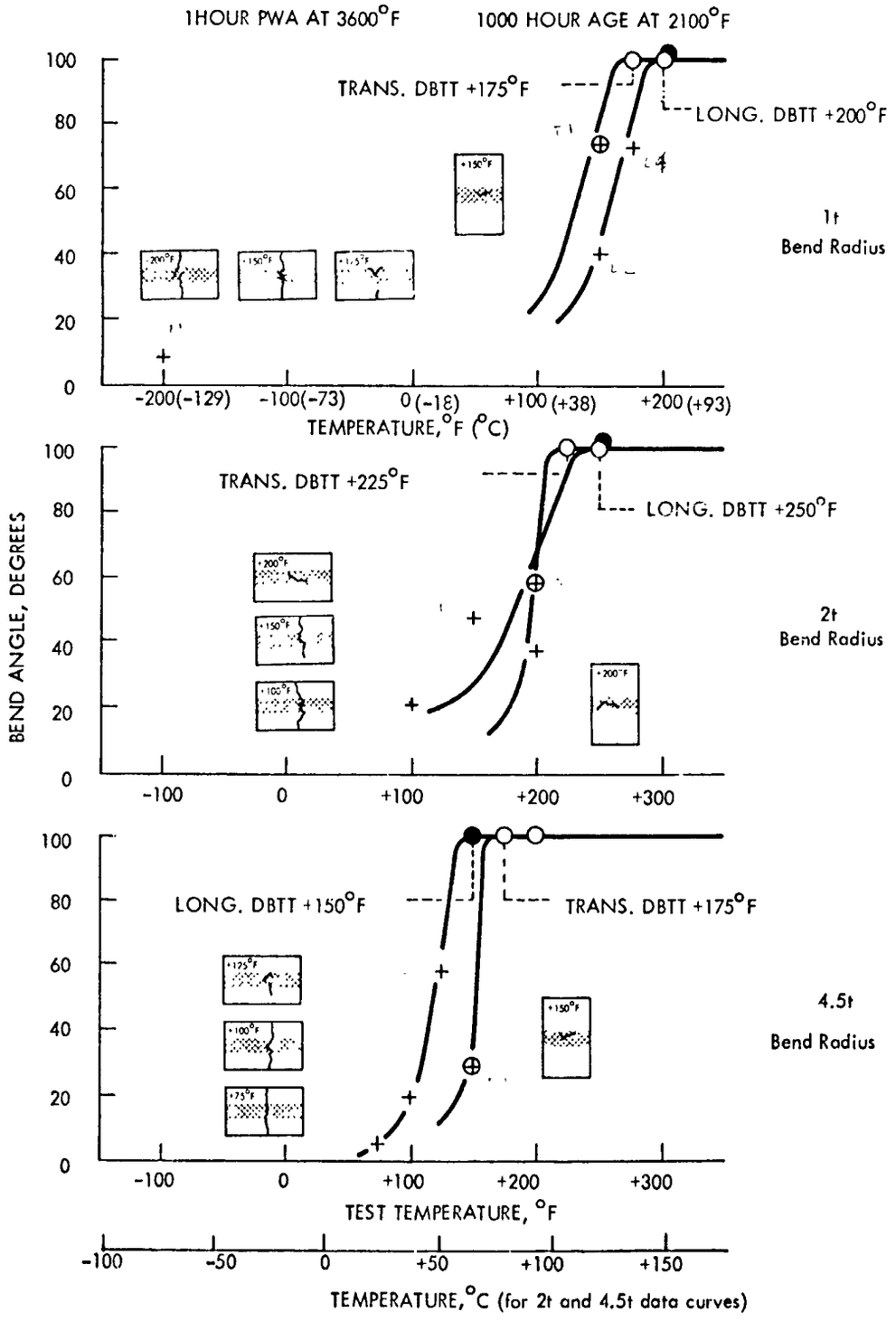

Figure A17. Bend Test Data for GTA Welds in 0.089 cm (0.035 inch) ASTAR-811C Sheet. 1 Hour PWA at 1982°C (3600°F). Aged 1000 Hours at 1149°C (2100°F).